CHEMICAL REVIEWS

Review

pubs.acs.org/CR

Self-Assembly of Perylene Imide Molecules into 1D Nanostructures: Methods, Morphologies, and Applications

Shuai Chen,[†,‡] Paul Slattum,[∥] Chuanyi Wang,[*,†] and Ling Zang[*,§]

[†]Laboratory of Environmental Sciences and Technology, Xinjiang Technical Institute of Physics & Chemistry, Key Laboratory of Functional Materials and Devices for Special Environments, Chinese Academy of Sciences, Urumqi 830011, China

[‡]The Graduate School of Chinese Academy of Science, Beijing 100049, China

[§]Nano Institute of Utah and Department of Materials Science and Engineering, University of Utah, Salt Lake City, Utah 84112, United States

[∥]Vaporsens Inc., Salt Lake City, Utah 84112, United States

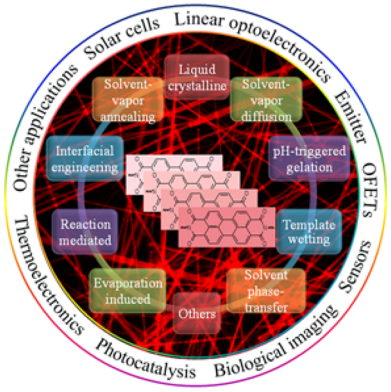

CONTENTS

1. INTRODUCTION

Supramolecular self-assembly, since its beginning in the later 1980s, has attracted increasing attention as a breakthrough methodology in the fields of nanoscience and nanotechnology.[1,2] In contrast to "top-down" approaches such as the templating method, electron-spinning, and nanolithography, and other "bottom-up" approaches such as physical vapor deposition, molecular self-assembly is usually conducted in the solution phase and is governed by weak noncovalent interactions.[2−4] In the last decades, great efforts have been directed to the solution-processable self-assembly of π-conjugated small molecules, oligomers, or polymers into shape-defined nanostructures, offering an attractive pathway to construct well-organized functional nanomaterials, which help bridge the gap between natural and artificial systems.[3−8] These nanostructures and corresponding morphologies are cooperatively controlled by noncovalent forces including H-bonding, dipole−dipole attraction, $\pi-\pi$ stacking, van der Waals force, hydrophobic effect, electrostatic interaction, and metal−ligand coordination. In most cases, intermolecular intrinsic $\pi-\pi$ stacking and highly directional H-bonding have been demonstrated as the major driving forces, which often act in cooperation with one or more other noncovalent interactions.[4,9] Nevertheless, these interactions are highly dependent on the molecular structures and are sensitive to external environmental parameters such as solvent, temperature, concentration, and fabrication process.[2,4,6] For self-assembly on a substrate, the surface characteristics like polarity play a critical role in precisely controlling the morphology of molecular assemblies thus produced.[6]

Among a large number of functional nanostructures with dimensionality distinguished between zero-dimensional (0D), one-dimensional (1D), two-dimensional (2D), and three-

Received: May 26, 2015
Published: October 6, 2015

DOI: 10.1021/acs.chemrev.5b00312
Chem. Rev. 2015, 115, 11967−11998

dimensional (3D), 1D nanostructures of organic semiconductors with morphologies including nanowires, nanobelts, nanorods, nanotubes, and helices have merited intensive study over the past two decades. These 1D nanostructures hold great potential for development into next generation electronic and optoelectronic nanodevices,[10,11] not only due to their small size (essential for device miniaturization) and large surface area (conducive to surface modification), but more importantly to the 1D confined properties, such as fluorescence polarization, waveguiding, $\pi-\pi$ stacking-mediated exciton diffusion, and charge transport. Consequently, self-assembly of π-conjugated organic molecules into 1D nanostructures has been an active and rapidly developing field as covered in some excellent reviews.[6,10−17] Up to now, most self-assembly studies have been focused on organic semiconductors that are p-type in nature (i.e., electron donating), such as conducting polymers.[6,9,10,18,19] Comparatively, less research progress and practical applications have been made on n-type semiconductors, especially the controlled 1D self-assembly of small molecules into larger functional nanostructures, which still remains as an important challenge due to their poor stability under ambient conditions.[20,21]

One exceptional n-type organic material has emerged from this research, perylene-3,4,9,10-tetracarboxylic imide, also called perylene imide, and is here denoted in short as PI. PIs, particularly the diimides (PDIs), as well as the oligomers and analogues, demonstrate both high thermal stability and photostability under ambient conditions,[22,23] making them feasible for self-assembly processing and applications in optoelectronic devices.[24] Numerous PDI molecules have been fabricated into well-defined supramolecular nanostructures; these successes have also inspired the research of self-assembly of many other n-type organic semiconductor molecules.[14,21] The presence of electron-withdrawing imide fragments in PIs allows them to be easily reduced chemically or electrochemically into stable anionic radicals while remaining stable to oxidation.[21] Their resistance to oxidation is the primary reason why PIs usually act as stable n-type materials.[23] Together with their other features, including facile structural functionalization, outstanding light-harvesting in the visible region, and near-unity fluorescence quantum yields in the molecular state, PIs have been recognized as an ideal candidate for fabricating organic optoelectronic materials and devices (Figure 1), such as organic photovoltaics (OPVs), organic field effect transistors (OFETs), dye lasers, fluorescent sensors, and organic light-emitting diodes (OLEDs).[20,22,24] Well-defined 1D nanostructures (Figure 1) of PIs can be fabricated via supramolecular self-assembly processes both in bulk solution and on solid substrates.[14,21,25−29] The 1D self-assembly is mainly driven by the intrinsic $\pi-\pi$ stacking interaction between the aromatic perylene planes, which favors the 1D growth of assembly, in cooperation with other intermolecular noncovalent interactions.[14,21,26] In comparison with the individual molecules or bulk-phase materials, 1D nanostructures of PIs exhibit uniaxial optical and electronic properties along the 1D $\pi-\pi$ stacking direction, which provides great potential for application in optoelectronic devices, especially at the nanoscale.[14,21,24,26,29] Research in the relevant fields has received increasing attention in recent years.[2,4,9,14,16,21,25−29] Although several excellent reviews have previously been published on the broader topics of molecular self-assembly including some PIs,[14,21,26,29] it still remains crucial to provide a deep, extensive review especially focused on various molecular designs of PIs. Structural

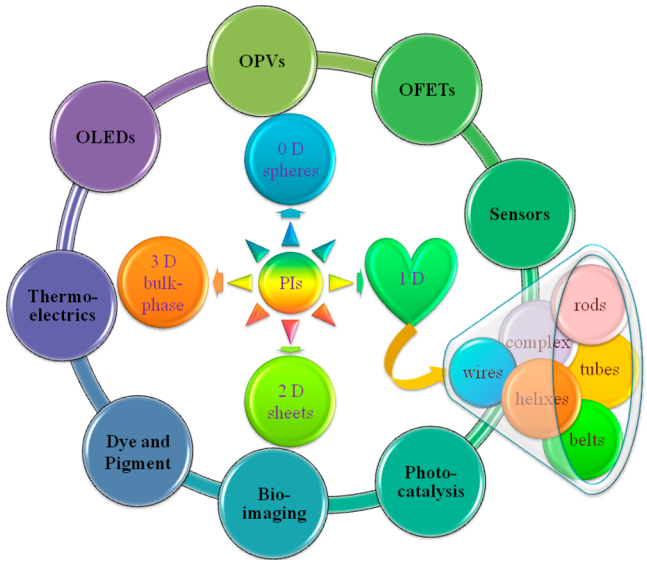

Figure 1. Main applications of PIs with various morphologies in tunable dimensions.

modification at side chains and bay substitutions play critical roles in controlling the morphology and optoelectronic properties of molecular assembly. Considering the rapid development in the 1D self-assembly of PI, a comprehensive and systematic review, covering both the advances of fabrication methods and promising applications, is of considerable interest.

This Review aims to present a comprehensive picture of 1D self-assembly of PIs, providing a deep understanding of recent progress as well as possible challenges and breakthroughs coming in the near future. First, the basic molecular design and synthetic strategies of PI molecules are described. A complete overview of the 1D self-assembly methodology of PIs then is presented, followed by a summary of the inspiring applications and relevant prospects of the 1D assemblies in photonic and electronic devices. Along with this, some novel analogue PI molecules and their involvement in 1D self-assembly are discussed. Last, the future challenges and opportunities of 1D self-assembly of PIs are briefly discussed. This Review provides insight into the general relationship between molecular structure, noncovalent interactions, self-assembly processing (conditions), and resulting morphology of assembly. The goal of this Review is to promote new research efforts in 1D organic nanostructures and relevant applications in optoelectronics, which will likely bring unprecedented properties and functionality as compared to the bulk-phase materials.

2. MOLECULAR SYNTHESIS

Desired chemical and physical properties of PIs are significantly dependent on the side-group functionalization at the imide *N,N′* positions, the 1, 6, 7, 12 positions of the perylene core (also known as "bay" positions), and even at the 2, 5, 8, 11 positions (so-called "ortho-" positions) (Figure 2).[22] A review focusing on this aspect was published in 2011, where a common method first adopted by Langhals et al. in the 1990s was recommended for the synthesis of symmetric and asymmetric imide-substituted PIs.[23] In a typical synthetic route, commercially available starting molecule perylene tetracarboxylic dianhydride (PTCDA; Figure 2) reacts with primary amines in high boiling-point solvents (commonly,

DOI: 10.1021/acs.chemrev.5b00312
Chem. Rev. 2015, 115, 11967−11998

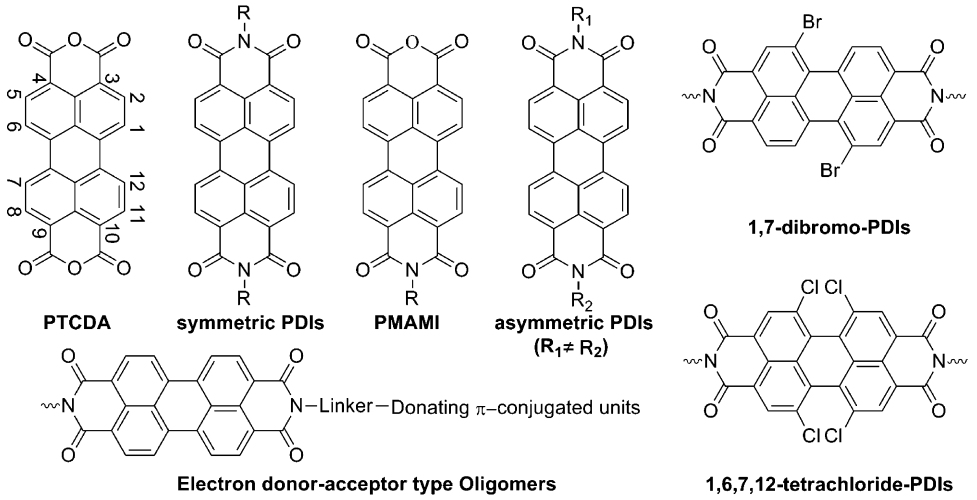

Figure 2. Fundamental chemical structures of PTCDA with the numbering of the positions in the ring system, symmetric and asymmetric *N,N′*-PDIs, most common precursors PMAMI, dibromo- and tetrachloro-PDIs, as well as a typical oligomer configuration.

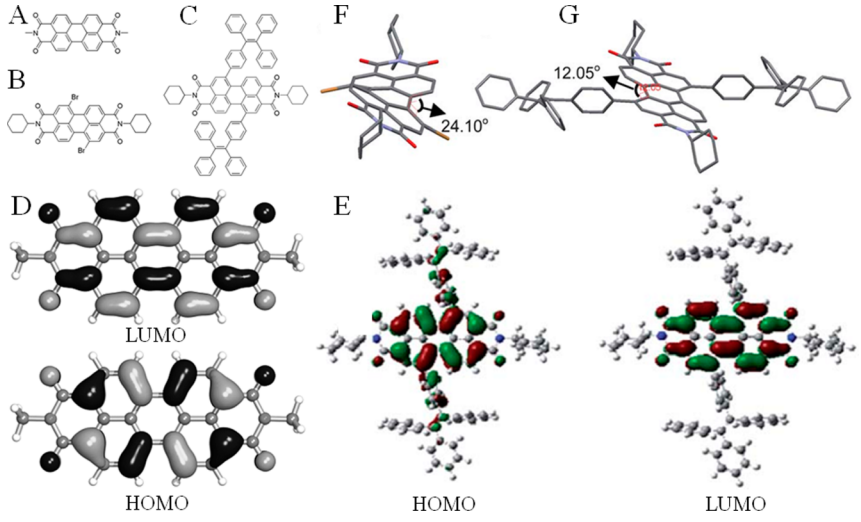

Figure 3. Chemical structures of *N,N′*-dimethyl-PDI (A), *N,N′*-dicyclohexyl-1,7-dibromo-PDI (B), and *N,N′*-dicyclohexyl-1,7-ditetraphenylethenyl-PDI (C). The frontier orbitals of *N,N′*-dimethyl-PDI (D) and *N,N′*-dicyclohexyl-1,7-ditetraphenylethenyl-PDI (E) according to DFT calculations. The optimal structures of *N,N′*-dicyclohexyl-1,7-dibromo-PDI (F) and *N,N′*-dicyclohexyl-1,7-ditetraphenylethenyl-PDI (G), calculated by the semiempirical AM1 method. Reproduced with permission from refs 23 and 30. Copyright 2011 American Chemical Society and 2012 Royal Society of Chemistry, respectively.

imidazole or quinoline). In most cases, direct imidization to symmetric PDIs (Figure 2) from aliphatic amines is feasible, giving higher yields than that of aromatic amines. For asymmetric PDIs (Figure 2), an indirect synthetic route with the aid of a precursor, perylene monoanhydride monoimide (PMAMI; Figure 2) from partial hydrolysis of symmetric PDIs, is often necessary.

In general, the substitution at the two imide positions has little effect on the electronic property of PDIs (e.g., energy levels, redox potentials), thus resulting in no significant change of the molecular absorption or emission features.[23] This is because the imide positions are the nodes of the HOMO and LUMO orbitals of the molecule, as shown in Figure 3D and E.[23] On the contrary, substitution at the bay positions often changes significantly the optical and electronic properties, especially when electron-donating moieties are attached.[30] The orbital energy shifting, in combination with the disturbing of the planar π-conjugation, can explain such performance changes.[30,31] For example, a twist angle of 24.10° was observed for the perylene plane when the 1,7-positions of PDI are substituted with dibromo moieties (Figure 3B and F).[30] It should be pointed out that the extent of the twisting of perylene plane is not necessarily proportional to the size of the substituents at bay area. Indeed, replacing the dibromo groups by much more bulky ditetraphenylethenyl moieties at the same bay positions (Figure 3C) resulted in a twist angle of only 12.05° (Figure 3G).[30] This difference is likely due to the π-conjugation system incorporating the substitution and propeller-like shape of the tetraphenylethenyl structure itself. Such tunable molecular planarity affects the solubility of PDI molecules, and on the other hand the significantly twisted π-conjugation weakens the $\pi-\pi$ stacking interaction. For the synthesis of bay-substituted PDIs, dibromo (predominantly 1,7 regioisomers; Figure 2) and tetrachloride (1, 6, 7, and 12 positions) derivatives of PTCDA or PDI are key intermediates for subsequent imidization or nucleophilic substitution.[23]

Besides the monomeric molecules described above, oligomers (often dimers and trimers) of PDIs have also been

DOI: 10.1021/acs.chemrev.5b00312
Chem. Rev. 2015, 115, 11967−11998

investigated by condensing PTCDA or PMAMI with diamines. Additionally, donor−acceptor (D−A) type oligomers (Figure 2) combining PDI moieties with other aromatic units can be obtained following similar amidation strategy with minor modifications. Such oligomers often exhibit enhanced charge transfer, which together with the unique linear geometry makes these molecules promising candidates for applications in electronics and optoelectronics, particularly the unimolecular electronics (e.g., single molecule rectifier).[31−34]

3. SELF-ASSEMBLY

The core of PDIs is a planar π-conjugated system, prone to $\pi-\pi$ stacking into crystal aggregates with an interlayer distance of ca. 3.4 Å (similar to that in graphite).[21] The aggregation behavior of PDIs can be monitored in situ by measuring relevant UV−vis absorption spectra. Monomeric PDI molecules in solution usually have three characteristic vibronic absorption peaks around 400−550 nm for the lowest energy electronic transitions. A red-shift in absorption peaks is often observed for molecular aggregation.[23,31] In addition, the transformation from isolated PDI molecules into condensed phase is often accompanied by significant fluorescence quenching.[28] Interestingly, the molecular stacking conformation in 1D nanostructures can be readily demonstrated by polarized fluorescence spectroscopy due to their optically uniaxial property along the $\pi-\pi$ stacking axis.[35] It should be noted that, unlike in the pigment industry, where insoluble PDIs are desirable, for the applications in organic optoelectronics and the supramolecular self-assembly studies, PDIs with reasonable solubility in common solvents are needed.[21,23] Consequently, long alkyl side-chains or bulk substituents at the imide positions are used to improve the solubility of PDIs.[14] Because of the molecular orbital nodes at the imide positions, such side-chain attachments impose little effect on the electronic properties of PDI molecules, offering wide options to modify the side-chain structures to tune the $\pi-\pi$ stacking arrangement, which in turn allows for studying the structure−property relationship of PDI assemblies.[14,21,26,29] On the contrary, bay-substitution often significantly disturbs the well-organized self-assembly of PDIs.[29] In many cases, steric effects imparted by bay substituents can lead to a twisting of the PDI plane, that is, a distortion of the π-systems from planarity, potentially increasing the solubility and restraining the crystal packing arrangement behavior induced by $\pi-\pi$ stacking.[23]

Note that the side-chain effect on the supramolecular self-assembly of PDIs is far from absolute. The incorporation of PDI building blocks into desired nanostructures and morphologies is also greatly altered by other noncovalent forces.[36,37] The tunable self-assembly of PDIs into well-defined 1D nanostructures is driven by the intrinsic cofacial $\pi-\pi$ stacking between adjacent PDIs ensuring molecular arrangement along the long axis, together with one or more other directional noncovalent forces, usually intermolecular H-bonding and hydrophobic effects trigged by modified side-chains of PDIs and solvent properties such as components, polarities, and pH.[21,23,25,28,38] These effects are exemplified by amphiphilic PDIs, in which self-assembly into 1D nanostructures can be subtly tuned by synergetic noncovalent interactions.[39,40] When performed on a substrate, the self-assembly becomes strongly dependent on the surface properties such as polarity, hydrophilic versus hydrophobic, and atomic orientation. The other environmental parameters, for example, temperature and solvent annealing, also play significant roles in tuning the molecular assembly process, for example, leading to the formation of more uniform nanofibers.[4,6,9] At early stages of the study on the self-assembly of PDI molecules, taking advantage of their inherent liquid crystalline characteristics arising from imide-substitution of polyether or alkyloxyl side-chains, solutions of monomeric PDIs were transferred onto various substrates resulting in the surface-assisted self-assembly of PDIs.[41−43] Monomer molecular structure, concentration, and temperature-dependent arrangement behavior both in solution and in the condensed state play critical roles in controlling the supramolecular morphology.[44,45] Although such template-supported nanostructuring of crystalline PDI molecules has been considerably explored via solution-casting and melt-assisted wetting, the resulting columnar nanostacks are much shorter than the desired long-range 1D nanostructures.[46−48] Thus, the main focus of this Review centers on solution-processable strategies for the self-assembly of PDIs into 1D nanostructures.[14] To gain a better understanding on the relationships among molecular structure, external environment, and nanostructured morphologies, the 1D self-assembly strategy has been divided into several approaches. These approaches include substrate-supported in situ self-assembly, solvent-phase interfacial self-assembly, and vapor-triggered self-assembly at the interface of solid/gas or liquid/gas systems. As the concise design of molecular structures is one of the key challenges in the development of functional PDI 1D nanofibers, a competitive balance between $\pi-\pi$ stacking and other noncovalent forces gives rise to the self-assembly of many imide-substituted PDIs as well as to some bay-substituted PDIs and ionic PDIs. Other self-assembly strategies include pH-triggered self-assembly in aqueous solution, and chemical reaction-mediated self-assembly of unsubstituted PTCDA and perylene diimide. In addition to the common rod-like and belt-like morphologies, 1D nanofibers with chiral/helical nanostructure similar to the double helix structure of DNA molecules, and heterogeneous "n−p" or "D−A" type nanostructures, which have attracted significant interest as building blocks in optoelectronics, are also presented.[37,49,50] Additionally, some studies on well-tailored 1D nanostructures of oligomeric and polymeric aromatic systems bearing PDI units deserve special attention in view of their promising performance in devices like organic solar cells (OSCs).[9]

3.1. Solvent-Phase Interfacial Self-Assembly

In the past decade, extensive efforts have been devoted to solution-phase self-assembly of PDI derivatives at interfaces to obtain 1D nanostructures with well-defined 1D morphologies (e.g., nanowire and nanobelt) under ambient conditions.[14,20] To date, such solution-processing strategies have been expanded into a series of approaches (Figure 4) such as bisolvent phase-transfer, solvent-vapor diffusion, and evaporation-triggered in situ self-assembly on a solid surface.[14,51−77] All methods are in relation to a mass transfer process between a good and a poor solvent (or vapor) with optimized binary solvent components and adjustable environmental parameters (e.g., solvent polarity, concentration, pH, temperature, etc.).[14] Good solvent refers to a solvent in which the PDI has a high degree of solubility and usually is a relatively polar aprotic solvent (e.g., $CHCl_3$), which is able to solvate the extended π-conjugated perylene systems, whereas extremely nonpolar solvents (e.g., hexane, methylcyclohexane) and some polar protic or hydrophilic solvents (e.g., CH_3OH, C_2H_5OH) often act as poor solvents because they favor $\pi-\pi$ stacking and/or H-

DOI: 10.1021/acs.chemrev.5b00312
Chem. Rev. 2015, 115, 11967−11998

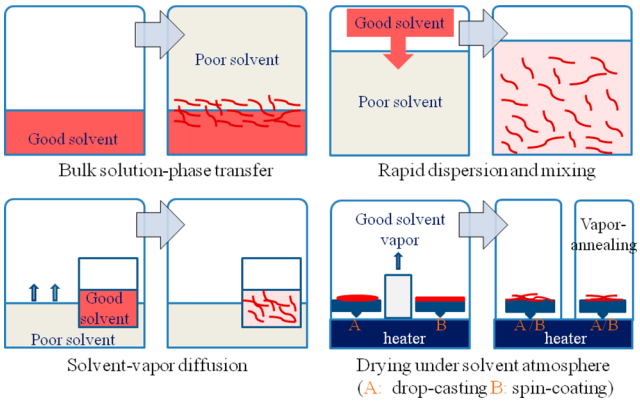

Figure 4. Diagrams showing the approaches relative to solvent-phase interfacial self-assembly strategy.

bonding.[14] However, the classification is far from absolute.[51−61] Successful self-assembly into shape-defined 1D nanostructures is finally determined by the balance between the solubility of PDI molecules and noncovalent intermolecular forces, in conjunction with proper molecular design.

3.1.1. Bulk Bisolvent Phase-Transfer Self-Assembly. The bisolvent phase-transfer self-assembly method is generally performed through interfacial diffusion from a large volume of poor solvent carefully decanted atop a concentrated solution of PIs molecules in a good solvent.[14,51−64] In the past decade, many studies have demonstrated the significant influence of side-chain modification (Figure 5) on the self-assembly and resultant morphologies of PDI nanostructures.[51−54]

The self-assembly of PDIs into nanostructures requires PDI monomers of sufficient solubility in good solvent, which is enhanced by branched or bulky imide substituents (e.g., 1-nonyldecyl, hexylheptyl). However, this type of substitution can create steric hindrance, which in turn can distort molecular stacking.[14,51] Efficient $\pi-\pi$ stacking interaction between the PDI monomers is critical for self-assembly into extended nanostructures. This stacking is enhanced by nonbulky, linear, or flexible side-chains (e.g., propoxyethyl).[14] Sufficient side-chain interaction via H-bonding or electrostatic interactions relative to solvent effect should also be considered before molecular design,[14,52] because hydrophobic interactions of side-chains in mixed solvents may inhibit molecular arrangement along the $\pi-\pi$ stacking long axis.[52,53] Clearly, the effect of side-chain substitution plays a critical role in self-assembly at the good/poor solvent interface and demonstrates that the self-packing conformations of PIs other than the $\pi-\pi$ stacking of perylene planes play a role in self-assembly.[14,52] For example, soluble PDI molecules bearing long linear alkyl chains (dodecyl and octadecyl, etc.) at the imide positions were found to form 1D nanobelts (Figure 6a−g) at the $CHCl_3/CH_3OH$ interface.[14,56−60] On the contrary, by virtue of tunable balance between $\pi-\pi$ stacking growth and solvophobic effect, self-assembly of PDIs bearing branched alkyl chains or bulky moieties resulted in shorter and wider 1D nanofibers (ribbons or rods; Figure 6h−k).[51−54] These nanoribbons or nanorods retain much of the native strong fluorescence of monomeric PDI molecules in contrast to the observed strong fluorescence quenching in the above-mentioned crystalline nanobelts.[54] Additionally, the contributions of other noncovalent forces such as van der Waals attraction between side-chains[61,62] and dipole−dipole interactions between PDIs molecules,[54] and solvent to the self-assembly process of ordered 1D nanofibers also have been revealed.[61]

Once the molecules are defined, varying volume ratios of the good/poor solvents are the most common strategy to control the self-assembly process.[14,54,56−58,62] Although defining the influence of solvent alone is difficult, it should be pointed out that excessive poor solvent as compared to good solvent is often necessary for forming optimal 1D nanofibers,[56−58] but not mandatory.[62] One exception involves amphipathic PDI molecules, which can be processed in aqueous media.[62] In this

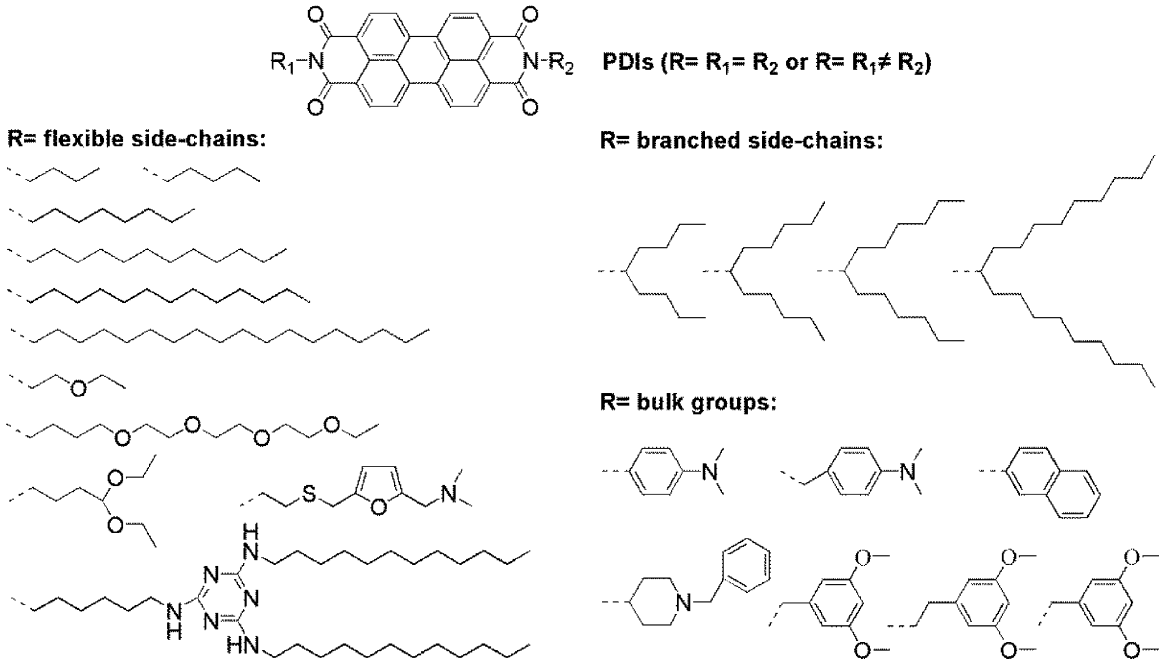

Figure 5. Molecular structures of PDIs bearing a variety of imide-substituents capable of bulk-phase bisolvent phase-transfer self-assembly reported in the past decade.

DOI: 10.1021/acs.chemrev.5b00312
Chem. Rev. 2015, 115, 11967−11998

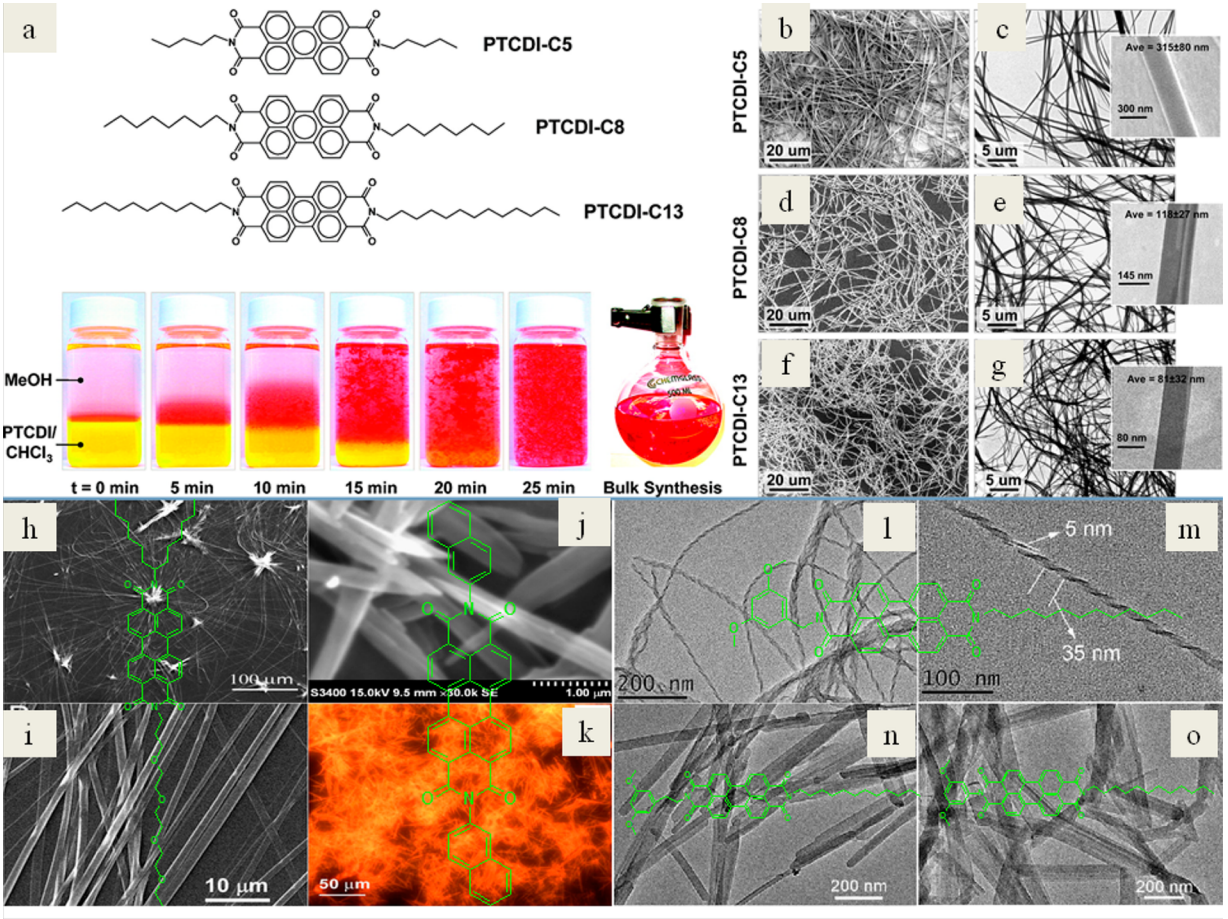

Figure 6. Schematic illustration of the effect by imide-substituents on the morphologies of 1D nanofibers of PDIs from bisolvent phase-transfer self-assembly. (a) Chemical structures of the three PDI derivatives modified with varying lengths of alkyl chains. (b) Optical photographs showing the time-course color and morphology change of a PDI solution caused by self-assembly. (b,d,f) SEM images of the PDI nanofibers. (c,e,g) TEM images of PDI nanofibers. (h) A large-area SEM image showing the growth of long nanobelts from the central seeding aggregates. (i) A zoom-in image showing the morphology of the nanobelts. (j) SEM image of nanorods assembled from a PDI. (k) Fluorescence microscopy image of the PDI nanorods. (l and m) TEM images of nanocoils assembled from a PDI. (n and o) TEM image of the nanoribbons assembled from a PDI. Reproduced (adapted) with permission from refs 54, 56, 62, and 64. Copyright 2014 Elsevier, 2007 American Chemical Society, and 2014 Royal Society of Chemistry, respectively.

case, the solvent polarity and the amount of H_2O (as a poor solvent) should be kept at a low level. The resulting morphology can be further adjusted via the type or length of the hydrophobic alkyl and hydrophilic oligoethyoxyl side chains.[62,63] In contrast to symmetric PDIs, these asymmetric PDIs molecules, especially those bearing hydrophilic electron donor moieties, provide more options for fabricating functionalized 1D nanofibers in aqueous media and thus pave the way for the development of future photoelectronic nanomaterials employing feasible, cost-effective, and environmentally friendly fabrication processes.[53,62]

Nevertheless, well-defined 1D nanobelts have been observed as the most favorable morphologies with lengths ranging from hundreds of nanometers to tens of micrometers (sometimes several millimeters) and aspect ratios (length over width) in magnitudes of ten to several hundreds.[14,51−61] Formation of these structures is primarily driven by the $\pi-\pi$ stacking interactions between PDI backbones, in cooperation with the hydrophobic interactions arising from solvent effects. In an alternative approach to self-assembly, a rapid dispersion method (Figure 4) has also been investigated, that is, rapidly injecting the PDI monomer dissolved in a minimum amount of good solvent into an excess volume of poor solvent followed by immediate mixing and/or long-time aging.[20,64] In some cases, shorter and more disordered 1D nanofibers were obtained than via the above-mentioned slow diffusion process.[14,52] However, through dedicated molecular design, there have been some surprising results. For example, a very stable coiled nanostructure was obtained from the rapid dispersion method as compared to the nanoribbons (Figure 6l−o) obtained from the $CHCl_3/C_2H_5OH$ interfacial self-assembly of asymmetric PDI molecule bearing methylene linked dimethoxyphenyl polar group and dodecyl side-chain.[64]

3.1.2. Solvent-Vapor Diffusion Self-Assembly. Largely due to the extreme steric hindrance, PIs containing only bulky branched alkyl side-chains have proven difficult to self-assemble into ordered 1D nanostructures via the above solution-phase self-assembly methods.[14] In 2008, Zang et al. developed an unconventional solvent-exchange crystallization process (Figure 4) controlled by slow diffusion within a sealed chamber between a $CHCl_3$ solution of 1-nonyldecyl-modified PMAMI and CH_3OH vapor. Because of the distorted molecular stacking, the resulting well-defined 1D nanofibers remain strongly fluorescent in the solid state. In cooperation with the

DOI: 10.1021/acs.chemrev.5b00312
Chem. Rev. 2015, 115, 11967−11998

exposed tetracarboxylic dianhydride moieties ensuring effective, selective binding with amines, these fibers were found to be useful in fluorescence sensors.[65] Although slow, the fact that the nanofibers generated from this process can be manipulated without significant structural disruption and fluorescence quenching makes them promising for practical applications in emitters and sensors.

3.1.3. In Situ Self-Assembly on Substrate Surface. 1D nanofibers have been prepared on appropriate solid surfaces via a self-assembly method, which is controlled by adjusting factors such as molecular structure, solvent nature (polarity, volatility, solubility, concentration), surface properties (polarity, atomic orientation, and flatness), and postassembly treatment (solvent or thermal annealing).[14] These methods can be classified as evaporation-triggered solution-phase self-assembly,[63,66−71] solvent-vapor-annealing facilitated self-assembly (Figure 4),[31,72−74] and self-assembly via drying under solvent atmosphere (Figure 4).[75,76]

The most basic case involves surface-supported aggregation by evaporation of solvent from a solution of PDIs: the aggregation behavior is tailored by $\pi-\pi$ stacking, electrostatic, H-bonding and solvation interactions, as well as surface polarity and evaporation temperature.[63,66−71] However, evaporation-triggered solution self-assembly often generates 1D nanostructures of PDIs exhibiting a low degree of uniformity, and it is beyond our focus in this Review. In the past decade, there has been significant work in this area along with various molecular design strategies.[63,66−71] Nevertheless, an appropriate balance between π-stacking and one or more other assembling parameters plays a critical role in producing ordered 1D nanostructures of well-defined morphologies. Zang et al. introduced a unique vapor-annealing treatment method, which enables the transfer of *N*,*N*′-di(propoxyethyl)-PDI and *N*,*N*′-di(dodecyl)-PDI (PDI-C12) assemblies from a thermodynamically unstable state formed from the fast evaporation of solvent during the spin-coating or drop-casting process on a substrate to a thermodynamically stable extended 1D stacking conformation.[35,72,73] A fine balance between molecular stacking and solubility, as well as the nature of the substrate surfaces, should be considered. Particularly, the solvent vapor (usually, good solvent) should be consistent with the surface polarity of the target substrate; for example, hydrophobic vapor of $CHCl_3$ solvent pairs well with hydrophilic substrates such as silicon oxide, glass, mica, and gold, whereas hydrophilic vapor of tetrahydrofuran (THF) solvent pairs well with hydrophobic substrates such as highly oriented pyrolytic graphite.[72,74]

Upon exposure to an optimal amount of solvent vapor, millimeter-long 1D nanofibers with remarkably high aspect ratios, exceeding 10^3, can be constructed from *N*,*N*′-di(1-ethylpropyl)-PDI molecules on polar substrates.[74] Such surface-assisted in situ fabrication approaches are quite favorable for optical or microscopy characterization directly after the formation of nanofibers, and for fabricating film-based devices.[35,73] Additionally, this method provides an opportunity for the fabrication of single PDI nanobelts that exhibit enhanced linearly polarized emission and charge carrier mobility along the 1D molecular stacking direction and meet the requirements for various orientation-sensitive optoelectronic applications and nanoelectronics.[35,73,75] An alternative method by which well-separated PDI nanofibers have been prepared is via another in situ solvent-vapor diffusion technique, the "drying under solvent atmosphere" method.[75,76]

As seen in Figure 7, elongated 1D nanowires with lengths of several millimeters and aspect ratios of up to 10^4 have been fabricated directly by slowly drying $CHCl_3$ solutions of bulky-substituent-modified *N*,*N*′-di(9,9′-spirobifluorene-2yl)-PDI directly on desired substrates while under $CHCl_3$ atmosphere.[75,76] This method allows the direction of nanowire growth to be regulated by using prestructured lines on plastic substrates or pre-etched inorganic/metal substrates. It is an ideal method for preparing large-area oriented nanofibril coatings, which may find broad applications, for example, OFETs and OLEDs.[35,73,75]

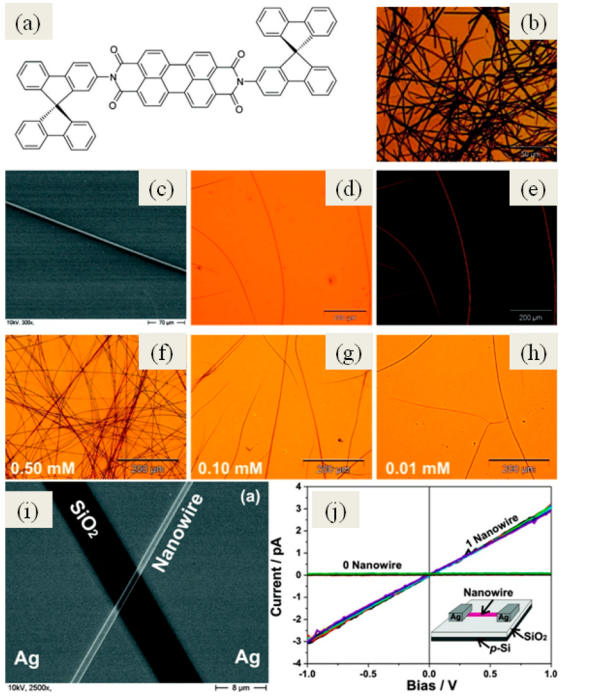

Figure 7. (a) Chemical structure of *N*,*N*′-di(9,9′-spirobifluorene-2yl)-PDI (Spiro-PDI). (b) Optical micrograph of Spiro-PDI nanowires obtained from the bisolvent phase-transfer method (0.25 mM $CHCl_3$ solution/CH_3OH). (c−e) Scanning electron microscopy, optical microscopy, and fluorescence microscopy images of wires obtained from drying under solvent atmosphere technique (0.01 mM $CHCl_3$ solution). (f−h) Optical micrographs of wires obtained from drying under $CHCl_3$ atmosphere with different concentration of Spiro-PDI $CHCl_3$ solution. (i) SEM image of a typical single Spiro-PDI nanowire device contacted with silver electrodes, and (j) current−voltage (*I*−*V*) characteristics of a top-contacted single Spiro-PDI nanowire acquired in the dark and under ambient atmosphere. Inset: Schematic diagram of the electrical measurement of single Spiro-PDI nanowire. Reprinted (adapted) with permission from ref 75. Copyright 2011 American Chemical Society.

In brief, these bulk-phase solvent-transfer methods offer promising routes to prepare large-scale robust 1D nanofibers of PDIs that display excellent structural qualities with high levels of chemical purity, and also benefit from the simplicity of the fabrication method.[14,77] The processes allow for easier manipulation and transfer of PDI nanofibers from solution to polar or nonpolar (e.g., carbon) solid surfaces under ambient conditions than substrate-supported in situ self-assembly and vacuum deposition processes.[6,14,21,73] Furthermore, the solvent-vapor annealing approach can be applied as an effective postassembly treatment to eliminate the defects and grain boundaries formed during solution-phase self-assembly processes.[78] As a result, these versatile strategies have been applied to the fabrication of regular 1D nanostructures of other π-

DOI: 10.1021/acs.chemrev.5b00312
Chem. Rev. 2015, 115, 11967−11998

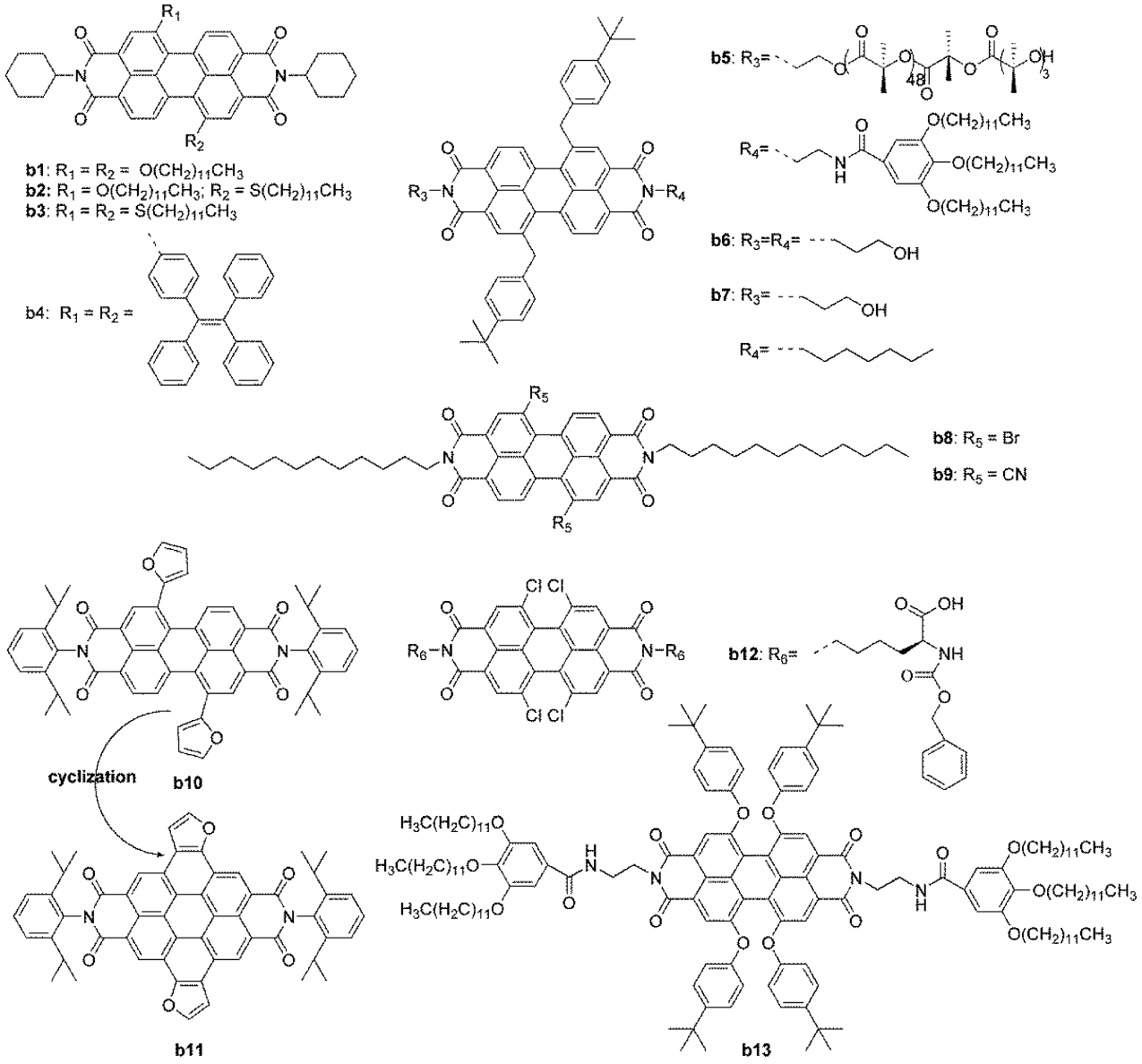

Figure 8. Chemical structures of bay-substituted PDIs molecules (b1−b13), which have been applied for 1D self-assembly.

conjugated organic systems,[79−81] and inorganic semiconductors.[82] However, such solution-processable self-assembly normally leads to entangled mesh-like networks of nanofibers when deposited on substrates.[14,75] While this tangled morphology may be beneficial to applications in gas sensors, it may weaken the device performance because of a significant number of charge traps.[77] Efforts to prepare ordered arrays composed of single crystalline nanofiber of PDIs are underway, and a breakthrough in this field may be imminent.[75−77] Initial work may center on template- or scaffold (e.g., oligomer/polymer)-assisted directional self-assembly. There remains much room for broadening ideas of phase-transfer self-assembly of PIs when other issues such as chirality,[83] molecular configuration,[36,37,84−89] pH,[40,90−95] and nanoheterojunction[96−98] are introduced into this field, and these will be discussed in the following sections.

3.2. Self-Assembly of Bay-Substituted PDIs

In contrast to structural modification at the imide (*N*,*N*′) positions, there is little research regarding the self-assembly of bay-substituted PDIs into 1D nanostructures. The self-assembly of bay-substituted PDIs is challenging because of the twist in the planarity of the perylene backbone due to steric interactions of the bay substituents.[23] However, unlike imide-substitution (even with bulky or branched groups), functionalization of PDIs at bay positions often significantly influences their optical and electronic properties, as well as solubility.[23] Thus, these molecules have garnered increased attention and endeavor to meet the challenge of self-assembly of these PDI derivatives (Figure 8) into well-defined 1D nanostructures. Generally, the fundamental strategies outlined above for solution-processable self-assembly are still followed; however, bay-substituted PDIs are more sensitive to solvent effects (Figures 9 and 10).[36,37,84] The twisting of the PDI cores should be precisely tuned through careful design at the molecular level to achieve the desired morphology of 1D nanostructures.

Through a rapid dispersion process by injecting the $CHCl_3$ solutions of PDIs (b1, b2, b3; Figure 8) bearing symmetric or asymmetric bay-substitution of dodycyloxy and thiododecyl groups into larger volumes of CH_3OH, b1 self-assembled into

DOI: 10.1021/acs.chemrev.5b00312
Chem. Rev. 2015, 115, 11967−11998

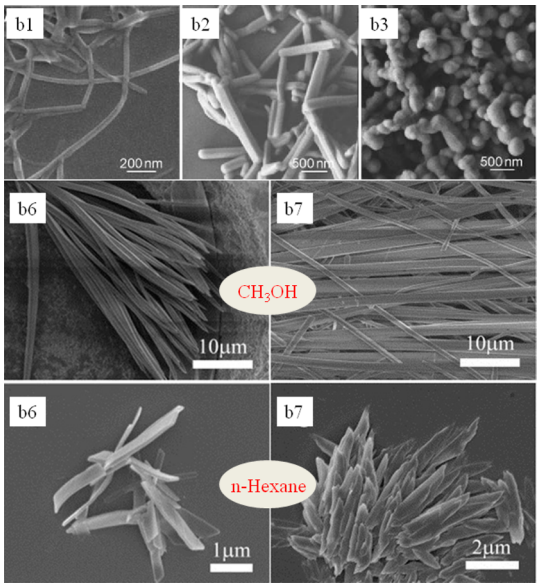

Figure 9. Effect of substituents at the bay-area and solvent environment on the 1D morphologies of self-assembled PDIs nanostructures. Chemical structures of b1, b2, b3, b6, and b7 are given in Figure 8. Adapted with permission from refs 84 and 39. Copyright 2007 Wiley-VCH and 2012 Elsevier, respectively.

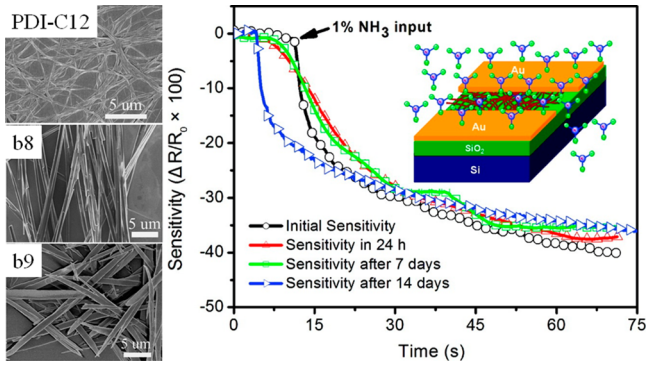

Figure 10. Influence of bay-substitution on the morphologies of PDI nanofibers, and the enhanced sensing performance of 1,7-dicyano-PDI (b9) for NH_3 vapor. Adapted with permission from ref 36. Copyright 2011 American Chemical Society.

1D nanowires several micrometers long, whereas b2 and b3 self-assembled into 1D nanorods and 0D spherical nanoparticles, respectively (Figure 9). Such dramatic morphology differences result from the strength of the $\pi-\pi$ interactions between the PDI units in the order b1 > b2 > b3, in line with the coplanar feature of the methoxy groups with perylene core and larger degree of distortion of the perylene system induced by thiododecyl groups.[84] On the contrary, if the bay-substituents are unaltered, the structures and morphologies are highly dependent on the substituents at the imide positions.[37,39] As one example, nanostructures prepared from 1,7-di(*p*-*t*-butylphenoxy)-PDIs substituted with long helical semicrystalline oligo(L-lactic acid)$_n$ (O-LLA) chains at one imide nitrogen (b5, Figure 8) via injecting CH_2Cl_2 solutions of these PDIs into excessive CH_3OH were observed to be short wide 1D nanoribbons with left-handed helicity due to the liquid-crystalline nature of the O-LLA chain. Comparatively, shorter O-LLA segments induced the formation of long narrow nanofibers.[37] In addition, well-defined 1D nanobelts (Figure 9) with an aspect ratio of 500 were obtained from amphiphilic b6 (Figure 8) bearing two hydroxyethyl groups at imide positions from $CHCl_3/CH_3OH$ systems.[39] The asymmetric analogue b7 (Figure 8) bearing both hydroxyethyl and hexyl side-chains produced 1D nanobelts (Figure 9) exhibiting a smaller aspect ratio (150), but having an electrical conductivity (3.3×10^{-3} S cm^{-1}) about 1 magnitude higher than that of b6 due to fewer structural defects and more efficient π-stacking and side-chain interactions.[39]

However, when bay substituents are cyclized (e.g., from b10 to b11; Figure 8), the steric hindrance of these core-enlarged molecules is weakened and promotes their tendency to construct uniform 1D nanofibers via $\pi-\pi$ stacking of coplanar aromatic cores along the longitudinal axis.[86] These core-extended PDI molecules and their self-assembled nanostructures exhibit extensive optical absorption, covering the visible and near-infrared region, due to their expanded π-conjugation.[20,22] Additionally, highly conductive (1 order of magnitude greater than nanobelts fabricated from b6[39]) 1D nanobelts of CBZ-L-lysine-substituted tetrachloride b12 (Figure 8) were obtained via phase-transfer self-assembly in acetone/H_2O mixtures (Figure 11).[49] Here, the H-bonding interactions between the carboxyl groups of the lysine side-chains play a critical role in optimizing molecular packing, and such an effect is dependent on solvent polarity, for which a strong polarity usually enhances nucleation, thus leading to formation of less ordered molecular aggregates. The well-ordered $\pi-\pi$ stacking

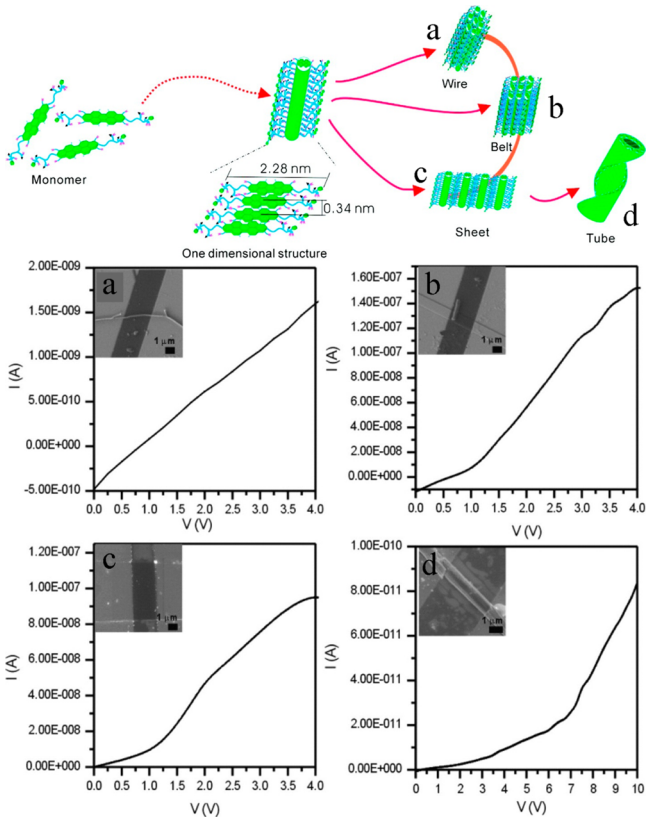

Figure 11. Concentration-dependent self-assembly of PDI (b12, Figure 8) molecules from 45% H_2O/acetone mixtures when tuning the concentration of b12 in acetone from (a) 100 μM, (b) 300 μM, (c) 800 μM to (d) 1 mM, and the effect of morphologies (a, nanowire; b, nanobelt; c, nanosheet; d, nanotube) on the *I*–*V* curves. Adapted with permission from ref 49. Copyright 2011 American Chemical Society.

DOI: 10.1021/acs.chemrev.5b00312
Chem. Rev. 2015, 115, 11967–11998

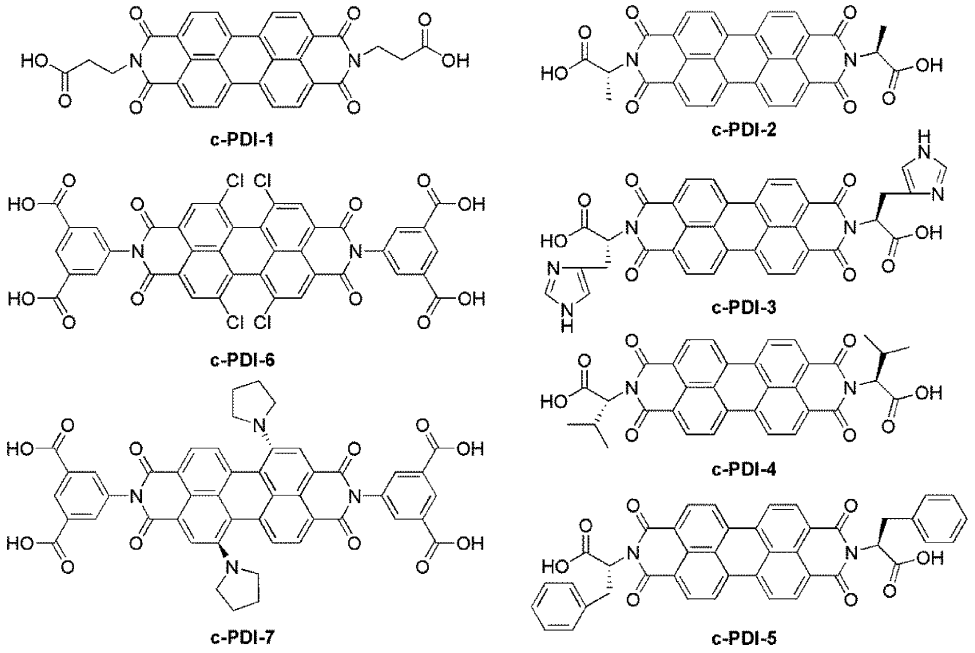

Figure 12. Chemical structures of reported PDI molecules used for pH-triggered hydrogelation in aqueous solution.

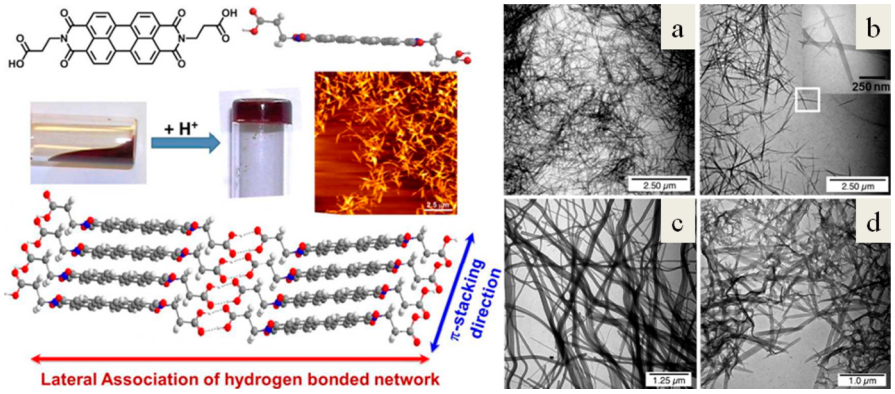

Figure 13. Left: (top) Molecular structure and configuration of building block molecule c-PDI-1; (center) addition of acid to the basic aqueous solution of PA-PDI leads to formation of hydrogel composed of uniform nanofibers as imaged by AFM; (bottom) schematic diagram showing the concerted intermolecular $\pi-\pi$ stacking and H-bonding interactions that form the nanofibril structure. Right: Large-area TEM image of densely packed c-PDI-1 nanofiber network, which were synthesized by the gelation method (a,b) and 1D nanofibers synthesized by the phase-transfer method through injecting CH_3OH (c) and THF (d) into aqueous TEA solutions. Reproduced with permission from ref 90. Copyright 2013 Royal Society of Chemistry.

structures and the existence of carboxyl acid and hydroxyl moieties in the side-chains provide the possibility of self-doping and are believed to play a crucial role in the excellent conductive properties of 1D nanofibers of these amphiphilic PDIs (Figure 11).[49] For rigid molecules bearing bulky and twisted moieties both at imide and at bay positions, evaporation-triggered in situ self-assembly on substrates seems to be a preferred method. For example, the b4 molecule modified with a bulky p-type tetraphenylethenyl group (Figure 8) has been successfully self-assembled into well-organized 1D nanofibers by slowly evaporating the solvents from H_2O/THF, CH_3OH/CH_2Cl_2, hexane/CH_2Cl_2, or CH_3OH/dioxane mixtures. Such 1D self-assembly benefits from the moderate molecular planarity of b4 as shown in Figure 3, which still enables effective $\pi-\pi$ stacking, leading to 1D growth of molecular aggregation. In a similar case, the solvent-dependent organogelation process for orderly 1D self-assembly of core-planar b13 (Figure 8) bearing bulk electron-rich trialkoxyphenyl moieties into 1D nanofibers has been observed.[87,88] Unconventionally, 1D morphologies of PDIs bearing bay-substituted pyridyloxy groups can be finely controlled by the cooperation of solvophobic and H-bonding interactions with additional forces such as charge−charge interactions and charge−dipole interactions. The latter can be attributed to the fine-tuning of the protonation of pyridyloxy groups by adjusting the surrounding acidic aqueous environment.[38,89]

Despite the difficulty and challenge of self-assembly, bay-functionalization of PDIs provides much leeway to modify the optoelectronic performance of their 1D nanofibers as compared to that of imide-substitution alone. Because of the unavoidable deviations from planarity of the perylene cores, 1D nanofibers of bay-modified PDIs often retain the intense fluorescence emission performance of monomeric building blocks.[30,37,85] For example, well-defined 1D nanobelts of b8 exhibit a fluorescence quantum yield as high as 2.83%, which is 140 times that of PDI-C12.[85] By attaching electron-donating or -accepting moieties at

DOI: 10.1021/acs.chemrev.5b00312
Chem. Rev. 2015, 115, 11967−11998

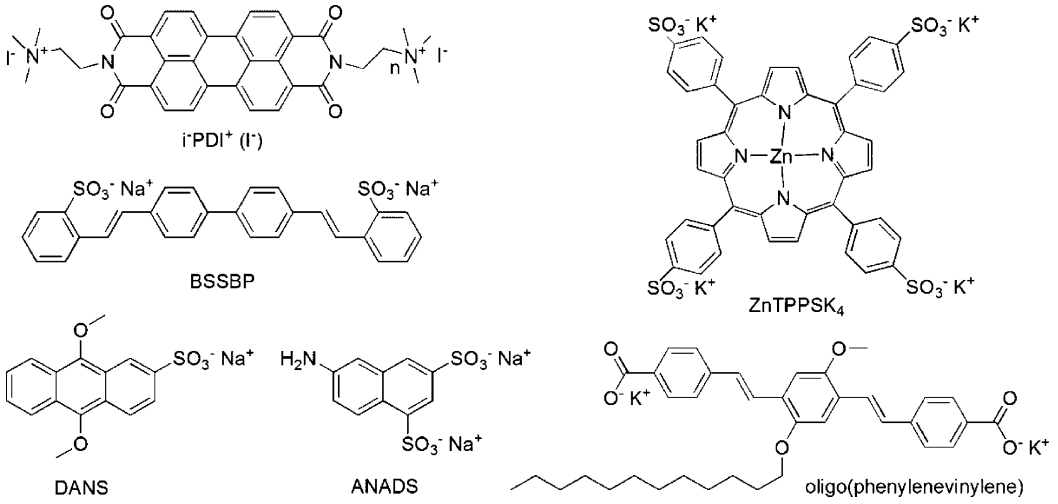

Figure 14. Chemical structures of ionic PDI molecules capable of 1D self-assembly and reported organic counterions used as electron dopants in π-conjugated backbones.

the bay positions of PDIs, one can significantly tune the electronic properties of the molecules and thus the molecular aggregate through intramolecular and intermolecular charge-transfer interactions.[30] Particularly, the 1,7-dibromo- and 1,6,7,12-tetrachloro-bay-substituted PDIs are among the mostly used intermediates for constructing more complex building blocks by linking the halogen sites to special functional groups, such as electron-donating groups, oligomers, or polymers. These bay-substituted PDI supramolecules provide more structural flexibility for optimizing the self-assembly process, as well as the electronic and optoelectronic properties of the molecular assembly, such as exciton diffusion, charge transfer, and recombination, which are tightly correlated to the application in OLEDs, OCSs, and gas sensors.

3.3. pH-Triggered Self-Assembly in Aqueous Solution

The use of water rather than organic solvents reduces waste and is considered to be a green alternative for industrial applications. Through tailoring the hydrophilic substituents, the amphiphilic PDIs can self-assemble in aqueous solutions, leading to the formation of well-defined nanofibers. Particularly for the hydrophilic substituents that are pH sensitive (i.e., subject to protonation and deprotonation), the self-assembly and the resulted morphology of nanofibers can be tuned by changing the pH, which controlled the hydrogelation processing as was recently observed for the PDIs substituted with carboxylic acid groups (Figure 12).[40,90]

In 2013, Zang and co-workers reported a pH-triggered hydrogelation route enabling the fabrication of c-PDI-1 (Figure 12) molecules into well-defined 1D nanobelts. Self-assembly was triggered through lowering the pH of aqueous triethylamine (TEA) solutions (pH $\approx$ 9.0) of c-PDI-1 by the addition of hydrochloric acid (Figure 13). Comparatively, as seen in Figure 13, the size of nanobelts obtained with this method is shorter and narrower than those obtained from a solvent phase-transfer method, due to Ostwald ripening during the phase-transfer processing.[90] According to the variation of amino acid functional groups, uniform 1D nanofibers of amino-acid-functionalized PDIs (c-PDI-2, c-PDI-3, and c-PDI-4, but not c-PDI-5; Figure 12) have been fabricated both from viscous aqueous solutions (pH $\approx$ 10) and xerogels through moderately adjusting the solution pH by glucono-δ-lactone (slowly hydrolyzing to gluconic acid).[91] Regardless of the methods and the carboxylic acid side chains used, such 1D self-assembly is dominated by synergistic $\pi-\pi$ stacking, H-bonding, and hydrophobic/hydrophilic interactions.[90,91]

More recently, a similar self-assembly strategy was applied to a series of tera-carboxylic acid-substituted PDI derivatives, c-PDI-6 and c-PDI-7 (Figure 12). These PDI molecules are water-soluble in part due to the twisted perylene cores: irregular 1D nanofibers can be successfully fabricated from coassembly of c-PDI-6 and c-PDI-7 using a mole ratio of 1:4 upon lowering the pH of aqueous solution to the optimum level. Nevertheless, the formed nanofibers show an efficient Förster-type resonant excitation energy transfer from the excited state of c-PDI-7 (energy donor) to the ground state of c-PDI-6 (energy collector), resulting in amplification of emission both in aqueous solution and in the solid films with a remarkable light-harvesting efficiency (as high as 98.1%).[40] Similar endeavors to improve light-harvesting or photoconductive properties of self-assembled PDIs with various morphologies and uniformity have also been made for another series of amphiphilic PDIs via controlled aggregation processes such as pH adjusted double-solvent self-assembly or gelation in water, organic solvents, or mixed systems.[92−94]

3.4. Aqueous Self-Assembly of Ionic PDIs

In addition to carboxyl group functionalized PDIs, other attempts have also been carried out to control 1D self-assembly of ionic PDIs from aqueous solutions.[95−98] Wei et al. have fabricated 1D nanotubes (with lengths of several micrometers and outer diameters of approximately 100−300 nm) on substrates from aqueous solution of *N,N′*-bis(2-(trimethyl)-ammonium iodide)ethylene)-PDI (i-PDI$^+$ (I$^-$); Figure 14) after evaporating water slowly at room temperature.[95] In contrast, 1D rectangular nanorods with an average width of approximately 200−300 nm and lengths up to tens of micrometers are generated from evaporation of CH_3OH solution of i-PDI$^+$ (I$^-$).[95] Beyond the morphology differences arising from the crystallizing−etching or nucleation−growth mechanism, these 1D nanofibers are capable of sensing reducing agent vapors, such as hydrazine or phenylhydrazine, indicated by 2−3 orders of magnitude enhancement of electrical conductivity.[95]

Fukuzumi's group later constructed a series of D−A complexes in water composed of electron-deficient 1D nanofibers of i-PDI$^+$ (I$^-$) as the host and variable guest

DOI: 10.1021/acs.chemrev.5b00312
Chem. Rev. 2015, 115, 11967−11998

electron donors, including meso-tetrakis(4-sulfonatophenyl)-porphyrin zinc tetrapotassium ($ZnTPPSK_4$), disodium 4,4′-bis(2-sulfonatostyryl)-biphenyl (BSSBP), sodium 9,10-dimethoxyanthracene-2-sulfonate (DANS), and disodium 6-amino-1,3-naphthalenedisulfonate (ANADS), shown in Figure 14.[96,97] These complexes are built through the strong favorable $\pi-\pi$ stacking and ionic interactions strengthened by water. Photoinduced electron injection from inserted porphyrins and subsequent electron transport, due to the intermolecular electron delocalization along the long axis of i-PDI nanostacks, and the high polarity of aqueous medium, results in a fast charge separation (1.4 ps), which is 3000-fold higher than the rate of charge recombination for $ZnTPPSK_4^-$/i-PDI^+ (Figure 15).[96] On the contrary, a rapid charge separation (0.70 ps) and

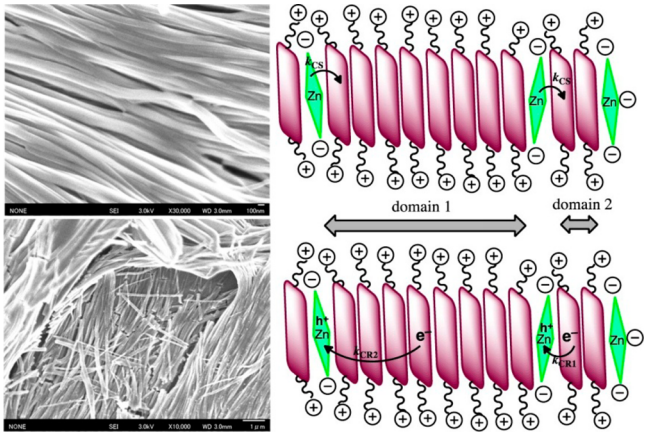

Figure 15. SEM images of i-PDI^+ (I^-) nanofibers obtained from aqueous solutions, and representative illustration of the charge separation and charge recombination between the stacks of i-PDI^+ (I^-) and randomly distributed $ZnTPPSK_4$. Adapted with permission from ref 96. Copyright 2012 American Chemical Society.

relatively slow charge recombination (485 ps) are detected for $BSSBP^-$/i-PDI due to a larger π-extent, at least 10^5 times higher than the lifetimes of charge separated states in $DANS^-$/i-PDI^+ and $ANADS^-$/i-PDI^+.[97]

George et al. presented a cofacial assembly technique for the mixed self-assembly of a wedge-shaped noncovalent amphiphilic D/A molecule pair, oligo(phenylenevinylene)/i-PDI^+ (Figure 14), in aqueous solution.[98] The formed 1D nanotubes exhibit a length of more than 15 millimeters with a diameter of 35−50 nm, and a promising conductivity up to 0.02 S cm^{-1} without external doping. This high conductive character is quite remarkable and desirable for electronic applications. Many PDIs and other organic semiconductors lack sufficient conductivity without appropriate doping.[98−100] Thus, 1D nanostructures of i-PDI^+ embedded with electron dopants possessing π-conjugated backbones due to strong $\pi-\pi$ stacking, in concert with interactions such as charge−charge, electrostatic, and hydrophilic actions, could work as promising candidates for organic photoelectronics, especially those requiring aqueous processing.

3.5. Chemical Reaction-Mediated Self-Assembly of Unsubstituted PIs

Unlike solution-phase self-assembly of soluble PIs, assembly of insoluble nonsubstituted PIs (PDINH) remained a great challenge for a long time. Through a unique chemical-reaction-mediated self-assembly procedure, Fu and co-workers brought the difficult 1D nanostructure of PDINH into reality in 2011.[101] They elaborately self-assembled uniform 1D nanobelts of PDINH with lengths of tens of micrometers via an oxidation−reduction process using soluble PDINH dianions ($PDINH^{2-}$) as medial precursors (Figure 16a). A similar work was done by Balakrishnan et al., who successfully achieved highly crystalline 1D nanobelts of insoluble PTCDA, with lengths up to 2−3 mm via in situ chemical conversion reaction of a soluble precursor, perylene tetracarboxylic acid (PTCA), as seen in Figure 16b.[102] While the exact mechanisms are still unclear, it is now believed that synergistic $\pi-\pi$ stacking and other noncovalent interactions in conjunction with nucleation and crystallization govern these self-assembly processes.[101,102] Nevertheless, such desirable chemical-reaction-mediated self-assembly surely provides new insight into developing 1D nanofibers from functionalized insoluble organic semiconductor molecules, for example, PMAMI.

3.6. Self-Assembly of Oligomers

Electronic D−A type PDI-based copolymers/oligomers (Figure 2) have been shown to play an important role in optoelectronic applications.[22,103] Although quite challenging, solution-processable self-assembly of these PDIs has made it possible to take advantage of the resulting 1D charge-transfer nanostructure. In recent years, Yagai and Ma's groups investigated the effect of the bridge-linker as well as side-chain influence for the self-assembly of a series of oligomethylene-linked PDI dimers, O-1 (n = 5−10), and amino acid linked electronic D−A dyads, O-2 (Figure 17), respectively.[104,105] Specifically, self-assemblies of O-1 (n = 7) show 1D columnar nanofiber morphology with a high-aspect ratio arising from the strong intermolecular $\pi-\pi$ stacking interactions, giving rise to a 3-fold increase of charge-carrier mobility.[104] Well-defined 1D nanofibers formed from amphiphilic D−A dyads with long-linker (O-2, n = 5) hold more promise than O-1 for optoelectronic devices because of their optimal intramolecular charge transport and better D−A phase separation.[105]

3.7. Interfacial Engineering of Nanofibril Heterojunctions

Unlike most reports thus far on the fabrication of photoconductive 1D nanostructure from self-assembly of covalently linked D−A molecules, Zang's group has successfully explored a remarkably simple method to construct photoconductive organic nanofibril heterojunctions via interfacial engineering (Figure 18). This strategy relies on the hydrophobic interaction between the long alkyl side-chains of self-assembled nanofibers of PDIs (A) and optimized D molecules (electron donors with HOMO levels higher than that of PDIs), enabling efficient inhibition of charge recombination via spatial separation of the D/A complex, in conjunction with intermolecular transfer of charge carriers along the $\pi-\pi$ stacking of PDIs. Also, the nanofibril heterojunctions possess wide D/A interfaces for increased charge separation and long-range charge-transport pathways. As a result, these hybrid materials exhibit high, air-stable, and reversible photoconductivity, and rapid photoresponse with photocurrent on/off ratios of up to 10^4.[78,106] Such well-ordered D/A heterojunction nanofibril composites fabricated through controllable molecular design and engineering that avoid complicated molecular synthesis are especially desirable for large-area fabrication of high-performance organic optoelectronic devices.

DOI: 10.1021/acs.chemrev.5b00312
Chem. Rev. 2015, 115, 11967−11998

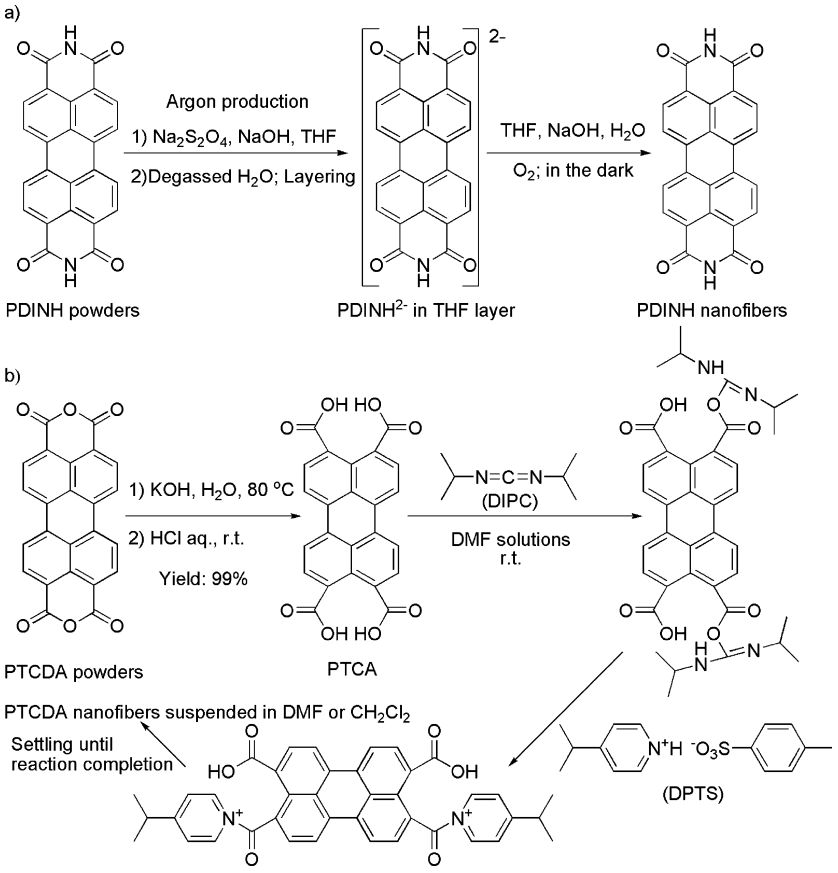

Figure 16. Schematic depiction of the general chemical reactions during the 1D self-assembly processes of (a) PDINH and (b) PTCDA molecules into 1D nanofibers.

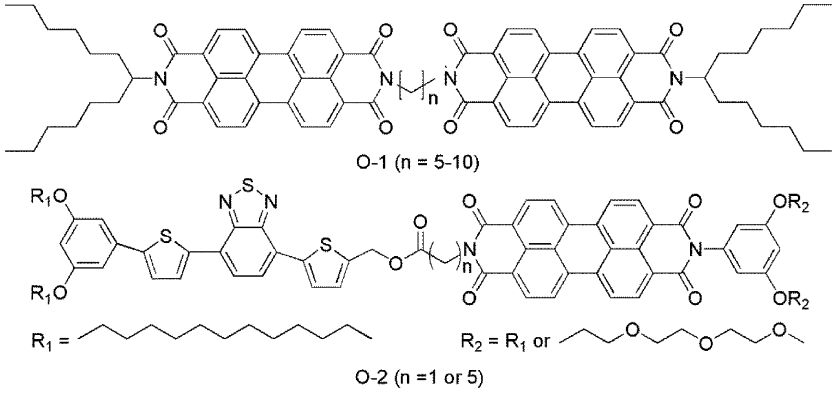

Figure 17. Chemical structures of oligomethylene linked PDI dimmers (O-1) and amino acid linked D−A PDI dyads (O-2).

3.8. Self-Assembly and Chiral/Helical Nanostructures

In comparison with conventional 1D morphologies, supramolecular nanostructures exhibiting chirality or helicity are more appealing as surrogates for natural biological systems. Inspired by this, many efforts have been carried out to create 1D helices via artificial self-assembly of π-conjugated molecules by utilizing cooperative noncovalent forces.[107,108] Among them, self-assembly of chiral PDI molecules or chiral self-assembly of achiral molecules into 1D helical nanostructures through intelligent molecular design and precise control of noncovalent forces represent one of the most attractive and promising fields.[83,109−112] Some exciting results have been obtained on thermodynamic-controlled evaporation of the binary (good/poor) solvent mixtures of amphiphilic PDIs (Figure 19), resulting in 1D helical nanostructures consistent with the morphologies in solution phase as listed in Table 1.[83,109−112] These processes were conducted by controlling environmental parameters such as the nature of the solvents (e.g., polarity), the volume ratio of the good/poor solvents, and temperature.

The chirality of side groups and the solvent polarity provide the original driving force for chiral assemblies of PDIs. The arrangement of helical morphologies (e.g., handedness, shape) is further modulated by $\pi-\pi$ stacking, H-bonding, and hydrophobic interaction in the binary solutions.[83,109,110] As an example, amphiphilic PDIs (H1−H4, Figure 19) bearing chiral galactosyl-substituents have been frequently employed to construct 1D nanofibers with helicity.[83,109−112] Through a bisolvent phase-transfer strategy by injecting a poor solvent into

DOI: 10.1021/acs.chemrev.5b00312
Chem. Rev. 2015, 115, 11967−11998

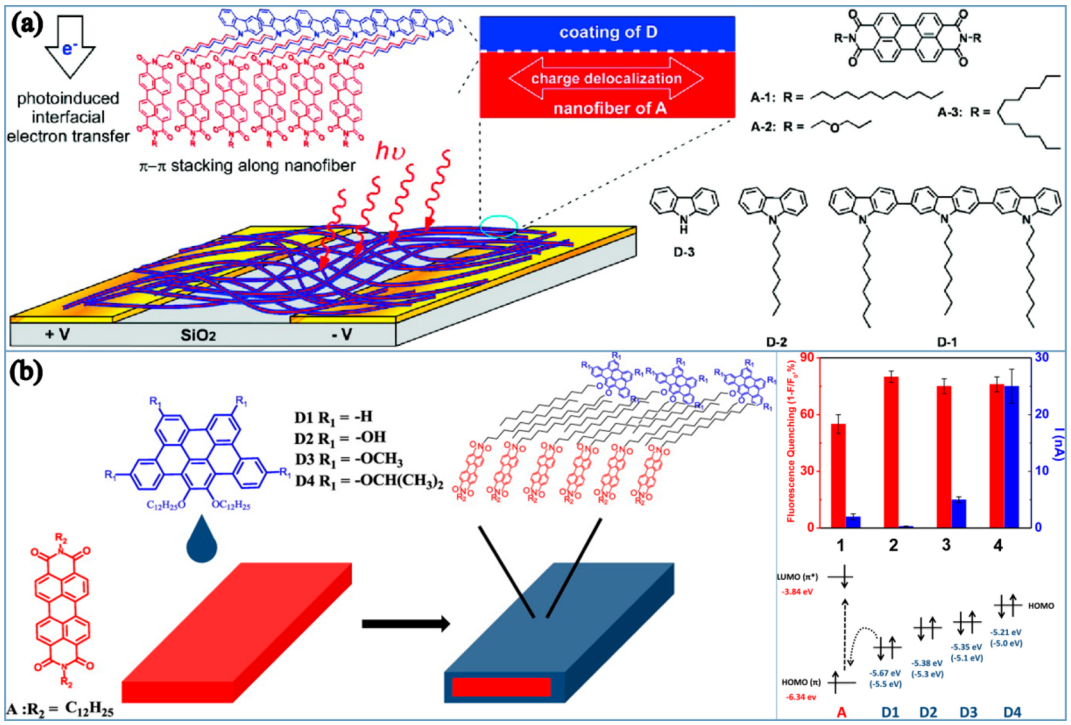

Figure 18. (a) Schematic illustration of nanofibril heterojunction composed of electron donor (D-1–D-3) coated PDI nanofibers that function as electron acceptors (A-1–A-3). The optimized choice is D-2/A-1. Adapted with permission from ref 106. Copyright 2011 American Chemical Society. (b) Left: Schematic illustration of core–shell structured nanofibril heterojunction composed of D1–D4 coating and PDI-C12 nanofibers. Right: Comparison of fluorescence quenching (red) and photocurrent generation (blue) between the PDI-C12 nanofibers coated with the four donor molecules, and the electronic energy levels of PDI-C12 and D1–D4. Adapted with permission from ref 78. Copyright 2013 American Chemical Society.

a solution of PDIs in a good solvent, both left-handed and right-handed superhelical as well as achiral planar nanofibers can be generated from asymmetric or symmetric molecules by adjusting the volume ratios of mixed solutions.[83,109–112] Thermodynamically controlled self-assembly and kinetic nucleation mechanisms are believed to control these processes. More recently, 1,6,7,12-tetrachloro bay-substitution, which can weaken the π–π stacking of H2 molecules, has been used to tune the helical self-assembly behavior of the sugar-substituted H4 (Figure 20).[111,112]

Another interesting work is chiral self-assembly of bolaamphiphile PDIs (H5–H8; Figure 19) bearing two hydrophilic peptide side groups. Among the different peptide substitutions, chiral nanofibers could only be formed from H5 through self-assembly in an aqueous buffer or organo-gelation method.[94] The intermolecular arrangement is determined by a balance between the π–π stacking interaction and peptide-mediated H-bonding and electrostatic interactions.[91] The later two are in turn dependent on the pH of aqueous solutions or the polarity (hydrophobicity) of organic solvents for the organo-gelation process.

Temperature, which affects the intermolecular interaction of glucose molecules, has been identified as another factor governing the chiral self-assembly of PDIs substituted by glucose moieties (Figure 20).[112] The chiral morphology of the assembled nanostructures has been found to be not only dependent on the molecular structure and solvent property, but also dependent on the thermal treatment of heating–cooling as shown in Figure 20.[113] These observations suggest that for given building block molecules, the self-assembly may be tuned significantly by external stimuli such as heating or mechanical forces, leading to the formation of nanostructures in different morphologies.[113]

Chiral nanostructure PDIs can also be formed through substrate (or scaffold)-assisted self-assembly; that is, attaching PDIs to the side groups of rigid, helical polyisocyanopeptides leads to π–π stacking along the helical backbone of polymer, forming a nanofiber structure consisting of a single stack of PDIs.[114] The rigid scaffold of polymer allows for good control over the configuration of molecular stacks, providing a novel way to design and fabricate the 1D nanomaterials based on π–π stacking, for which the electronic property (e.g., charge transport) can be tuned and optimized by changing the polymer backbone structure. The individual nanofibers comprising a single stack of PDIs were also assembled from the molecules substituted at the imide positions by two short peptides connected to long alkyl chains, for example, oligo(L-alanine)-poly(isobutylene), as shown in Figure 19.[50] The supramolecular helicity thus formed along the long axis of nanofiber helps suppress lateral aggregation, allowing for linear alignment of individual nanofibers to produce a tight bundle with cross-section size of microns. This two-step fabrication method offers an alternative way to parallel align nanofibers so as to enhance the charge transport along the π–π stacking.

Regardless of the fabricating processes, in most cases, the chirality or helicity of the resultant nanostructures originates from the existence of chiral substituents of the PDI cores.[109] However, by virtue of tunable molecular structures, together with noncovalent interactions arising from external environments, achiral PDI molecules can also self-assemble into a variety of well-defined helical 1D nanofibers, including left-handed, right-handed, and double helix morphologies.[113,115,116]

DOI: 10.1021/acs.chemrev.5b00312
Chem. Rev. 2015, 115, 11967–11998

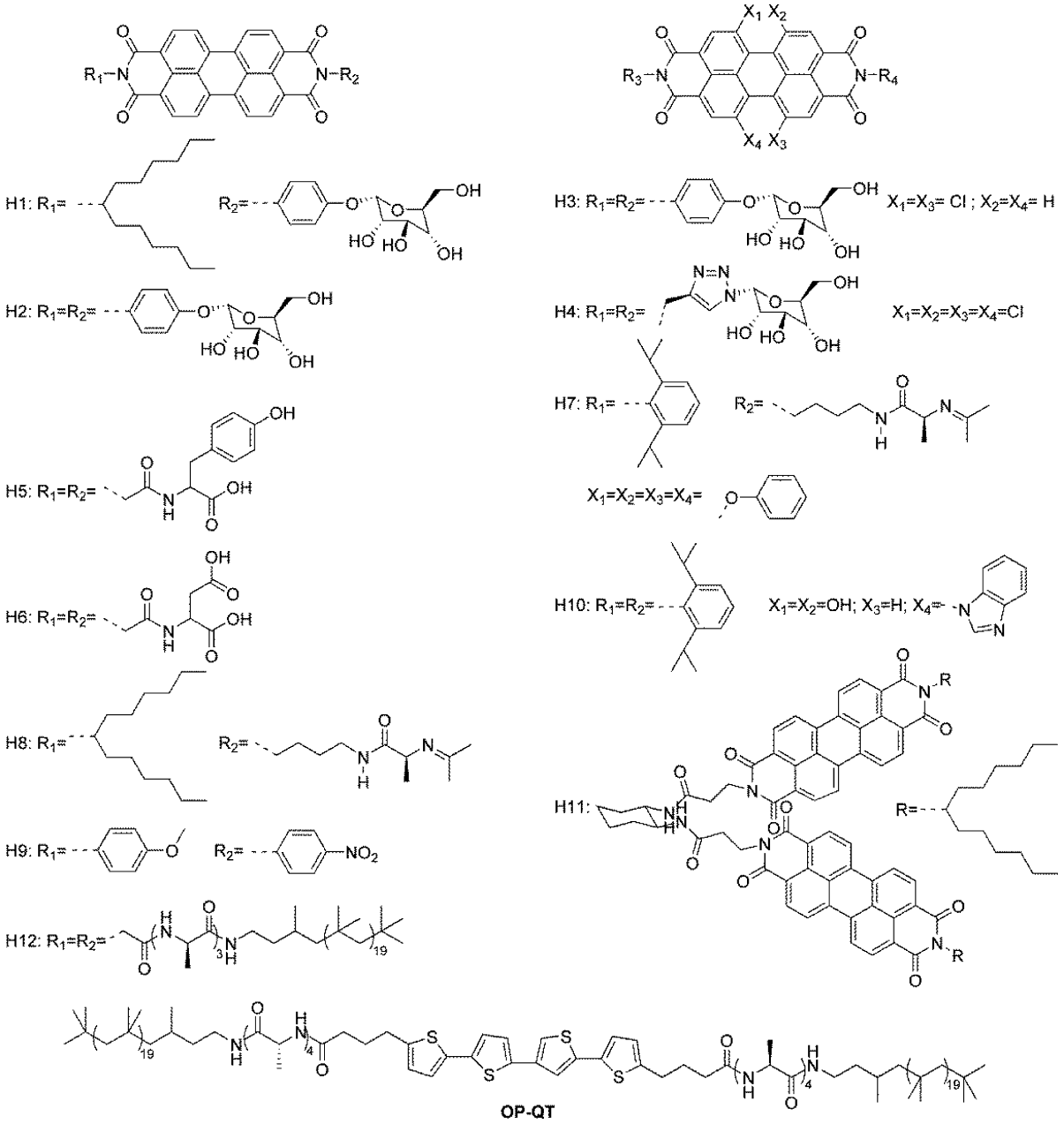

Figure 19. Structures of some PDI molecules capable of helical self-assembly.

Pioneering work was carried out in 2008 by Chen's group, where both left- and right-handed helical nanoribbons were obtained from an asymmetric PDI monomer bearing achiral imide substituents, *N*-(4-methoxyphenyl)-*N*′-(4-nitrophenyl)-PDI (H9; Figure 19).[115] The nanostructures were formed by deposition of a $CHCl_3$ solution of H9 onto the surface of glass substrates. In addition to common noncovalent interactions, the steric requirements and electrophile (4-nitrophenyl)-nucleophile (4-methoxyphenyl) interactions play a key role. More interestingly, double-helical fibers of H9 similar to the structure of DNA were also observed on the surface of carbon-coated copper grids due to their hydrophobic character.[115] Moreover, the influence of heterocycle or heteroatom substitution at the bay region on the self-assembly and final hierarchical structures was revealed. Bay-substitution-triggered intramolecular charge-transfer performance of D−A structure in combination with *J*-aggregation and H-bonding interactions results in specific 1D double-helical nanofibers from H10 (Figure 19). These fibers exhibit specific practical applications, for example, integration into devices for fluorescence sensing of metal ions such as Hg^{2+} and Pb^{2+}.[116] Overall, these strategies pave new ways to develop functional 1D helical nanostructures.

Recently, a water-triggered helical self-assembly of a cationic amphiphile bearing a pyridinium and a long-chain glutamine in organic media has been reported.[117] This method can be used to construct various chiral or helical 1D nanostructures of ionic PDI amphiphiles. Nevertheless, precise control of helical self-assembly of PDIs remains very challenging, both in solution and on surfaces, as well as at interfaces. The relationship between the chiral/helical 1D nanostructures and final function deserves further exploration. Fortunately, the chirality and self-assembly process can be monitored by spectroscopic techniques such as circular dichroism (CD), UV−vis, fluorescence, atomic force microscopy (AFM), and scanning

DOI: 10.1021/acs.chemrev.5b00312
Chem. Rev. 2015, 115, 11967−11998

Table 1. Self-Assembly Conditions and Resulting 1D Helical Morphologies with Different Chiralities of Some Reported PDIs (Figure 19)[a]

PDIs	condition	morphology	chirality	ref
H1	40/60−50/50 THF/H_2O	nanowires	right-handed	109
	80/20 THF/H_2O; 80/20−50/50 $CHCl_3$/*n*-octane		left-handed	
H2	80/20−60/40 DMF/H_2O	nanoribbons	achiral	110
	40/60−20/80 DMF/H_2O	nanowires	left-handed	
	DMF (or DMAC)/C_2H_5OH		left-handed	83
	DMSO (EG or NMP)/C_2H_5OH		right-handed	
	80/20 DMF/H_2O		left-handed	111
	80/40 DMF/H_2O (or C_2H_5OH)		right-handed	
H3	80/20 DMF/H_2O (or C_2H_5OH)	nanowires	right-handed	
H4	4 °C CH_3OH/H_2O	nanoribbons	twisted	112
	25 °C	microplates	achiral	
H5	buffer solution (pH = 10.8); DMSO; DMF; THF; acetone	nanowires	chiral	94
H6	DMF	nanowires	chiral	
	H_2O; DMSO	nanospheres	achiral	
H7 H8	deposition of PDI solutions of $CHCl_3$ or *p*-xylene onto graphite, silica, or mica that seeded with scaffolds of polyisocyanopeptides	nanowires	helical supercoils	114
H9	on glass $CHCl_3$	nanoribbons	chiral	115
	on C-coated Cu grids	nanowires	double helix	
H10	50/50 CH_2Cl_2/CH_3OH on Si wafer	nanowires	left-handed, right-handed, double-helix	116
H11	dilute benzonitrile solution of gels of R-isomer through heat−cooling	nanowires	right-handed	113
H12	thermal annealing of $Cl_2(CH)_2Cl_2$ solution of nanofibril H12/OP-QT and then solution-spinning of microfibers on CH_3OH	complex microfibers	hierarchical	50

[a] *N*,*N*-Dimethylformamide (DMF), *N*,*N*-dimethylacetamide (DMAC), dimethyl sulfoxide (DMSO), ethylene glycol (EG), *N*-methyl-2-pyrrolidone (NMP).

and transmission electron microscopy (SEM and TEM) measurements, and analyzed with assistance of theoretical calculation.[83,109] Moreover, due to the high rigidity imparted by the helical stacking arrangement, such 1D chiral nanostructures, especially single nanoribbons, often display enhanced sensitivity (as compared to the achiral nanostructures) when employed in chemiresistor sensors for vapor detection of reducing reagents like hydrazine.[110]

4. APPLICATIONS

In the past decade, 1D nanofibers of PDIs have been extensively used as building blocks for organic optoelectronic devices, representing one of the most active research fields in chemistry and materials science, particularly in the fields of nanoscience and nanotechnology. Here, we summarize recent advances in this field, from well-known OSCs, OFETs, linear optoelectronic devices, sensors, to novel uses in photocatalysis as well as potential thermoelectric applications.

4.1. OSCs

In recent years, OSCs, one indispensable branch of photovoltaics, became increasingly attractive and important to convert clean solar energy into electrical power, taking advantage of their flexible processing, low-cost and large-area fabrication, and rapidly increasing performances.[103] Since their origins in the 1980s, OSCs have been ranked as the most active prospect in the field of organic optoelectronics utilizing PIs.[22,103] Two excellent reviews have been previously published with focus on the decades' research progress in this field.[22,103] Because n-type PIs possess unique natures such as large charge mobilities, favorable electron affinities, air stability, facile molecular design, and broad solar spectrum coverage, they have been exploited as a promising alternative to the commonly used fullerene derivatives in bulk p−n heterojunction solar cells, as well as photosensitizers in dye-sensitized solar cells.[21,103] Photoinduced electron transfer from electron-rich units (donors) to electron-deficient aromatic cores (acceptors) and subsequent charge transport have been proven necessary to fabricate efficient OSCs.[22,29,103] Thus, in addition to the molecular design of D−A type PDIs or copolymers/oligomers, defined architecture represents another particularly desired facet in the development of more advanced OSC devices in the future.[118]

Previous studies have shown that hierarchical supramolecular architectures via well-defined molecular assembly are very promising candidates for highly efficient OSCs, especially bulk heterojunction solar cells.[118−120] The preparation of such architectures relies on the control of synergistic noncovalent interactions (frequently $\pi-\pi$ stacking, H-bonding, electrostatic interaction, solvophobic force, ionic bond, and metal−ligand coordination) in the fabricating process. Thus, it enables researchers to improve the photovoltaic performance of bulk heterojunction OSCs through constructing 1D crystalline nanostructures of PDIs.[22,78,104−106,118,121] Encouragingly, these uniform 1D materials can be constructed via facile solution-processable self-assembly, which represents a facile strategy to produce low-cost and large-area OSCs as compared to the conventional vacuum-deposition method. Generally speaking, 1D self-assembly of PIs can work in two charge-transfer systems. In the first system, the D/A complex (noncovalent amphiphilic pair of π-conjugated donor molecule plus PI unit) is coassembled via solution processing, for example, 1D rod-like nanostructures of complex (n-1/p-1; Figure 21) consisting of aspartic acid-modified PDI and π-conjugated phenazine,[116] or highly conductive 1D nanotubes of complex (n-2/p-2; Figure 21) with extended π-conjugated oligo(phenylenevinylene) and PDI units.[98] In the second case, significant progress has been achieved from mixing preassembled 1D nanofibers of PDIs with appropriate hole transport conjugated polymers via solution processing in bulk heterojunction solar cells, for example, D/A heterojunction blends (Figure 22, ①) of PDI (n-3; Figure 21) xerogels (in the

DOI: 10.1021/acs.chemrev.5b00312
Chem. Rev. 2015, 115, 11967−11998

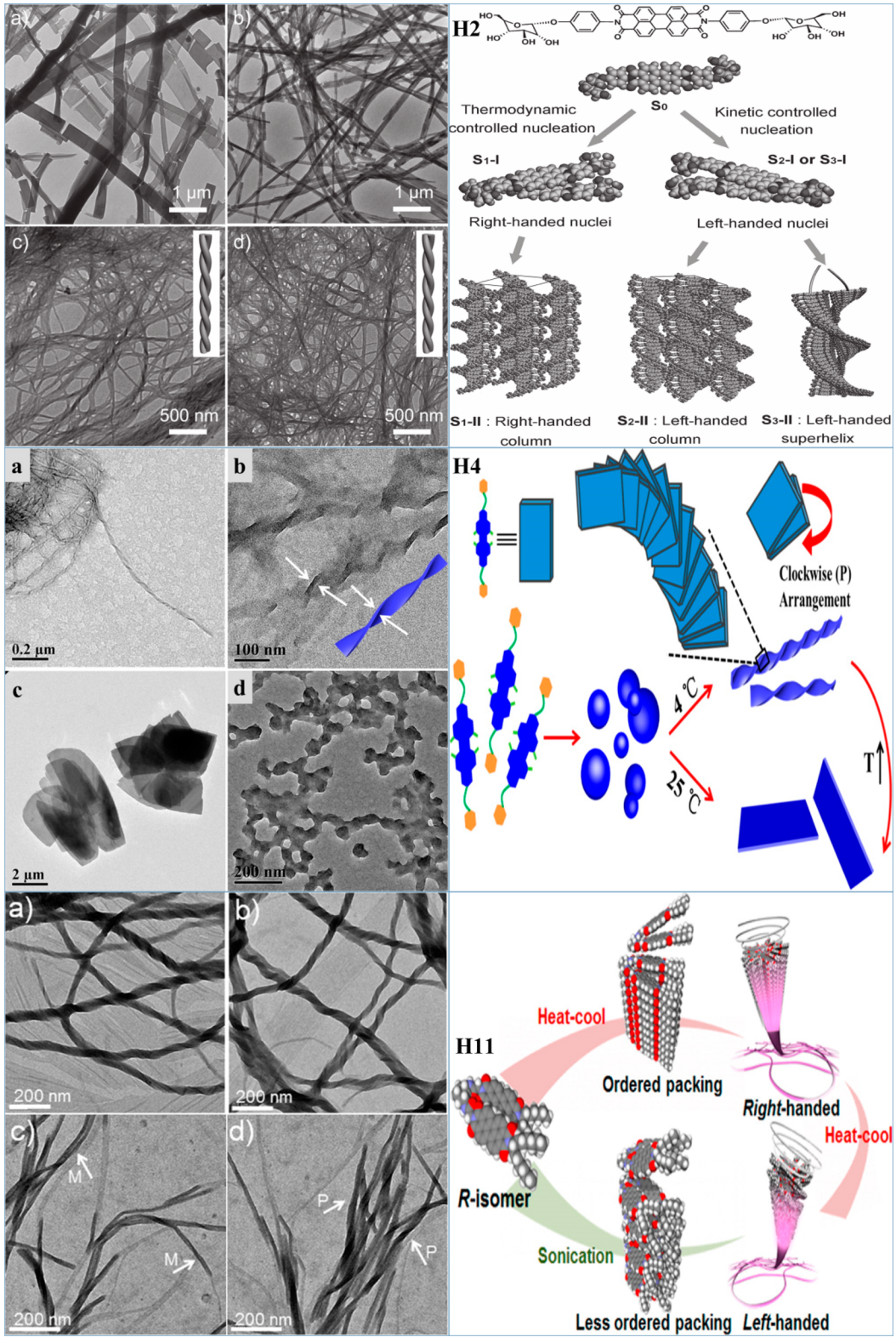

Figure 20. Illustration of the helical self-assembly processes of three chiral PDI molecules (H2, H4, and H11) and SEM images of the resulting 1D self-assemblies. Adapted with permission from ref 110. Copyright 2012 Wiley-VCH. Adapted with permission from refs 112 and 113. Copyright 2014 American Chemical Society.

presence of 1D nanowires) and amorphous hole conducting polymer, poly{*N*,*N*′-bis(4-methoxyphenyl)-*N*-phenyl-*N*′-4-vinylphenyl-[1,1′-biphenyl]-4,4′-diamine} (p-3; Figure 21).[121,122] A power conversion efficiency of 0.041% has been reached from such PDI (n-3)/p-3 heterojunction blends (Figure 22, ①).[121] A more inspiring result with a power conversion efficiency of about 1% was obtained for a system generated from the incorporation of micrometer-long PDI-C8 (n-4; Figure 21) nanoribbons with donor polymer poly[2-methoxy-5-(3′,7′-dimethyloctyloxy)-1,4-phenylenevinylene]

DOI: 10.1021/acs.chemrev.5b00312
Chem. Rev. 2015, 115, 11967−11998

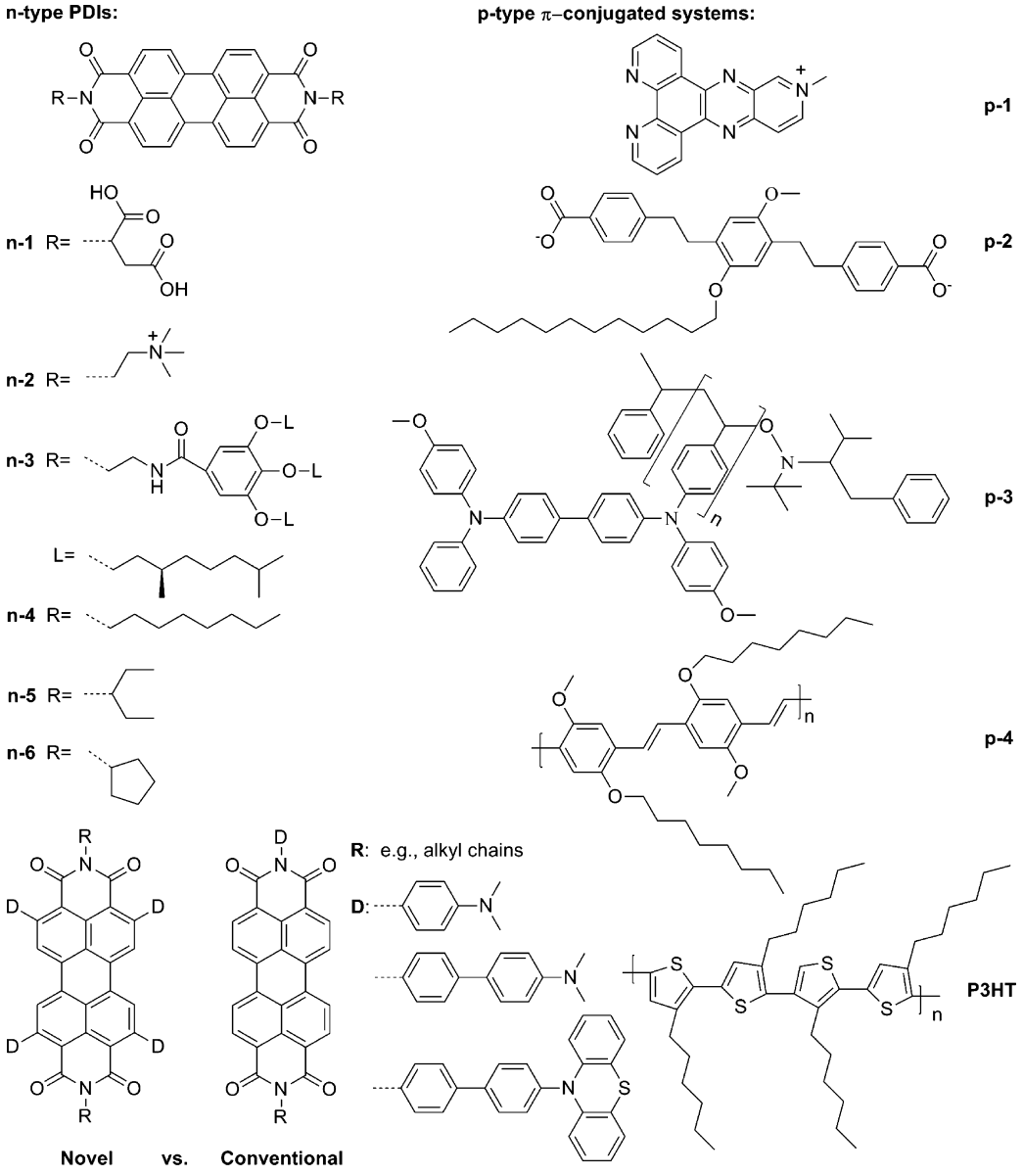

Figure 21. Chemical structures of PDIs and p-type π-conjugated molecules, oligomers, and polymers, which have been used for fabricating p−-n nanofibril heterojunction OSCs.

(p-4; Figure 21) or P3HT (Figure 21).[122] Similar and even more promising results are anticipated if the above-mentioned high photoconductive nanofibril D/A heterojunction is utilized.[78,106] In short, these improvements in power conversion probably arise from the enhancement of photoinduced electron generation and the large D/A interface area in light of nanoscale molecular interaction and phase separation, which enable efficient exciton dissociation and generate continuous pathways for rapid charge extraction.[22,118,121,122]

PDIs and polythiophenes (typically, P3HT) have been listed among the most promising organic electron acceptor and donor materials, respectively, in organic photovoltaics.[22,103] Many photovoltaic devices employ a combination of PDIs and P3HT in the form of blends, or covalently linked block copolymers/oligomers, for which the inhibition of pervasive charge recombination has been limited, thus preventing the further improvement of the photoconversion efficiency of the OSCs devices.[22,103] Accordingly, several recent advances have been achieved in attempting to bypass this problem, resulting in the design of ordered heterogeneous p−n nanojunctions (n-4/P3HT, n-5/P3HT, n-6/P3HT; Figure 21) via simple solution-evaporation processes on substrates (Figure 22, ②).[123−125] Among these achievements, one involves the self-assembly of PDI (n-5) molecules on P3HT backbones, which serve as the matrix and support.[123] Another involves the tailored coassembly of PDI (n-4) molecules and P3HT into hybrid "shish-kebab" nanostructures.[124] In the long run, 1D nanostructured heterojunctions can act as one of the most promising building blocks for organic photovoltaic devices, due to their long-range order, large contact area, unique charge carrier separation, and transport features.[124,125]

Additionally, functionalization of the shoulder (2-,5-,8-,11-) positions on the perylene core of PDIs holds great promise as photovoltaic functional materials by virtue of favorable balance between the planarity and HOMO/LUMO energy levels.[122] Very recently, Wasielewski's group developed a series of intriguing photoinduced charge-separated systems (Figure 22, ③).[126] With the assistance of the 1D supramolecular self-

DOI: 10.1021/acs.chemrev.5b00312
Chem. Rev. 2015, 115, 11967−11998

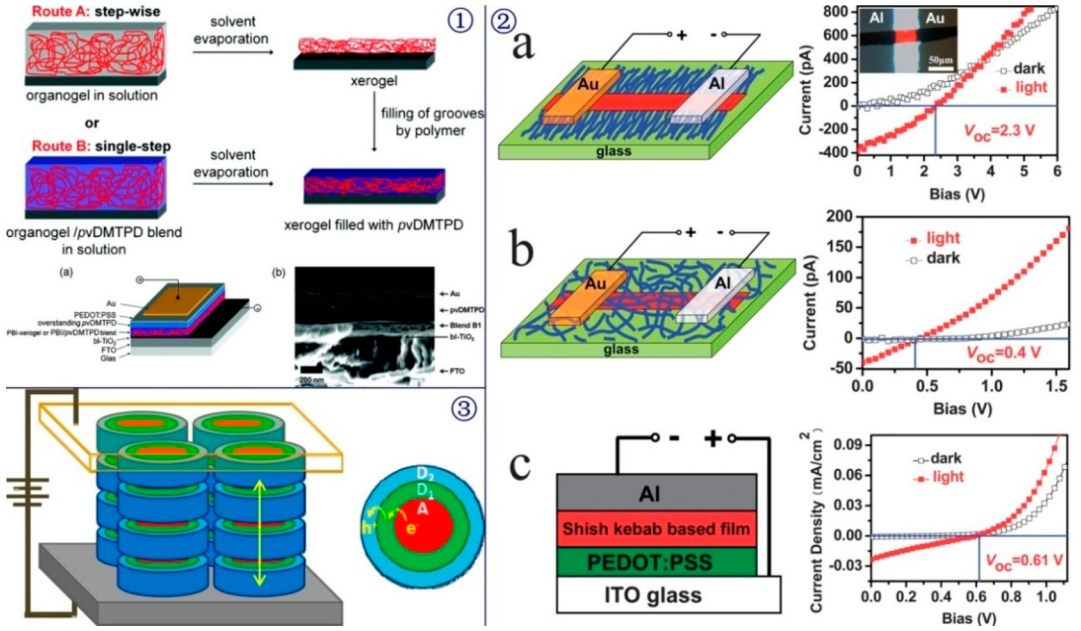

Figure 22. Schematic representation of three heterojunction OSC devices containing PDI nanofibers. ① Organogel-polymer for preparation of an interpenetrating organic bulk heterojunction. Route A: Formation of n-type xerogel with subsequent filling with p-type polymer. Route B: Concomitant embedding of the physical network by a blended approach. (a) General device architecture with inverted cell configuration. (b) SEM cross section of a typical blend device B1 prepared via route B. Adapted with permission from ref 121. Copyright 2009 American Chemical Society. ② Device architectures and the corresponding $I-V$ characteristics measured under dark and simulated AM 1.5G light illumination from a glass substrate. (a) PV device employing a discrete n-6/P3HT shish kebab-like structure; the inset shows the optical microscopic image of the device. (b) PV device based on n-6 single crystal covered by random P3HT fibers. (c) Solar cell employing the traditional sandwich structure with n-6/P3HT shish kebab-like structures as the photoactive layer. Reproduced with permission from ref 125. Copyright 2014 Royal Society of Chemistry. ③ The ideal architecture for an OPV active layer. In this case, red = acceptor, green = primary donor, blue = secondary donor. Adapted with permission from ref 126. Copyright 2014 American Chemical Society.

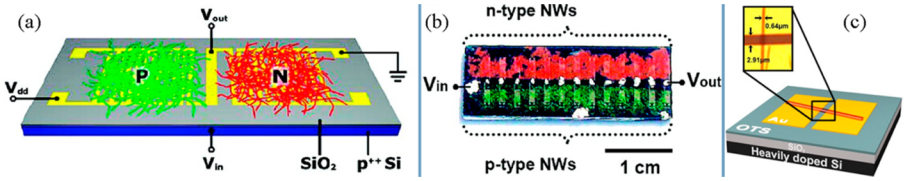

Figure 23. (a) Schematic of an inverter with p- and n-type nanowire networks covering interdigitated source-drain electrodes, and (b) a photograph of a substrate containing 13 discrete inverters of (a). Reproduced with permission from ref 56. Copyright 2007 The American Chemical Society. (c) A schematic diagram of a single nanowire OFET. The inset shows an optical micrograph of a device channel connected by a nanowire. Reproduced with permission from ref 77. Copyright 2013 American Chemical Society.

assembly technique (in virtue of the presence of headland soft side-chains), these ortho-functionalized PDIs may attract particular interest for achieving the object of commercial PDI-enrolled OSCs devices in the future.

Overall, the efficiencies observed for the photovoltaics devices employing PDI materials including nanofibers are still behind that of the fullerene-based systems. This is mostly due to the poor organization and/or phase segregation of the materials, which in turn limit the charge transport. To overcome this problem, columnar stacking of electron donor–acceptor molecules into segregated charge-transport channels (similar to Figure 22, ③) would be an ideal approach. Upon illumination, complete charge separation will occur through intramolecular photoinduced electron transfer from donor to acceptor. The electron thus generated will migrate along the $\pi-\pi$ stacking of PDIs (functioning as acceptor), while the hole will transport along the stack of the donor part. Such segregated charge-transport pathways will also help prevent the charge recombination. The extended columnar stacks (maybe in the format of fibril structure) will allow for long-range, continuous charge transport to reach the electrode. A combination of these structural features is expected to significantly improve the photoconversion efficiency. One challenge in constructing the ordered, segregated columnar stacking of donor–acceptor lies in the design and optimization of molecular structures that will maximize the intermolecular interaction (particularly $\pi-\pi$ stacking) to counterbalance the usual preference for donor/acceptor over acceptor/acceptor and donor/donor interactions.

4.2. OFETs

For flexible and lightweight organic electronics, such as integrated circuits, complementary inverts, and ring oscillators, high performance OFETs, in particular, organic thin film transistors (OTFTs), are highly desirable.[127,128] As compared to their p-type counterparts, the development of OFETs fabricated from n-type organic semiconductors is more suitable for use in areas such as complementary circuits. Recently, Liu et al. have reviewed the exciting previous quarter-century's

DOI: 10.1021/acs.chemrev.5b00312
Chem. Rev. 2015, 115, 11967–11998

progress in OFETs focusing on n-type and ambipolar semiconductors.[128] Similar to OSCs, it is believed that high charge carrier mobility, ambient stability, low cost, and facile processability are essential, and it is still challenging to prepare materials suited for practical applications in n-type OFETs.[128,129] However, it is the right time and opportunity to apply solution-processed 1D nanofibers of PDIs into this field.[56,128] Indeed, intermolecular $\pi-\pi$ stacking construction and ordered long-range nanostructure of 1D PDI nanofibers are beneficial to enhancing the performance of n-type OFETs due to their high electron affinity and good charge-transport properties.[56] Many attempts have been made to unveil the relationships between the molecular structures of PDIs and OFET performances.[56,77,93]

Commercially available molecules, PDI-C5, PDI-C8, and PDI-C13, have received considerable attention in this field.[56,77] Recent studies have demonstrated their bisolvent-phase self-assembled 1D nanowires feasible in fabricating n-type OFETs via the solution process (Figure 23a–c). Specifically, after combining these n-channel transistors with p-channel hexathiapentacene nanowire OFETs, high performance complementary inverters can be built as shown in Figure 23a.[56] Although there are no distinct differences in the electron affinities (or LUMO levels) and morphology due to the imide nodes in *N,N′*-substituted PDIs, the longer alkyl chain results in increased electron mobility for OFET devices.[56] Moreover, PDI-C8 and PDI-C13 have been proven to be a much better choice for the application of PDIs in the OFET field, due to their band-like charge transport.[56,77,129,130] In the future, advances are expected through optimizing the molecular structure of PDIs with electron-withdrawing moieties (−CN, $-C_3F_7$, etc.), which may tune their LUMO energy levels.[128] Additionally, in view of the redox capacity of PDIs, some PDI nanostructures possess high photoconductivity, due to their facile reduction in the photoexcited state (chemical doping) in cooperation with efficient $\pi-\pi$ stacking, leading to a long-lived charge-separated state.[14] As a proof, hydrazine-doped metal-loorganic nanowires with ∼2 nm lamellae consisting of Zn^{2+} doped *N,N′*-di(phenyl-3,5-dicarboxylic acid)-PDI radical anions have been used to construct efficient OFETs devices leading to a high electron mobility (13 $cm^2\ V^{-1}\ s^{-1}$) at a low operating voltage of 1 V under ambient conditions.[93] Further progress may be derived from the photoconductive 1D nanofibers of L-alanine-modified PDI in the presence of unusually air/water-stable perylene radical anions.[91]

The fabrication strategy often imposes a significant effect on the morphology and sequent device performance.[128,129] Recently, the remarkable environmental stability of nanofiber-based OFETs (including OTFT devices) has been demonstrated when compared to conventional thin-film transistors.[56] The effective interdigitation of ordered PDI-C8 and PDI-C13 nanowires on the solid surface, which reduces the penetration of environmental contaminants and minimization of charge traps, is imperative to support this.[56,77] On the other hand, novel configurations (for example, bottom-gate bottom-contact instead of normal bottom-gate top-contact) will provide much more room to improve the environmental stability of OFET devices.[127] Hence, further structural modifications in line with device constitution are still among the most important issues for the application of PDIs in n-type OFETs with long-term stability. By combining solution-phase self-assembly with etching or templating technology, it will likely be possible to construct nanowire arrays of PDIs, further enhancing the OFETs efficiency toward commercial demands.

4.3. Linear Optoelectronics

Linear optoelectronic properties, that is, the uniaxial emission and conductivity along the $\pi-\pi$ stacking direction of individual nanofibers, make PDI-based 1D self-assemblies ideal candidates for orientation-sensitive applications, such as polarized OLEDs, nanolasers, optical waveguides, flat-panel displays, optical sensors, or switches with high selectivity in response to polarized light, and other angle-dependent optical as well as electrical nanodevices.[14,58,87,131,132]

In the past decade, great progress has been made by Zang and his co-workers who have demonstrated impressive linearly polarized emission from $\pi-\pi$ stacked 1D nanobelts of *N,N′*-di(propoxyethyl)-PDI employing cross-polarized optical (using near-field scanning optical microscope; NSOM) and electron diffraction microscopy.[20,35,72] Similarly, maximum anisotropic birefringence occurs when a single nanofiber of PDI-C8 is aligned 45° to the direction of the polarizer of NSOM (Figure 24A–C).[58] Reddy et al. have proposed a model to explain such

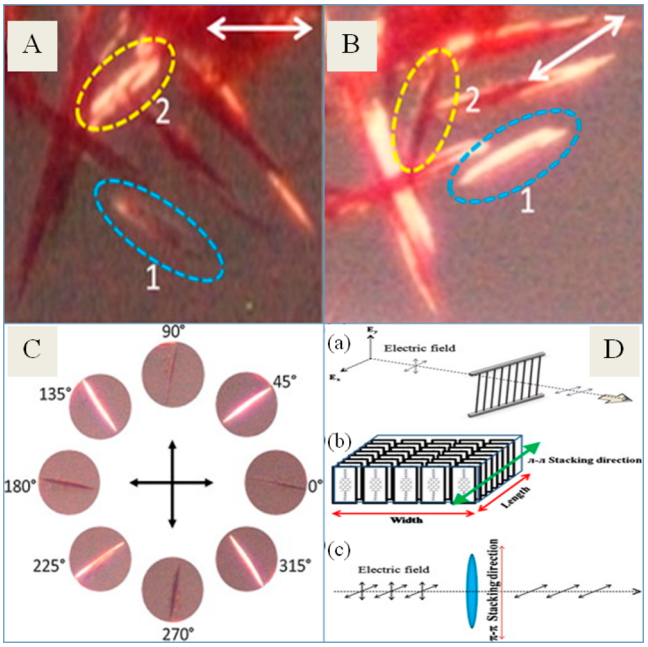

Figure 24. Cross-polarized microscopy images of PDI-C8 microstructures of the same area of the sample, (A) taken before rotation and (B) taken after 45° rotation of the sample. (C) A single microstructure under cross-polarized microscope: successive rotation of the sample showed alternate appearance of maximum birefringence as the microstructure was aligned 45° to either of the polarizers. The crossed polarizers are indicated as arrows. (D) Schematic diagram showing (a) linearly polarized emission from a wire-grid polarizer, (b) $\pi-\pi$ stacking of PDI-C8 molecules in a 1D microstructure, and (c) linearly polarized emission from PDI-C8 1D microstructure. Adapted with permission from ref 58. Copyright 2013 Elsevier.

phenomena (Figure 24D).[58] Additionally, an electrically modulated ultralong optical waveguide, based on 1D microwires (lengths of several hundred micrometers to millimeters) of PDI-C8, has been fabricated by template-assisted assembly on the surface of graphene oxide.[133]

Generally, *H*-type aggregates of PDIs have been demonstrated to be more suitable for optical applications than *J*-aggregates.[134] However, although $\pi-\pi$ stacking can facilitate

DOI: 10.1021/acs.chemrev.5b00312
Chem. Rev. 2015, 115, 11967–11998

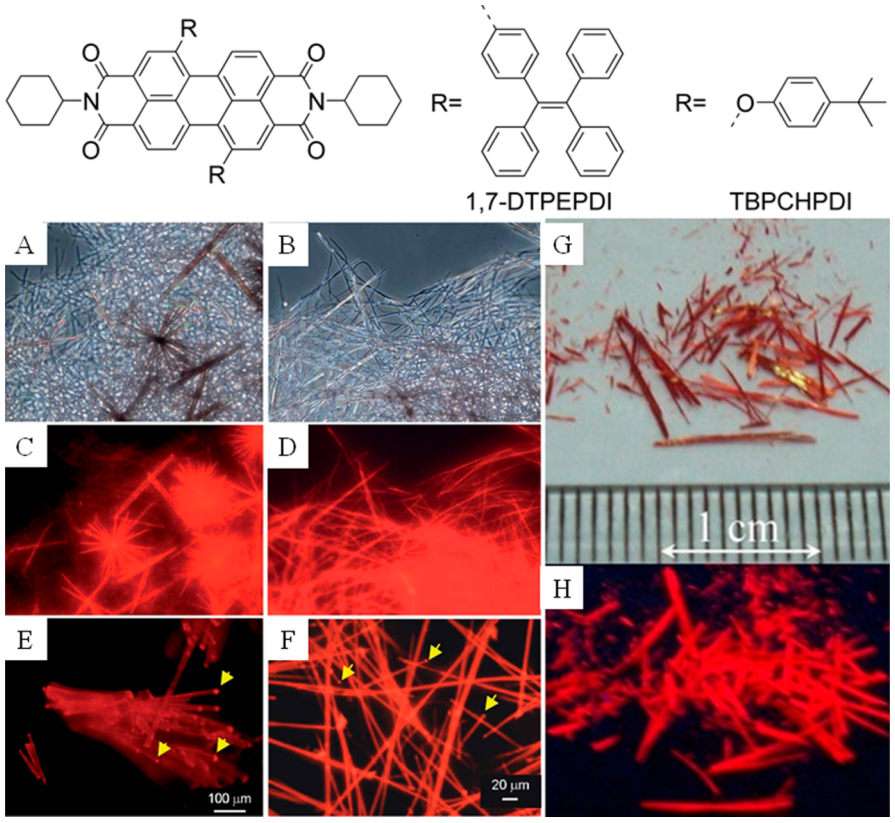

Figure 25. Polarized optical microscopic images of the microcrystals obtained from a CH_3OH/CH_2Cl_2 mixture (A), the fibrils formed by 1,7-DTPEPDI (b4) molecules in a H_2O/THF mixture (B). (C) and (D) are the confocal fluorescence images corresponding to the microstructures shown in (A) and (B), respectively. Images showing the waveguide properties of the microcrystals (E) and fibrils (F); some brighter spots are indicated by arrows. Excitation wavelength is 488 nm. Adapted with permission from ref 30. Copyright 2012 The Royal Society of Chemistry. The photographs of TBPCHPDI crystals under day light (G) and upon illumination with UV light. (H) The inset is the molecular structure of TBPCHPDI. Adapted with permission from ref 135. Copyright 2014 Elsevier.

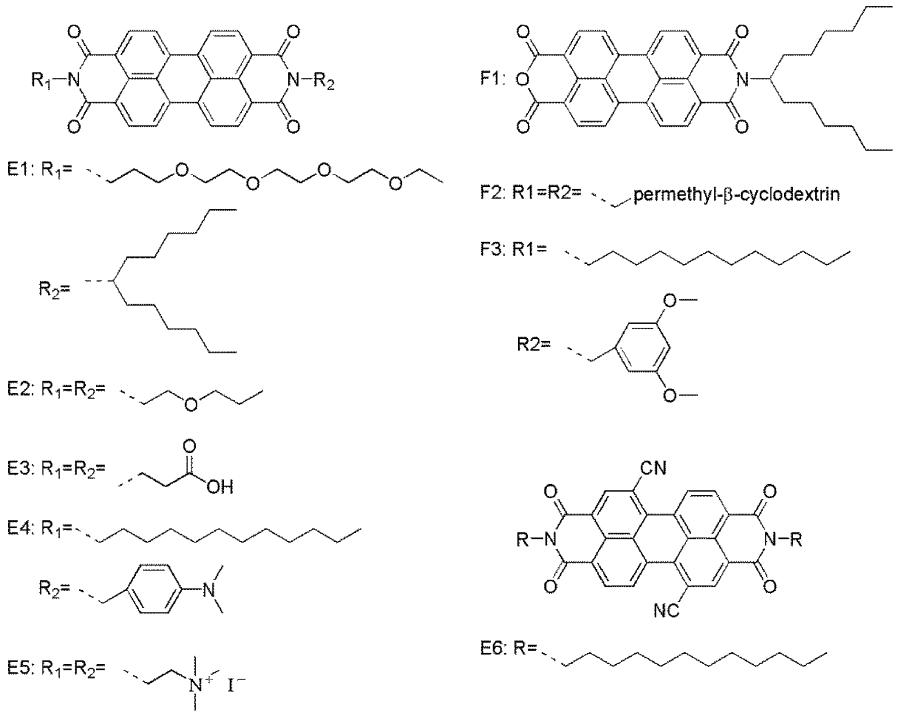

Figure 26. Structures of reported PIs molecules, which have been fabricated into 1D nanofiber for the detection of organic vapors.

DOI: 10.1021/acs.chemrev.5b00312
Chem. Rev. 2015, 115, 11967−11998

energy and charge transport along the long axis of a solid *H*-type nanofiber, PDI molecules normally lose their high fluorescence due to an aggregation-related quenching effect, which still limits their linear optical properties in real devices.[131,132] To fabricate strong fluorescent nanofibers of PDIs, a balance between effective molecular stacking and retention of the desired fluorescence must be maintained via appropriate side-chain substitution.

As discovered by Zang et al., 1D nanobelts of *N*,*N*′-dicyclohexyl-substituted PDI show persistent strong polarized and self-waveguided fluorescence emission arising from a so-called "flip-flap" stacking morphology.[131,134] Taking additional advantage of steric interactions of rigid *p*-*tert*-butylphenoxy substituents at the bay positions, a high electron mobility (1.8 $cm^2\ V^{-1}\ s^{-1}$) from needle crystals of TBPCHPDI (Figure 25G,H) was observed, while maintaining strong red fluorescence with a quantum yield of 0.32.[135] The above-mentioned work shed light on constructing future fluorescent devices through well-tailored structural design to control the intermolecular $\pi-\pi$ interactions. As a proof, well-ordered 1D microfibers of 1,7-DTPEPDI (b4) possessing both D−A structure and bay-modification via p-type tetraphenylethene substitution have shown pronounced red-emission and waveguide activity (Figure 25A−E).[30] Furthermore, because emission in the solid state has been detected, the potential influence of solvent-triggered and shape-dependent optical behavior can be avoided.[72,135−137] Uniform belt-like 1D structures of PDI nanofibers that possess higher purities and larger smooth surfaces also favor better waveguide properties.[14,137] Besides devices described above, Bao and co-workers fabricated n-channel organic phototransistors from single-crystalline nanowires of *N*,*N*′-di(2-phenylethyl)-PDI showing favorable light sensitivity and photoconductivity especially in a bottom-contact conformation.[138] Future exploitation of strong emissive and light-responsive *H*-type 1D nanofibers of PDIs will be of great interest for application in low-cost, lightweight, flexible, and mini-scale optoelectronic devices.

4.4. Chemical Vapor Sensing

Variation in electrical resistance and fluorescence of semiconducting materials induced by surface adsorption of gas analytes has received increasing attention for application in sensors.[14,19,36] In the past decade, because of their n-type semiconductor character (i.e., electron-deficient feature), PDI-based nanofibers have been extensively studied by Zang's and others' groups for sensing a wide range of reducing gaseous species (i.e., electron donating), such as CO, NO, volatile organic amines (e.g., hydrazine), and even weakly reducing ammonia (NH_3), by measuring the change in electrical or fluorescent signals (Figures 26, 27, and Table 2).[14,36,55,65] These materials have demonstrated rapid response with high sensitivity (sensing response within milliseconds along with detection limits as low as in ppt range), good selectivity, and quick recovery.[36,55,65]

Generally, the vapor sensing applications take advantage of several features of PDIs: (1) excellent photostability (zero photo bleaching);[14,55] (2) strong surface adsorption of analytes as well as strong contact with electrodes especially in the presence of bare anhydride moieties or carboxylic side chains in asymmetric PDIs (e.g., F1, E3);[65,90,93,95] (3) long-range exciton migration and strong π-electron delocalization within 1D nanofibers, arising from a well-organized molecular arrangement leading to increased charge carrier mobility (electrical

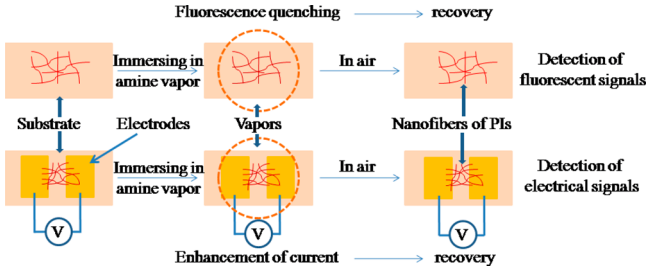

Figure 27. Schematic presentation of the device for characterizing the fluorescent emission or *I*−*V* properties of PDI nanofibers for amine vapor sensing.

conductivity) and amplified fluorescence quenching upon adsorption of analytes capable of electron donation (reducing analytes);[55,62,139] and (4) unlimited substitution at the imide positions without affecting HOMO/LUMO electronic levels because these positions are nodes of the molecular orbitals, leading to structural diversity and a high degree of selectivity. Of course, this means that the core-substituted effect should be taken seriously. Indeed, electron-withdrawing −CN group attachment can enhance the ammonia sensitivity of PDI (E6) nanobelts via decreasing the reduction potential PDI molecules.[36] (5) PDI nanofibers form mesh-like highly porous films, which provide large surface area for adsorption of gaseous analytes and expedient diffusion of the analytes through the 3D network.[14,53,65,139] Sometimes, fine structural design can amplify such gas intaking effects. Wei's group demonstrated that the 1D nanotubes of ionic PDI (E5) possessed better sensory properties (shorter response time and stronger resistance decrease) upon exposure to the vapor of hydrazine or phenylhydrazine than their nanorods, due to the greater surface area and increased contact time.[95] The addition of the polar 3,5-dimethoxybenzyl side-group and dodecyl chain, which creates a balanced interplay among molecular steric hindrance, $\pi-\pi$ interactions, and hydrophobic interactions, gave rise to a morphology of bilayer nanocoils following self-assembly of PDI (F3), which was processed through the injection of its $CHCl_3$ solution (0.14 mM) into larger volume of C_2H_5OH followed by aging for 3 days. Unlike the above helical systems formed from various amphiphilic molecules, such nanocoils are thermodynamically stable in matrix solvent phase. Even without bay-substitution, they display an efficient fluorescent emission (with a quantum yield of 25%). A significantly enhanced sensitivity of these porous nanocoils for vapor detection of amines has been obtained, nearly 3 orders of magnitude greater than that reported for the 1D nanofibers.[64,65] (6) Photocurrent within PDI nanostructures can be enhanced by introducing suitable donor moieties on PDI cores. For example, PDI (E4) nanoribbons, which have dark currents in the pA range, exhibit a photocurrent on/off ratio, for example, ca. 10^3 upon illumination with white light.[53] More promising, the enhanced photocurrent of PDI (E4) leads to the development of a sensing device capable of detecting oxidizing species such as nitro-based explosives (e.g., DNT) and oxygen by monitoring a decrease in photocurrent.[53]

The above sensing observations will likely inspire future development of commercial optoelectronic sensors based on PDI nanofibers coated onto appropriate substrates (e.g., glass), electrode pairs, or embedded into analyte-sensitive films (e.g., poly(vinylidene fluoride) (PVDF) membranes[139]) capable of detecting vapor analytes. Commercial sensors coated onto

DOI: 10.1021/acs.chemrev.5b00312
Chem. Rev. 2015, 115, 11967−11998

Table 2. Self-Assembled 1D Nanofibers of PIs (As Listed in Figure 26) as Sensors for Vapor Detection of Volatile Organic Compounds (VOCs) by Electrical or Fluorescent Signals

samples	1D morphology	VOCs	detection signals	detection limits	ref
F1	nanobelts	hydrazine	fluorescence quenching	1 ppb	65
		aniline		200 ppt	
F2	nanorods	organic amines		33 ppm (aniline)	139
		nitro-based compounds			
F3	nanocoils	aniline		0.8 ppt	64
		phenethylamine		3 ppt	
		octylamine		0.2 ppb	
		triethylamine		4 ppb	
		dibutylamine		12 ppb	
E1	nanobelts	hydrazine	electrical current increase		62
E2	nanobelts	hydrazine			55
E3	nanobelts	diethylamine			91
E4	nanobelts	oxygen	photocurrent decrease		53
		nitro-based explosives			
E5	nanotubes	hydrazine	electrical current increase by 3 orders of magnitude		96
	nanorods	phenylhydrazine	electrical current increase by 2 orders of magnitude		
E6	nanobelt	NH_3	electrical current increase		36

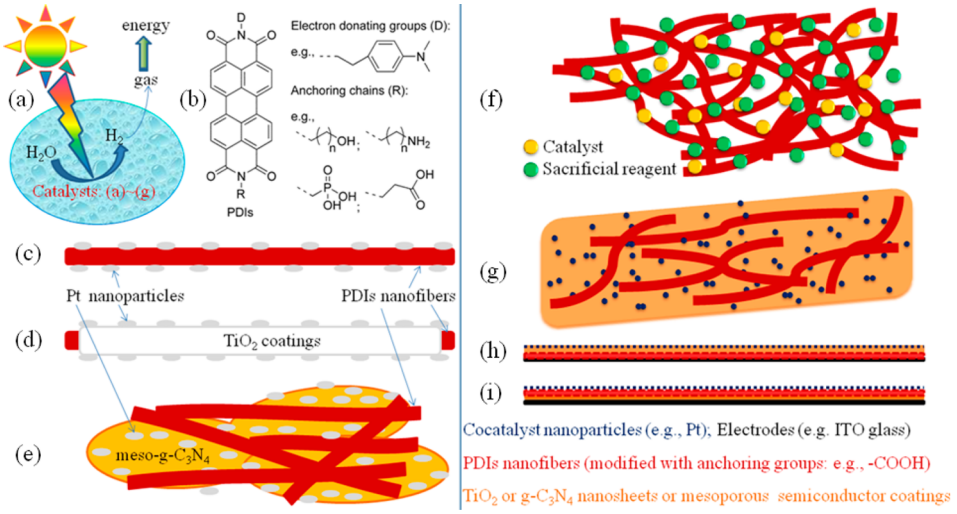

Figure 28. (a) Schematic presentation of the solar-irradiated photocatalytic water-splitting for H_2 production; (b) optimized molecular structures of PDIs (just taking imide-substitution as examples) in relation to photocatalysis field; (c–e) scheme of reported hybrid photocatalyst composites enrolled by PDI nanoassemblies; and (f–i) scheme of possible conformation of 3D photocatalytic hydrogel systems or photoelectrocatalytic device containing nanostructured PDIs coatings.

flexible supports (like paper) capable of real-time detection of certain vapor analytes are also expected.

4.5. Photocatalysis

Photocatalysis (including photoelectrocatalysis) has long been another attractive area for utilizing solar energy. In this field, solar-induced water-splitting over semiconductor photocatalysts (Figure 28a) has gained intense interest, providing an ideal approach to generate the clean and renewable energy source, hydrogen.[140−143] Among the large number of photocatalysts, titanium dioxide (TiO_2) and graphitic carbon nitride (g-C_3N_4) have been recognized as the most important inorganic and organic semiconductor photocatalysts, respectively.[143,144] Despite their appealing features (low cost, effective, and stable) in line with many promising results, they exhibit low photoconversion efficiency, which limits their use in practical applications, mainly due to the poor visible-light absorption and rapid recombination of photogenerated electrons and holes.[143,144] Consequently, increasing research efforts have been invested to overcome these obstacles.

Recently, PDIs have been enrolled in this field mainly as dye-sensitizers in a series of hybrid photocatalyst composites. These composites benefit from PDI's excellent environmental stability, strong visible-light absorption, tunable redox potentials (molecular orbital energy levels) arising from variable structural functionalization, and matched energy levels as well as effective binding ability with TiO_2 or g-C_3N_4 (Figure 28c–e).[145−147] Significant efforts have been focused on tuning the electron D−A structure of PDI molecules and fabricating 1D nanostructures of PDIs in an effort to achieve efficient charge-transfer mobility through controlled initial intramolecular charge transfer of PDIs and intermolecular charge separation among composites (Figure 28b).[145−147] Appropriate selection of the electron-donating moiety attached to the electron-deficient PDI core is critical to achieve extended lifetimes of photoinitiated charge separation following visible-light illumi-

DOI: 10.1021/acs.chemrev.5b00312
Chem. Rev. 2015, 115, 11967−11998

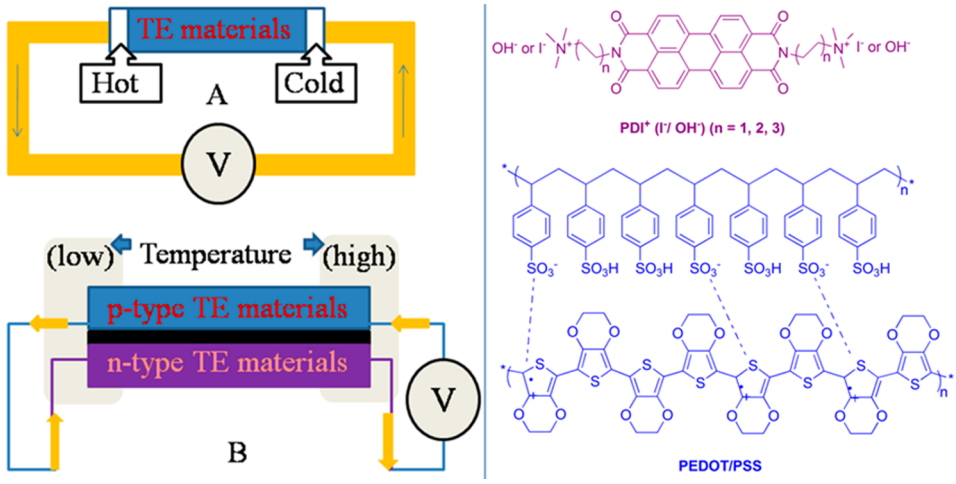

Figure 29. Schematic illustration of general thermoelectric (TE) architectures (A and B) and corresponding current directions, as well as molecular structures of candidate PDI^+/I^- or OH^- (n-type) and PEDOT/PSS (p-type) TE materials.

nation.[28,126,148] Such efficient charge transfer can also be found in organic/inorganic hybrid D−A nanostructures, for instance, PDI/ZnS/CdSe and PDI/CdS.[149−151] On the other hand, well-ordered organic/inorganic or organic/organic interfaces, as shown in Figure 28c−i, are very important for organic electronic and optoelectronic devices.[21] These interfaces have been constructed by in situ growth or deposition of PDI assemblies on solid surfaces.[148] PDIs are particularly interesting for this purpose due to their facile self-organization into 1D nanostructures (especially nanofibers), effective molecular binding, as well as efficient charge transport both at the interface and within the PDI nanofiber itself.[148]

Additionally, with the assistance of anchoring group (e.g., −COOH, $-PO_3H$, and $-NH_2$; Figure 28b) functionalization, PDI can form a strong complex with semiconductor photocatalyst components, forming a composite system with effective visible-light response and effective interfacial charge transfer.[152,153] Such anchoring groups can also serve as active sites on the surface of composite photocatalysts to anchor cocatalysts, such as Pt or Ru nanoparticles with narrow and uniform particle size.[154] PDI molecules can be combined with multiwalled carbon nanotubes or graphene nanosheets, and the resulting complexes can be dispersed in water, as well as in some organic solvents, while still preserving the intrinsic electronic properties of the individual complex components for photocatalysis.[155,156] When the complex PDI components are formed into 1D self-assemblies with well-ordered crystalline structure, further enhancement of exciton and charge transport can be realized. Using systems such as these (Figure 28f−i), photocatalytic activity has been observed, for example, the photoelectrocatalytic splitting of water or degradation of organic pollutant under visible light irradiation, when constructing self-assembled PDI nanofiber coatings together with spin-coated electrodes (e.g., indium tin oxide (ITO)), nanoparticles, or nanosheets of catalysts and cocatalyst (e.g., CoO_x) nanoparticles layer-by-layer onto solid substrates.[60,153,157]

In brief, the remarkable properties of PDIs with appropriate 1D morphology and anchoring groups make them ideal photosensitizers for use with photocatalyst components such as inorganic semiconductors (e.g., metal oxides and sulfides),[158] g-C_3N_4,[159] and carbon materials (e.g., graphene, oxide graphene, and carbon nanotube).[160−163] Although research to further increase catalytic efficiency is still underway, appropriate nanoscale engineering (particularly at interfaces) of these composite materials will open new scenarios for photocatalyst development (e.g., Figure 28f−i). The development of novel PDI molecules satisfying the requirements of D−A type, solution-processable 1D self-assembly capability, and strong binding force with other semiconductors is still highly desirable, although challenging.

4.6. Thermoelectricity

In addition to photovoltaic and photocatalytic devices used to convert solar energy into electricity and chemical energy, there is another active research field: the development of highly efficient thermoelectric materials for use in other green power-generation devices (Figure 29A and B) that can transform heat from abundant waste and natural heat resources into electricity.[100,164,165] While not as efficient as their inorganic counterparts (already in commercial applications), organic thermoelectric materials are more flexible, lower-cost, and apt for large-area processing.[100,166] In recent years, significant progress has been made for p-type conducting polymers,[166−168] especially poly(3,4-ethylenedioxy-thiophene)/poly-(styrenesulfonate) (PEDOT/PSS; Figure 29).[169] However, n-type organic thermoelectric materials have been largely ignored due to stability issues.[100]

PDIs may be capable of meeting these challenges due to their unique stability. Recently, Segalman et al. observed thermoelectric performance from a series of water-soluble PDIs (PDI^+ (n = 1, 2, 3), Figure 29) with I^- counterions functioning as charged doping groups.[99] Even more attractive properties were observed from solution processed thin films of PDI^+ using OH^- as a counterion, PDI^+OH^- (n = 3; Figure 29), which displayed the highest n-type thermoelectric performance of solution-processed organic materials reported to date, a thermoelectric power factor of as high as 1.4 $\mu W\ m^{-1}\ K^{-2}$, along with an electrical conductivity of 0.5 $S\ cm^{-1}$.[99] Theoretically, thermoelectric performance is believed to be strongly associated with charge-carrier mobility (resulting from the conformational change), carrier concentration (in relation to doping degree), and intrinsic thermal conductivity of the selected materials.[166] Thus, further gains in thermoelectric efficiency may be realized by using self-assembly techniques to convert $PDI^+(I^-$ or $OH^-)$ and other PDIs into 1D structures with the possibility of

DOI: 10.1021/acs.chemrev.5b00312
Chem. Rev. 2015, 115, 11967−11998

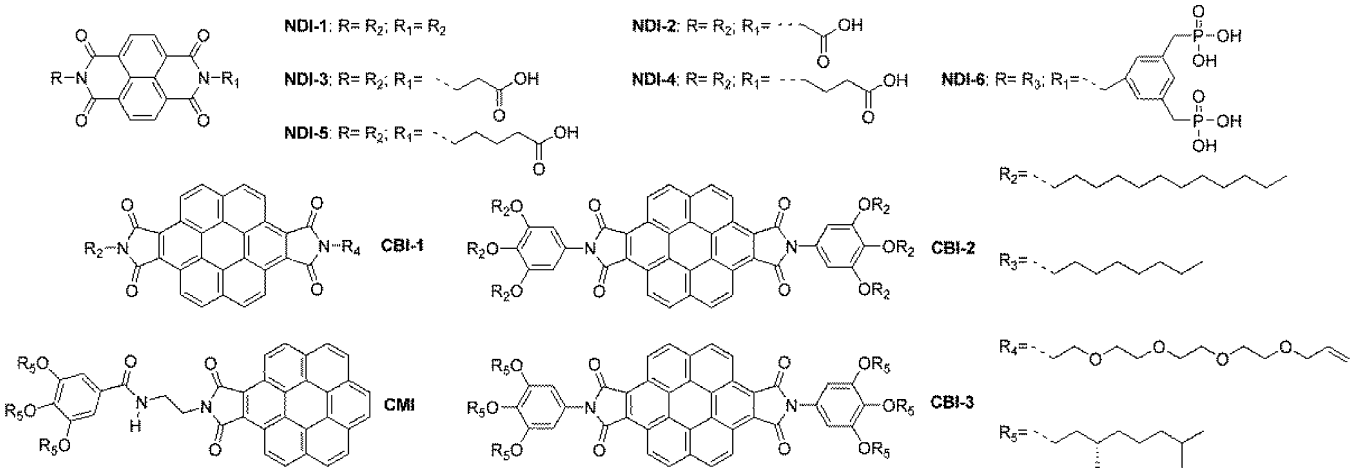

Figure 30. Molecular structures of n-type naphthalene and coronene diimides or monoimides.

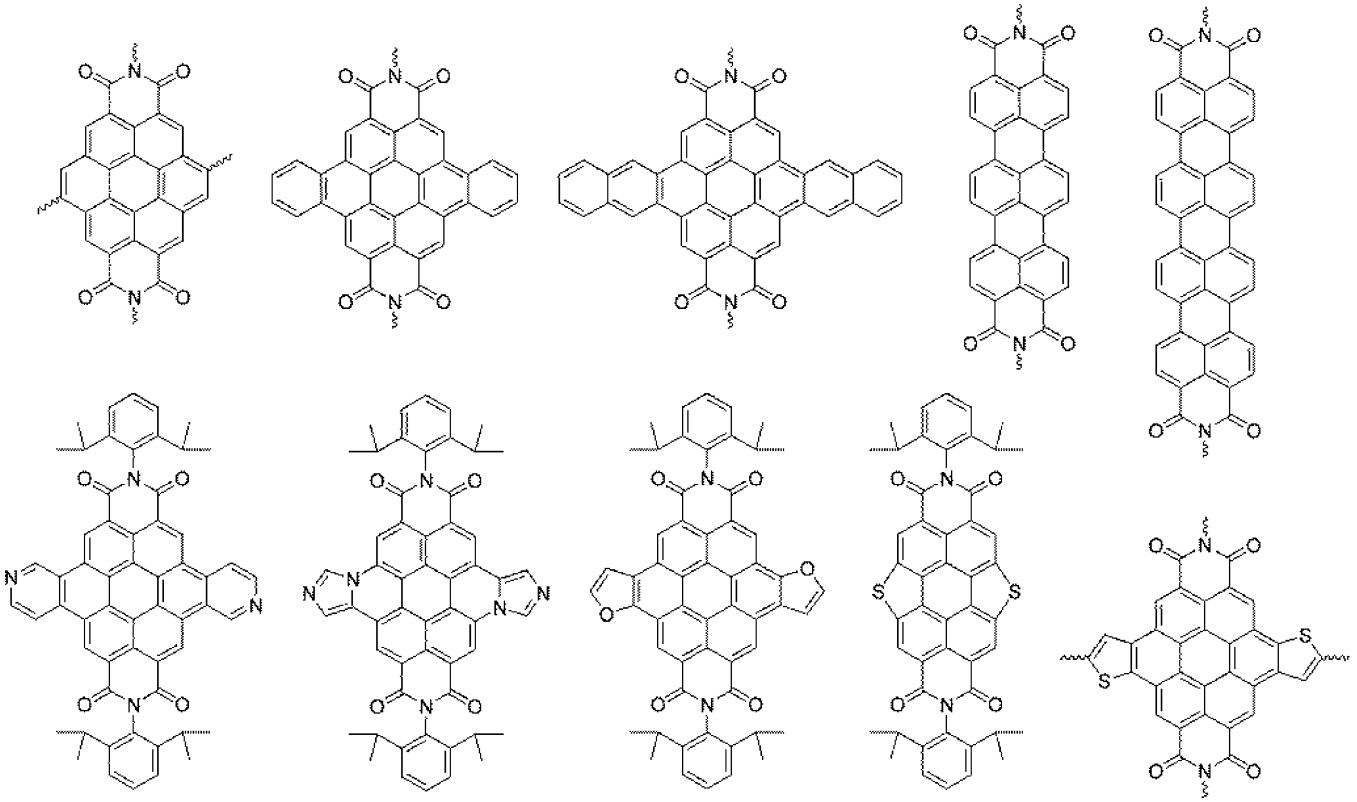

Figure 31. Molecular structures of aromatic benzene ring and N-/O-/S-heterocycle core-extended PDIs.

constructing flexible, stable, and efficient thermoelectric devices at the nanoscale. Nanofiber complexes combining p-type conducting polymers and PDIs via coassembly may result in organic TE devices (as shown in Figure 29B) that are efficient enough for practical applications, especially when doped by counterions (like I^-).[6,98,167,168]

5. ANALOGUES OF PIs

Although most of the efforts on 1D self-assembly of n-type semiconductors have been focused on PIs, similar concepts of molecular design and fabricating strategies outlined above have also been applied to other related molecules.

George and Ghosh's groups have presented promising results regarding the controlled self-assembly of a series of naphthalene and coronene diimide or monoimide molecules (NDI-1−6, CBI-1−3, and CMI) as represented in Figure 30.[170−175] Application of self-assembled 1D nanotapes of NDI-1 has been explored both in the film and in the *J*-aggregated state in solution for sensing volatile organic vapors such as $CHCl_3$ by making use of their reversible vapor- and thermo-chromism.[170] Self-assembly of NDIs (NDI-2−5) has led to a range of morphologies from 2D nanosheets to 1D nanofibers in the $CHCl_3$/methylcyclohexane system. The ultimate morphology observed depends on competition between 1D growth due to π-stacking (enhanced by H-bonding) and orthogonal directions (varying from the alkyl spacers between the NDI core and the carboxylic acid group). These nanostructures exhibit tunable photoluminescence colors spanning nearly the entire red-green-

DOI: 10.1021/acs.chemrev.5b00312
Chem. Rev. 2015, 115, 11967−11998

blue region and uncommonly high electrical conductivities of up to 10^{-4} S cm^{-1}.[173] In addition, Bhoscale and co-workers explored the pH-triggered 1D self-assembly of water-soluble NDI-6 and the enhanced fluorescence emission of nanoassemblies in both basic and acidic aqueous solutions.[174] The presence of the pH-sensitive phosphonic acid group (hydrophilic) and a long octyl chain (hydrophobic) enables tuning of the $\pi-\pi$ stacking behavior of aromatic core.[174]

Through tuning solvent composition, the coronene-based amphiphilic CBI-1 was self-assembled into 1D nanotubes and nanotapes in THF/H_2O through $\pi-\pi$ stacking and solvophobic interactions.[175] More complex compounds, such as the achiral CBI-2 and the chiral CBI-3, are also workable for fabricating 1D fibers in nonpolar methylcyclohexane via $\pi-\pi$ stacking and van der Waals interactions.[172] More importantly, a rare chiral amplification phenomenon related to supramolecular coassemblies of both CBI-2 and CBI-3 has been demonstrated.[172] A similar approach has also been used to form fluorescent nanofibers of CMI via H-bonding-induced frustrated dipolar assembly in toluene and methylcyclohexane.[171] These observations may inspire the exploration of more π-conjugated molecules possessing similar imide structure and rigid planar geometry for 1D columnar $\pi-\pi$ stacking. Comparative studies among these molecules, in conjunction with the p-type counterparts, will facilitate the design and optimization of organic electronic and optoelectronic nanodevices in the future. Although dyes combining visible-light-responsive NDIs or PIs with effective transition-metal (e.g., Ru and Ir) ligands have been used to fabricate dye-sensitized solar cells (DSCs) and near-infrared (NIR)-phosphorescence devices,[176,177] further morphology modification of these imide−metal complexes still remains challenging.

In recent years, expansion of the aromatic core of PDIs (Figure 31) has been intensively explored, aiming to tune the optoelectronic properties of these building blocks, for example, to extend the light response into the near IR region.[22,178] These core-extended molecules have shown remarkable optical and electrochemical properties.[22,24,178] Generally, expansion of the aromatic core along the long molecular axis of PDI molecule induces a bathochromic shift to NIR, whereas a hypsochromic shift occurs with enlargement along the short molecular axis.[22] As discussed above, PDIs with bay substitution often exhibit strong steric effects, inducing torsion of the planar perylene core.[22] However, it has been indicated that cyclization of the bay substitution groups will result in planar aromatic core systems, thus making $\pi-\pi$ stacking of these bay-extended molecules possible.[22,85] Moreover, the enlarged aromatic core system makes the introduction of bulky side groups at the imide positions possible, without significantly weakening their self-assembly ability.[178]

In addition to the above analogues, there has been increasing interest in the annulation of PDIs with diverse heterocycles in the bay regions (Figure 31).[86,179] S- and O-heterocycle annulated PDI analogues have served as suitable candidates for the OSCs, sensors, and other devices. This is largely due to their ability to have electron-donating moieties incorporated in their thiophene or furan units.[86,179] With the aid of attaching solubilizing 2,6-diisopropylphenyl groups, these N-/S-heterocyclic PDI molecules exhibit good solubility in various polar organic solvents, but poor solubility in solvents like hexane. Such solubility offers the capability to control the self-assembly of such molecules into 1D nanostructures (e.g., wires and rods) via tuning solvent polarity, thus regulating $\pi-\pi$ stacking, H-bonding, and electrostatic interactions.[86,180,181] The characteristics of heterocycles have significantly influenced the aggregation performance of various N-heterocycle-embedded PDIs. With the aid of facile solvent control, the π-rich thiazole ring containing PDIs demonstrates excellent 1D self-assembly ability, due to their strong $\pi-\pi$ stacking capability. Well-defined 1D nanofibers have been achieved after evaporation from casting their CH_3CN or pyridine (both are good solvents) solutions onto silicon slides. Uniform nanofibers are also formed following a slow solution diffusion process using *n*-hexane (poor solvent) and pyridine (good solvent) as discussed in section 3.1.1.[181] PDIs in which the bay region is annulated with a pyridine ring (Figure 31) represent a novel class of molecules in the supramolecular self-assembly field.[177] Because of the more challenging and complicated organic synthesis of these core-extended molecules, further optimization of synthetic methodologies deserves more attention in the future. These large molecules may be difficult to self-assemble via solution processing due to their poor solubility.[178] Nevertheless, the ordered 1D nanostructures of PI analogues, such as these that allow further chemical functionalization, may be appealing for developing novel optoelectronic nanodevices.

6. CONCLUSIONS AND OUTLOOK

This Review covers the developments in the field of 1D self-assembled nanostructure of PIs-based molecules achieved in the past decade. Abundant structural design, well-defined morphologies, facile device fabrication, and excellent optoelectronic performances make these 1D PIs nanomaterials very promising in diverse fields. While many improvements have been made, current materials still fall short of the level needed for successful commercial application in practical optoelectronics and other areas, such as photocatalytic and thermoelectric devices. On one hand, there is an unavoidable trade-off between morphology control and optoelectronic or physicochemical performance, structural design, and interfacial mismatch of devices.[182] On the other hand, while a large amount of research has focused on morphology control and property optimization, very little work has been done on precise control of the self-assembly process of PIs, and thus in-depth appreciation of the microcosmic and dynamic self-assembly process. Other than spectroscopic tools and the work of Würthner and Kim et al. on discrete dimerization of PDIs,[64,183−185] currently only theoretical calculations (normally, density functional theory, DFT) and molecular simulations have been used in studying the self-assembly kinetics. In view of novel solution-dispersible applications (e.g., photocatalytic systems), optimized PIs/semiconductor pairs with effective binding force and interfacial charge separation ability are still rare. Future challenges and prospects will be still centered on these aspects. Furthermore, in addition to structural design,[186,187] the cooperation of "bottom-up" 1D self-assembly, together with conventional "top-down" techniques and novel nanoscale engineering, may provide new ways to meet the challenge for real device development.[6,19,188−190] Research into the use of 1D PIs nanofibers in practical devices is currently in progress. Relevant fabrication techniques and morphology control should also provide an important reference for other molecular systems.

DOI: 10.1021/acs.chemrev.5b00312
Chem. Rev. 2015, 115, 11967−11998

AUTHOR INFORMATION

Corresponding Authors

*E-mail: cywang@ms.xjb.ac.cn.
*E-mail: lzang@eng.utah.edu.

Notes

The authors declare no competing financial interest.

Biographies

Shuai Chen obtained a Bachelor of Science Degree at Qufu Normal University in 2007, a Master Degree in Engineering at Jiangxi Key Laboratory of Organic Chemistry of Jiangxi Science & Technology Normal University in 2012 under the supervision of Prof. Jingkun Xu studying the preparation, characterization, and applications of conducting polymers, and then a Ph.D. degree at Xinjiang Technical Institute of Physics & Chemistry of Chinese Academy of Sciences in 2015 under the supervision of Prof. Chuanyi Wang and Prof. Ling Zang studying the synthesis and self-assembly of perylene imides, as well as their applications in the optoelectronic and photocatalytic fields. Currently, he is a teacher at Jiangxi Science & Technology Normal University. His present research includes organic synthesis, the design and fabrication of organic functional polymers and nanomaterials, and their performances and applications in the organic electronic and optoelectronic fields.

Paul Slattum obtained a Master of Science Degree at The University of Wisconsin-Madison in 1990, under the supervison of Dr. Howard Zimmerman. Paul has over 20 years of experience in synthetic organic chemistry. He is an author on 11 papers in peer reviewed journals, and holds 11 patents in the fields of self-assembly, medicinal chemistry, and bioconjugation. At MirusBio Corp., he helped to develop nanoparticles for the in vivo delivery of nucleic acids and a series of reagents for the covalent labelling of nucleic acids. He is currently an employee of Vaporsens, Inc. and visiting scientist at University of Utah where he designs and synthesizes new perylene-based building blocks used in nanofibril-based sensors for the trace detection of explosive, narcotic, and toxic industrial chemical vapor.

Chuanyi Wang is a "One Hundred Talents Program" professor at Xinjiang Technical Institute of Physics & Chemistry (XTIPC) of Chinese Academy of Sciences (CAS). He obtained his Ph.D. degree from Institute of Photographic Chemistry of CAS in 1998, worked in Germany (Institute for Solar Energy Research in Hannover and Free University Berlin) as an Alexander von Humboldt research fellow with Prof. Detlef Bahnemann from 1999 to 2000, and then worked in the U.S. (Tufts University and Missouri University-Kansas City) as a research faculty from 2000 to 2010. Currently, Dr. Wang serves as the Director of Laboratory of Environment of Science & Technology of XTIPC, CAS, and Head of the CAS-SAFEA International Partnership Program for Creative Research Teams as well as CAS Cross-Cooperation Research Team. His research covers catalysis and photo/electro-catalysis at nanostructured materials including material design, synthesis, functionality evaluation, and in situ surface probe studies with focus on applications in photo/electrochemical energy conversion and environmental remediation.

Ling Zang is a USTAR professor at University of Utah, affiliated with the Department of Materials Science and Engineering, Department of Chemistry, and Nano Institute of Utah. He received his B.S. in chemistry from Tsinghua University and Ph.D. in chemistry from the Chinese Academy of Sciences. His current research focuses on nanoscale imaging and molecular probing, organic semiconductors and nanostructures, optoelectronic sensors, and nanodevices, with the goal to achieve practical applications in the areas of national security, renewable energy, and clean environment.

ACKNOWLEDGMENTS

All individual contributions in the cited references are gratefully acknowledged, and any omission is regretted. We gratefully acknowledge financial support from the National Natural Science Foundation of China (Grant no. 21173261), the CAS/SAFEA International Partnership Program for Creative Research Teams, the CAS "Cross Cooperation Program for Creative Research Teams" (Grant no. Y251821601), and the National Science Foundation (CHE 0641353, CHE 0931466, CBET 730667).

REFERENCES

(1) Whitesides, G. M.; Mathias, J. P.; Seto, C. T. Molecular Self-Assembly and Nanochemistry: A Chemical Strategy for the Synthesis of Nanostructures. *Science* **1991**, *254*, 1312−1319.
(2) Ariga, K.; Hill, J. P.; Lee, M. V.; Vinu, A.; Charvet, R.; Acharya, S. Challenges and Breakthroughs in Recent Research on Self-Assembly. *Sci. Technol. Adv. Mater.* **2008**, *9*, 014109.
(3) Whitesides, G. M.; Simanek, E. E.; Mathias, J. P.; Seto, C. T.; Chin, D. N.; Mammen, M.; Gordon, D. M. Noncovalent Synthesis: Using Physical-Organic Chemistry to Make Aggregates. *Acc. Chem. Res.* **1995**, *28*, 37−44.
(4) Hoeben, F. J. M.; Jonkheijm, P.; Meijer, E. W.; Schenning, A. P. H. J. About Supramolecular Assemblies of π-Conjugated Systems. *Chem. Rev.* **2005**, *105*, 1491−1546.
(5) Zhang, Z. K.; Ma, R. J.; Shi, L. Q. Cooperative Macromolecular Self-Assembly toward Polymeric Assemblies with Multiple and Bioactive Functions. *Acc. Chem. Res.* **2014**, *47*, 1426−1437.
(6) Schenning, A. P. H. J.; Meijer, E. W. Supramolecular Electronics; Nanowires from Self-Assembled π-Conjugated Systems. *Chem. Commun.* **2005**, 3245−3258.
(7) Wu, J. S.; Pisula, W.; Müllen, K. Graphenes as Potential Material for Electronics. *Chem. Rev.* **2007**, *107*, 718−747.
(8) Würthner, F. Supramolecular Polymerization: Living It Up. *Nat. Chem.* **2014**, *6*, 171−173.
(9) González-Rodríguez, D.; Schenning, A. P. H. J. Hydrogen-Bonded Supramolecular π-Functional Materials. *Chem. Mater.* **2011**, *23*, 310−325.
(10) Nguyen, T. Q.; Martel, R.; Bushey, M.; Avouris, P.; Carlsen, A.; Nuckolls, C.; Brus, L. Self-Assembly of 1-D Organic Semiconductor Nanostructures. *Phys. Chem. Chem. Phys.* **2007**, *9*, 1515−1532.
(11) Kim, F. S.; Ren, G. Q.; Jenekhe, S. A. One-Dimensional Nanostructures of π-Conjugated Molecular Systems: Assembly, Properties, and Applications from Photovoltaics, Sensors, and Nanophotonics to Nanoelectronics. *Chem. Mater.* **2011**, *23*, 682−732.
(12) Meijer, E. W.; Schenning, A. P. H. J. Chemistry: Material Marriage in Electronics. *Nature* **2002**, *419*, 353−354.
(13) Wang, X.; Li, Y. D. Solution-Based Synthetic Strategies for 1-D Nanostructures. *Inorg. Chem.* **2006**, *45*, 7522−7534.
(14) Zang, L.; Che, Y. K.; Moore, J. S. One-Dimensional Self-Assembly of Planar π-Conjugated Molecules: Adaptable Building Blocks for Organic Nanodevices. *Acc. Chem. Res.* **2008**, *41*, 1596−1608.
(15) Zhao, Y. S.; Fu, H. B.; Peng, A. D.; Ma, Y.; Liao, Q.; Yao, J. N. Construction and Optoelectronic Properties of Organic One-Dimensional Nanostructures. *Acc. Chem. Res.* **2010**, *43*, 409−418.
(16) Su, B.; Wu, Y. C.; Jiang, L. The Art of Aligning One-Dimensional (1D) Nanostructures. *Chem. Soc. Rev.* **2012**, *41*, 7832−7856.
(17) Dasgupta, N. P.; Sun, J. W.; Liu, C.; Brittman, S.; Andrews, S. C.; Lim, J.; Gao, H. W.; Yan, R. X.; Yang, P. D. 25th Anniversary Article: Semiconductor Nanowires-Synthesis, Characterization, and Applications. *Adv. Mater.* **2014**, *26*, 2137−2184.
(18) Aida, T.; Meijer, E. W.; Stupp, S. I. Functional Supramolecular Polymers. *Science* **2012**, *335*, 813−817.

DOI: 10.1021/acs.chemrev.5b00312
Chem. Rev. 2015, 115, 11967−11998

(19) Lee, D. Y.; Zhang, C. Y.; Gao, H. F. Facile Production of Polypyrrole Nanofibers Using a Freeze-Drying Method. *Macromol. Chem. Phys.* **2014**, *215*, 669−674.
(20) Balakrishnan, K.; Datar, A.; Oitker, R.; Chen, H.; Zuo, J. M.; Zang, L. Nanobelt Self-Assembly from an Organic n-Type Semiconductor: Propoxyethyl-PTCDI. *J. Am. Chem. Soc.* **2005**, *127*, 10496−10497.
(21) Würthner, F. Perylene Bisimide Dyes as Versatile Building Blocks for Functional Supramolecular Architectures. *Chem. Commun.* **2004**, 1564−1579.
(22) Li, C.; Wonneberger, H. Perylene Imides for Organic Photovoltaics: Yesterday, Today, and Tomorrow. *Adv. Mater.* **2012**, *24*, 613−636.
(23) Huang, C.; Barlow, S.; Marder, S. R. Perylene-3,4,9,10-Tetracarboxylic Acid Diimides: Synthesis, Physical Properties, and Use in Organic Electronics. *J. Org. Chem.* **2011**, *76*, 2386−2407.
(24) Zhan, X. W.; Facchetti, A.; Barlow, S.; Marks, T. J.; Ratner, M. A.; Wasielewski, M. R.; Marder, S. R. Rylene and Related Diimides for Organic Electronics. *Adv. Mater.* **2011**, *23*, 268−284.
(25) Elemans, J. A. A. W.; van Hameren, R.; Nolte, R. J. M.; Rowan, A. E. Molecular Materials by Self-Assembly of Porphyrins, Phthalocyanines, and Perylenes. *Adv. Mater.* **2006**, *18*, 1251−1266.
(26) Görl, D.; Zhang, X.; Würthner, F. Molecular Assemblies of Perylene Bisimide Dyes in Water. *Angew. Chem., Int. Ed.* **2012**, *51*, 6328−6348.
(27) Hasegawa, M.; Iyoda, M. Conducting Supramolecular Nanofibers and Nanorods. *Chem. Soc. Rev.* **2010**, *39*, 2420−2427.
(28) Yao, W.; Zhao, Y. S. Tailoring The Self-Assembled Structures and Photonic Properties of Organic Nanomaterials. *Nanoscale* **2014**, *6*, 3467−3473.
(29) Supura, M.; Fukuzumi, S. Energy and Electron Transfer of One-Dimensional Nanomaterials of Perylene Diimides. *ECS J. Solid State Sci. Technol.* **2013**, *2*, M3051−M3062.
(30) Zhao, Q. L.; Zhang, S.; Liu, Y.; Mei, J.; Chen, S. J.; Lu, P.; Qin, A. J.; Ma, Y. G.; Sun, J. Z.; Tang, B. Z. Tetraphenylethenyl-Modified Perylene Bisimide: Aggregation-Induced Red Emission, Electrochemical Properties and Ordered Microstructures. *J. Mater. Chem.* **2012**, *22*, 7387−7394.
(31) Liu, R. C.; Holman, M. W.; Zang, L.; Adams, D. M. Single-Molecule Spectroscopy of Intramolecular Electron Transfer in Donor-Bridge-Acceptor Systems. *J. Phys. Chem. A* **2003**, *107*, 6522−6526.
(32) Metzger, R. M. Unimolecular Electronics. *J. Mater. Chem.* **2008**, *18*, 4364−4396.
(33) Metzger, R. M. Unimolecular Electronics. *Chem. Rev.* **2015**, *115*, 5056−5115.
(34) Vajiravelu, S.; Ramunas, L.; Vidas, G. J.; Valentas, G.; Vygintas, J.; Valiyaveettil, S. Effect of Substituents on the Electron Transport Properties of Bay Substituted Perylene Diimide Derivatives. *J. Mater. Chem.* **2009**, *19*, 4268−4275.
(35) Datar, A.; Balakrishnan, K.; Yang, X. M.; Zuo, X. B.; Huang, J. L.; Oitker, R.; Yen, M.; Zhao, J. C.; Tiede, D. M.; Zang, L. Linearly Polarized Emission of an Organic Semiconductor Nanobelt. *J. Phys. Chem. B* **2006**, *110*, 12327−12332.
(36) Huang, Y. W.; Fu, L. N.; Zou, W. J.; Zhang, F. L.; Wei, Z. X. Ammonia Sensory Properties Based on Single-Crystalline Micro/Nanostructures of Perylenediimide Derivatives: Core-Substituted Effect. *J. Phys. Chem. C* **2011**, *115*, 10399−10404.
(37) Zhou, J.; Xue, L.; Shi, Y.; Li, X. Y.; Xue, Q. B.; Wang, S. Q. Synthesis and Self-Assembly of Perylenetetracarboxylic Diimide Derivatives with Helical Oligo(L-Lactic Acid)$_n$ Segments. *Langmuir* **2012**, *28*, 14386−14394.
(38) Ke, D. M.; Zhan, C. L.; Xu, S. P.; Ding, X. L.; Peng, A. D.; Sun, J.; He, S. G.; Li, A. D. Q.; Yao, J. N. Self-Assembled Hollow Nanospheres Strongly Enhance Photoluminescence. *J. Am. Chem. Soc.* **2011**, *133*, 11022−11025.
(39) Chen, Y. L.; Feng, Y. J.; Gao, J.; Bouvet, M. Self-Assembled Aggregates of Amphiphilic Perylene Diimide-Based Semiconductor Molecules: Effect of Morphology on Conductivity. *J. Colloid Interface Sci.* **2012**, *368*, 387−394.
(40) Sukul, P. K.; Datta, A.; Malik, S. Light Harvesting and Amplification of Emission of Donor Perylene-Acceptor Perylene Aggregates in Aqueous Medium. *Chem. - Eur. J.* **2014**, *20*, 3019−3022.
(41) Chen, Z. J.; Stepanenko, V.; Dehm, V.; Prins, P.; Siebbeles, L. D. A.; Seibt, J.; Marquetand, P.; Engel, V.; Würthner, F. Photoluminescence and Conductivity of Self-Assembled π-π Stacks of Perylene Bisimide Dyes. *Chem. - Eur. J.* **2007**, *13*, 436−449.
(42) Yagai, S.; Seki, T.; Karatsu, T.; Kitamura, A.; Würthner, F. Transformation from H- to J-Aggregated Perylene Bisimide Dyes by Complexation with Cyanurates. *Angew. Chem., Int. Ed.* **2008**, *47*, 3367−3371.
(43) Dössel, L. F.; Kamm, V.; Howard, I. A.; Laquai, F.; Pisula, W.; Feng, X. L.; Li, C.; Takase, M.; Kudernac, T.; Feyter, S. D.; Müllen, K. Synthesis and Controlled Self-Assembly of Covalently Linked Hexa *peri*-Hexabenzocoronene/Perylene Diimide Dyads as Models to Study Fundamental Energy and Electron Transfer Processes. *J. Am. Chem. Soc.* **2012**, *134*, 5876−5886.
(44) Marciniak, H.; Li, X. Q.; Würthner, F.; Lochbrunner, S. One-Dimensional Exciton Diffusion in Perylene Bisimide Aggregates. *J. Phys. Chem. A* **2011**, *115*, 648−654.
(45) Fennel, F.; Wolter, S.; Xie, Z. Q.; Plötz, P. A.; Kühn, O.; Würthner, F.; Lochbrunner, S. Biphasic Self-Assembly Pathways and Size-Dependent Photophysical Properties of Perylene Bisimide Dye Aggregates. *J. Am. Chem. Soc.* **2013**, *135*, 18722−18725.
(46) Bordo, K.; Schiek, M.; Rubahn, H. G. Nanowires and Nanotubes from π-Conjugated Organic Materials Fabricated by Template Wetting. *Appl. Phys. A: Mater. Sci. Process.* **2014**, *114*, 1067−1074.
(47) Muth, M. A.; Gupta, G.; Wicklein, A.; Orozco, M. C.; Albrecht, T. T.; Thelakkat, M. Crystalline vs Liquid Crystalline Perylene Bisimides: Improved Electron Mobility via Substituent Alteration. *J. Phys. Chem. C* **2014**, *118*, 92−102.
(48) Eakins, G. L.; Gallaher, J. K.; Keyzers, R. A.; Falber, A.; Webb, J. E. A.; Laos, A.; Tidhar, Y.; Weissman, H.; Rybtchinski, B.; Thordarson, P.; Hodgkiss, J. M. Thermodynamic Factors Impacting the Peptide-Driven Self-Assembly of Perylene Diimide Nanofibers. *J. Phys. Chem. B* **2014**, *118*, 8642−8651.
(49) Sun, Y.; He, C.; Sun, K.; Li, Y.; Dong, H. L.; Wang, Z. H.; Li, Z. B. Fine-Tuned Nanostructures Assembled from L-lysine-Functionalized Perylene Bisimides. *Langmuir* **2011**, *27*, 11364−11371.
(50) Marty, R.; Szilluweit, R.; Sánchez-Ferrer, A.; Bolisetty, S.; Adamcik, J.; Mezzenga, R.; Spitzner, E. C.; Feifer, M.; Steinmann, S. N.; Corminboeuf, C.; Frauenrath, H. Hierarchically Structured Microfibers of "Single Stack" Perylene Bisimide and Quaterthiophene Nanowires. *ACS Nano* **2013**, *7*, 8498−8508.
(51) Boobalan, G.; Imran, P. M.; Nagarajan, S. Self-Assembly, Optical and Electrical Properties of Fork-Tailed Perylene Bisimides. *Superlattices Microstruct.* **2012**, *51*, 921−932.
(52) Boobalan, G.; Imran, P. K. M.; Nagarajan, S. Luminescent One-Dimensional Nanostructures of Perylene Bisimides. *Spectrochim. Acta, Part A* **2013**, *113*, 340−345.
(53) Che, Y. K.; Yang, X. M.; Liu, G. L.; Yu, C.; Ji, H. W.; Zuo, J. M.; Zhao, J. C.; Zang, L. Ultrathin n-Type Organic Nanoribbons with High Photoconductivity and Application in Optoelectronic Vapor sensing of Explosives. *J. Am. Chem. Soc.* **2010**, *132*, 5743−5750.
(54) Boobalan, G.; Imran, P. M.; Ramkumar, S. G.; Nagarajan, S. Fabrication of Luminescent Perylene Bisimide Nanorods. *J. Lumin.* **2014**, *146*, 387−393.
(55) Che, Y.; Datar, A.; Yang, X. M.; Naddo, T.; Zhao, J. C.; Zang, L. Enhancing One-Dimensional Charge Transport Through Intermolecular π-Electron Delocalization: Conductivity Improvement for Organic Nanobelts. *J. Am. Chem. Soc.* **2007**, *129*, 6354−6355.
(56) Briseno, A. L.; Mannsfeld, S. C. B.; Reese, C.; Hancock, J. M.; Xiong, Y. J.; Jenekhe, S. A.; Bao, Z. N.; Xia, Y. N. Perylenediimide Nanowires and Their Use in Fabricating Field-Effect Transistors and Complementary Inverters. *Nano Lett.* **2007**, *7*, 2847−2853.
(57) Murugavelu, M.; Imran, P. K. M.; Sankaran, K. R.; Nagarajan, S. Self-Assembly and Photophysical Properties of a Minuscule Tailed Perylene Bisimide. *Mater. Sci. Semicond. Process.* **2013**, *16*, 461−466.

DOI: 10.1021/acs.chemrev.5b00312
Chem. Rev. 2015, 115, 11967−11998

(58) Ameena, M. Y.; Abhijith, T.; De, S.; Ray, S. K.; Reddy, V. S. Linearly Polarized Emission from PTCDI-C8 One-Dimensional Microstructures. *Org. Electron.* **2013**, *14*, 554−559.
(59) Boobalan, G.; Imran, P. K. M.; Manoharan, C.; Nagarajan, S. Fabrication of Highly Fluorescent Perylene Bisimide Nanofibers Through Interfacial Self-Assembly. *J. Colloid Interface Sci.* **2013**, *393*, 377−383.
(60) Senthilraja, A.; Krishnakumar, B.; Swaminathan, M.; Nagarajan, S. Self-Assembly, Photophysical and Electrochemical Properties and Activation of the TiO_2 Photocatalyst by Perylene Bisimide. *New J. Chem.* **2014**, *38*, 1573−1580.
(61) Boobalan, G.; Imran, P. M.; Nagarajan, S. Self-Assembly and Optical Properties of N,N'-Bis(4-(1-Benzylpiperidine))Perylene-3,4,9,10-Tetracarboxylic Diimide. *Supramol. Chem.* **2012**, *24*, 238−246.
(62) Che, Y. K.; Datar, A.; Balakrishnan, K.; Zang, L. Ultralong Nanobelts Self-Assembled from an Asymmetric Perylene Tetracarboxylic Diimide. *J. Am. Chem. Soc.* **2007**, *129*, 7234−7235.
(63) Islam, M. R.; Sundararajan, P. R. Self-Assembly of a Set of Hydrophilic-Solvophobic-Hydrophobic Coil-Rod-Coil Molecules Based on Perylene Diimide. *Phys. Chem. Chem. Phys.* **2013**, *15*, 21058−21069.
(64) Ma, Y. E. X. J.; Zhang, Y. F.; Zhang, Y. B.; Duan, R.; Ji, H. W.; Li, J.; Che, Y. K.; Zhao, J. C. Fluorescent Bilayer Nanocoils Assembled from an Asymmetric Perylene Diimide Molecule with Ultrasensitivity for Amine Vapors. *Chem. Commun.* **2014**, *50*, 13596−13599.
(65) Che, Y. K.; Yang, X. M.; Loser, S.; Zang, L. Expedient Vapor Probing of Organic Amines Using Fluorescent Nanofibers Fabricated from an n-Type Organic Semiconductor. *Nano Lett.* **2008**, *8*, 2219−2223.
(66) Chen, Z. J.; Fimmel, B.; Würthner, F. Solvent and Substituent Effects on Aggregation Constants of Perylene Bisimide π-Stacks − a Linear Free Energy Relationship Analysis. *Org. Biomol. Chem.* **2012**, *10*, 5845−5855.
(67) Usowicz, M. T.; Kelley, M. J.; Singer, K. D.; Duzhko, V. V. Tailored One- and Two-Dimensional Self-Assembly of a Perylene Diimide Derivative in Organic Solvents. *J. Phys. Chem. B* **2011**, *115*, 9703−9709.
(68) Shao, C. Z.; Grüne, M.; Stolte, M.; Würthner, F. Perylene Bisimide Dimer Aggregates: Fundamental Insights into Self-Assembly by NMR and UV/Vis Spectroscopy. *Chem. - Eur. J.* **2012**, *18*, 13665−13677.
(69) Ren, X. K.; Sun, B.; Tsai, C. C.; Tu, Y. F.; Leng, S. W.; Li, K. X.; Kang, Z.; Van Horn, R. M.; Li, X. P.; Zhu, M. F.; Wesdemiotis, C.; Zhang, W. B.; Cheng, S. Z. D. Synthesis, Self-Assembly, and Crystal Structure of a Shape-Persistent Polyhedral-Oligosilsesquioxane-Nanoparticle-Tethered Perylene Diimide. *J. Phys. Chem. B* **2010**, *114*, 4802−4810.
(70) Yang, X. G.; Yuan, H.; Zhao, Q. L.; Yang, Q.; Chen, X. H. Self-Assembly Constructed by Perylene Bisimide Derivatives Bearing Complementary Hydrogen-Bonding Moieties. *J. Cent. South Univ. Technol.* **2009**, *16*, 0206−0211.
(71) Würthner, F.; Hanke, B.; Lysetska, M.; Lambright, G.; Harms, G. S. Gelation of a Highly Fluorescent Urea-Functionalized Perylene Bisimide Dye. *Org. Lett.* **2005**, *7*, 967−970.
(72) Datar, A.; Oitker, R.; Zang, L. Surface-Assisted One-Dimensional Self-Assembly of a Perylene Based Semiconductor Molecule. *Chem. Commun.* **2006**, 1649−1651.
(73) Balakrishnan, K.; Datar, A.; Naddo, T.; Huang, J. L.; Oitker, R.; Yen, M.; Zhao, J. C.; Zang, L. Effect of Side-Chain Substituents on Self-Assembly of Perylene Diimide Molecules: Morphology Control. *J. Am. Chem. Soc.* **2006**, *128*, 7390−7398.
(74) Luca, G. D.; Liscio, A.; Maccagnani, P.; Nolde, F.; Palermo, V.; Müllen, K.; Samorì, P. Nucleation-Governed Reversible Self-Assembly of an Organic Semiconductor at Surfaces: Long-Range Mass Transport Forming Giant Functional Fibers. *Adv. Funct. Mater.* **2007**, *17*, 3791−3798.
(75) Lambrecht, J.; Saragi, T. P. I.; Onken, K.; Salbeck, J. Ultralong Single Organic Semiconducting Nano/Microwires Based on Spiro-Substituted Perylenetetracarboxylic Diimide. *ACS Appl. Mater. Interfaces* **2011**, *3*, 1809−1812.
(76) Lambrecht, J.; Saragi, T. P. I.; Salbeck, J. Self-Assembled Organic Micro-/Nanowires from an Air Stable n-Semiconducting Perylenediimide Derivative as Building Blocks for Organic Electronic Devices. *J. Mater. Chem.* **2011**, *21*, 18266−18270.
(77) Kim, B. J.; Yu, H.; Oh, J. H.; Kang, M. S.; Cho, J. H. Electrical Transport through Single Nanowires of Dialkyl Perylene Diimide. *J. Phys. Chem. C* **2013**, *117*, 10743−10749.
(78) Huang, H. L.; Chou, C. E.; Che, Y. K.; Li, L. G.; Wang, C.; Yang, X. M.; Peng, Z. H.; Zang, L. Morphology Control of Nanofibril Donor-Acceptor Heterojunction to Achieve High Photoconductivity: Exploration of New Molecular Design Rule. *J. Am. Chem. Soc.* **2013**, *135*, 16490−16496.
(79) Kim, D. H.; Lee, D. Y.; Lee, H. S.; Lee, W. H.; Kim, Y. H.; Han, J. I.; Cho, K. High-Mobility Organic Transistors Based on Single-Crystalline Microribbons of Triisopropylsilylethynyl Pentacene via Solution-Phase Self-Assembly. *Adv. Mater.* **2007**, *19*, 678−682.
(80) Jordan, B. J.; Ofir, Y.; Patra, D.; Caldwell, S. T.; Kennedy, A.; Joubanian, S.; Rabani, G.; Cooke, G.; Rotello, V. M. Controlled Self-Assembly of Organic Nanowires and Platelets Using Dipolar and Hydrogen-Bonding Interactions. *Small* **2008**, *4*, 2074−2078.
(81) Huang, H. L.; Gross, D. E.; Yang, X. M.; Moore, J. S.; Zang, L. One-Step Surface Doping of Organic Nanofibers to Achieve High Dark Conductivity and Chemiresistor Sensing of Amines. *ACS Appl. Mater. Interfaces* **2013**, *5*, 7704−7708.
(82) Shen, Y. T.; Lei, D.; Tan, J. H.; Feng, Y. Y.; Zhang, B.; Li, Y.; Dong, H. L.; Hu, W. P.; Feng, W. Topological Structural Transformations of Nanoparticle Self-Assemblies Mediated by Phase Transfer and Their Application as Organic-Inorganic Hybrid Photodetectors. *ACS Appl. Mater. Interfaces* **2013**, *5*, 12254−12261.
(83) Guo, Q.; Wang, J. C.; Zhu, L. Y.; Wei, Z. X. Modulating The Helicity of Sugar-Substituted Perylene Diimide Self-Assemblies by Solvent Polarilities. *Chin. J. Chem.* **2015**, *33*, 95−100.
(84) Su, W.; Zhang, Y. X.; Zhao, C. T.; Li, X. Y.; Jiang, J. Z. Self-Assembled Organic Nanostructures: Effect of Substituents on the Morphology. *ChemPhysChem* **2007**, *8*, 1857−1862.
(85) Zeng, T.; Sun, B.; Lordick, W.; Zhu, M. F. The Effect of 1,7-Bromine Substitution at Bay Area on Self-Assembly Behavior and Photo Physical Properties of Perylene Diimide. http://www.paper.edu.cn/releasepaper/content/201401-683.html, 2014.
(86) Yu, Y. W.; Li, Y. J.; Qin, Z. H.; Jiang, R. S.; Liu, H. B.; Li, Y. L. Designed Synthesis and Supramolecular Architectures of Furan-Substituted Perylene Diimide. *J. Colloid Interface Sci.* **2013**, *399*, 13−18.
(87) Li, X. Q.; Zhang, X.; Ghosh, S.; Würthner, F. Highly Fluorescent Lyotropic Mesophases and Organogels Based on *J*-Aggregates of Core-Twisted Perylene Bisimide Dyes. *Chem. - Eur. J.* **2008**, *14*, 8074−8078.
(88) Li, X. Q.; Stepanenko, V.; Chen, Z. J.; Prins, P.; Siebbeles, L. D. A.; Würthner, F. Functional Organogels from Highly Efficient Organogelator Based on Perylene Bisimide Semiconductor. *Chem. Commun.* **2006**, 3871−3873.
(89) Zhang, Z. G.; Zhan, C. L.; Zhang, X.; Zhang, S. L.; Huang, J. H.; Li, A. D. Q.; Yao, J. N. A Self-Assembly Phase Diagram from Amphiphilic Perylene Diimide. *Chem. - Eur. J.* **2012**, *18*, 12305−12313.
(90) Datar, A.; Balakrishnan, K.; Zang, L. One-Dimensional Self-Assembly of a Water Soluble Perylene Diimide Molecule by pH Triggered Hydrogelation. *Chem. Commun.* **2013**, *49*, 6894−6896.
(91) Draper, E. R.; Walsh, J. J.; McDonald, T. O.; Zwijnenburg, M. A.; Cameron, P. J.; Cowan, A. J.; Adams, D. J. Air-Stable Photoconductive Films Formed from Perylene Bisimide Gelators. *J. Mater. Chem. C* **2014**, *2*, 5570−5575.
(92) Shahar, C.; Baram, J.; Tidhar, Y.; Weissman, H.; Cohen, S. R.; Pinkas, I.; Rybtchinski, B. Self-Assembly of Light-Harvesting Crystalline Nanosheets in Aqueous Media. *ACS Nano* **2013**, *7*, 3547−3556.
(93) Arulkashmir, A.; Jain, B.; John, J. C.; Roy, K.; Krishnamoorthy, K. Chemically Doped Perylene Diimide Lamellae Based Field Effect

DOI: 10.1021/acs.chemrev.5b00312
Chem. Rev. 2015, 115, 11967−11998

Transistor with Low Operating Voltage and High Charge Carrier Mobility. *Chem. Commun.* **2014**, *50*, 326−328.
(94) Bai, S.; Debnath, S.; Javid, N.; Frederix, P. W. J. M.; Fleming, S.; Pappas, C.; Ulijn, R. V. Differential Self-Assembly and Tunable Emission of Aromatic Peptide Bola-Amphiphiles Containing Perylene Bisimide in Polar Solvents Including Water. *Langmuir* **2014**, *30*, 7576−7584.
(95) Huang, Y. W.; Quan, B. G.; Wei, Z. X.; Liu, G. T.; Sun, L. F. Self-Assembled Organic Functional Nanotubes and Nanorods and Their Sensory Properties. *J. Phys. Chem. C* **2009**, *113*, 3929−3933.
(96) Supur, M.; Fukuzumi, S. Photodriven Electron Transport within The Columnar Perylenediimide Nanostructures Self-assembled with Sulfonated Porphyrins in Water. *J. Phys. Chem. C* **2012**, *116*, 23274−23282.
(97) Supur, M.; Fukuzumi, S. Tuning The Photodriven Electron Transport within The Columnar Perylenediimide Stacks by Changing The π-Extent of The Electron Donors. *Phys. Chem. Chem. Phys.* **2013**, *15*, 2539−2546.
(98) Rao, K. V.; George, S. J. Supramolecular Alternate Co-Assembly through a Non-Covalent Amphiphilic Design: Conducting Nanotubes with a Mixed D-A Structure. *Chem. - Eur. J.* **2012**, *18*, 14286−14291.
(99) Russ, B.; Robb, M. J.; Brunetti, F. G.; Miller, P. L.; Perry, E. E.; Patel, S. N.; Ho, V.; Chang, W. B.; Urban, J. J.; Chabinyc, M. L.; et al. Power Factor Enhancement in Solution-Processed Organic n-Type Thermoelectrics through Molecular Design. *Adv. Mater.* **2014**, *26*, 3473−3477.
(100) Zhang, Q.; Sun, Y. M.; Xu, W.; Zhu, D. B. Organic Thermoelectric Materials: Emerging Green Energy Materials Converting Heat to Electricity Directly and Efficiently. *Adv. Mater.* **2014**, *26*, 6829−6851.
(101) Cao, X. Q.; Wu, Y. S.; Fu, H. B.; Yao, J. N. J. Self-Assembly of Perylenediimide Nanobelts and Their Size-Tunable Exciton Dynamic Properties. Phys. *J. Phys. Chem. Lett.* **2011**, *2*, 2163−2167.
(102) Sayyad, A. S.; Balakrishnan, K.; Ajayan, P. M. Chemical Reaction Mediated Self-Assembly of PTCDA into Nanofibers. *Nanoscale* **2011**, *3*, 3605−3608.
(103) Kozma, E.; Catellani, M. Perylene Diimides Based Materials For Organic Solar Cells. *Dyes Pigm.* **2013**, *98*, 160−179.
(104) Xu, L.; Hirono, M.; Seki, T.; Kurata, H.; Karatsu, T.; Kitamura, A.; Kuzuhara, D.; Yamada, H.; Ohba, T.; Saeki, A.; et al. Covalent Modular Approach for Dimension-Controlled Self-Organization of Perylene Bisimide Dyes. *Chem. - Eur. J.* **2013**, *19*, 6561−6565.
(105) Peng, J.; Zhai, F.; Guo, X. Y.; Jiang, X. P.; Ma, Y. G. Self-Assembly and Phase Separation of Amphiphilic Dyads Based on 4, 7-Bis (2-Thienyl) Benzothiodiazole and Perylene Diimide. *RSC Adv.* **2014**, *4*, 13078−13084.
(106) Che, Y. K.; Huang, H. L.; Xu, M.; Zhang, C. Y.; Bunes, B. R.; Yang, X. M.; Zang, L. Interfacial Engineering of Organic Nanofibril Heterojunctions into Highly Photoconductive Materials. *J. Am. Chem. Soc.* **2011**, *133*, 1087−1091.
(107) Huang, Y. W.; Wei, Z. X. Self-Assembly of Chiral Amphiphiles with π-Conjugated Tectons. *Chin. Sci. Bull.* **2012**, *57*, 4246−4256.
(108) Zhang, L.; Qin, L.; Wang, X. F.; Cao, H.; Liu, M. H. Supramolecular Chirality in Self-Assembled Soft Materials: Regulation of Chiral Nanostructures and Chiral Functions. *Adv. Mater.* **2014**, *26*, 6959−6964.
(109) Huang, Y. W.; Hu, J. C.; Kuang, W. F.; Wei, Z. X.; Faul, C. F. J. Modulating Helicity through Amphiphilicity-Tuning Supramolecular Interactions for The Controlled Assembly of Perylenes. *Chem. Commun.* **2011**, *47*, 5554−5556.
(110) Hu, J. C.; Kuang, W. F.; Deng, K.; Zou, W. J.; Huang, Y. W.; Wei, Z. X.; Faul, C. F. J. Self-Assembled Sugar-Substituted Perylene Diimide Nanostructures with Homochirality and High Gas Sensitivity. *Adv. Funct. Mater.* **2012**, *22*, 4149−4158.
(111) Huang, Y. W.; Wang, J. C.; Zhai, H. Y.; Zhu, L. Y.; Wei, Z. X. Helical Supramolecular Aggregates of Sugar-Based Perylene Dyes: The Effect of Core-Substituted Groups. *Soft Matter* **2014**, *10*, 7920−7924.
(112) Sun, K.; Xiao, C. Y.; Liu, C. M.; Fu, W. X.; Wang, Z. H.; Li, Z. B. Thermally Sensitive Self-Assembly of Glucose-Functionalized Tetrachloro-Perylene Bisimides: from Twisted Ribbons to Microplates. *Langmuir* **2014**, *30*, 11040−11045.
(113) Kumar, J.; Nakashima, T.; Kawai, T. Inversion of Supramolecular Chirality in Bichromophoric Perylene Bisimides: Influence of Temperature and Ultrasound. *Langmuir* **2014**, *30*, 6030−6037.
(114) Finlayson, C. E.; Friend, R. H.; Otten, M. B. J.; Schwartz, E.; Cornelissen, J. J. L. M.; Nolte, R. J. M.; Rowan, A. E.; Samorì, P.; Palermo, V.; Liscio, A.; et al. Electronic Transport Properties of Ensembles of Perylene-Substituted Poly-Isocyanopeptide Arrays. *Adv. Funct. Mater.* **2008**, *18*, 3947−3955.
(115) Yang, L. Y.; Shi, M. M.; Wang, M.; Chen, H. Z. Self-Assembled Helical Nanostructures from an Asymmetrical Perylene Diimide. *Chin. Chem. Lett.* **2008**, *19*, 1260−1263.
(116) Li, Y. J.; Qing, Z. H.; Yu, Y. W.; Liu, T. F.; Jiang, R. S.; Li, Y. L. Synthesis and Self-Assembly of Dihydroxyperylene Bisimides for the Tuning of Photophysical Properties. *Chem. - Asian J.* **2012**, *7*, 1934−1939.
(117) Liu, C. X.; Jin, Q. X.; Lv, K.; Zhang, L.; Liu, M. H. Water Tuned the Helical Nanostructures and Supramolecular Chirality in Organogels. *Chem. Commun.* **2014**, *50*, 3702−3705.
(118) Yan, Q. F.; Luo, Z. Y.; Cai, K.; Ma, Y. G.; Zhao, D. H. Chemical Designs of Functional Photoactive Molecular Assemblies. *Chem. Soc. Rev.* **2014**, *43*, 4199−4221.
(119) Gao, Y. Y.; Li, H. Z.; Yin, S. W.; Liu, G. X.; Cao, L.; Li, Y.; Wang, X. S.; Ou, Z. Z.; Wang, X. Supramolecular Electron Donor-Acceptor Complexes Formed by Perylene Diimide Derivative and Conjugated Phenazines. *New J. Chem.* **2014**, *38*, 5647−5653.
(120) Praveen, V. K.; Ranjith, C.; Bandini, E.; Ajayaghosh, A.; Armaroli, N. Oligo (Phenylenevinylene) Hybrids and Self-Assemblies: Versatile Materials for Excitation Energy Transfer. *Chem. Soc. Rev.* **2014**, *43*, 4222−4242.
(121) Wicklein, A.; Ghosh, S.; Sommer, M.; Würthner, F.; Thelakkat, M. Self-Assembly of Semiconductor Organogelator Nanowires for Photoinduced Charge Separation. *ACS Nano* **2009**, *3*, 1107−1114.
(122) Karak, S.; Ray, S. K.; Dhar, A. Photoinduced Charge Transfer and Photovoltaic Energy Conversion in Self-Assembled N,N'-Dioctyl-3,4,9,10-Perylenedicarboximide Nanoribbons. *Appl. Phys. Lett.* **2010**, *97*, 043306.
(123) Wiatrowskia, M.; Dobruchowska, E.; Maniukiewicz, W.; Pietsch, U.; Kowalski, J.; Szamel, Z.; Ulanski, J. Self-Assembly of Perylenediimide Based Semiconductor on Polymer Substrate. *Thin Solid Films* **2010**, *518*, 2266−2270.
(124) Bu, L. J.; Pentzer, E.; Bokel, F. A.; Emrick, T.; Hayward, R. C. Growth of Polythiophene/Perylene Tetracarboxydiimide Donor/Acceptor Shish-Kebab Nanostructures by Coupled Crystal Modification. *ACS Nano* **2012**, *6*, 10924−10929.
(125) Li, L. G.; Jacobs, D. L.; Bunes, B. R.; Huang, H. L.; Yang, X. M.; Zang, L. Anomalous High Photovoltages Observed in Shish Kebab-like Organic p-n Junction Nanostructures. *Polym. Chem.* **2014**, *5*, 309−313.
(126) Shoer, L. E.; Eaton, S. W.; Margulies, E. A.; Wasielewski, M. R. Photoinduced Electron Transfer in 2,5,8,11-Tetrakis-Donor-Substituted Perylene-3,4:9,10-Bis(dicarboximides). *J. Phys. Chem. B* **2015**, *119*, 7635−7643.
(127) Ma, L. C.; Guo, Y. L.; Wen, Y. G.; Liu, Y. Q.; Zhan, X. W. High-Mobility, Air Stable Bottom-Contact n-Channel Thin Film Transistors Based on N,N'-Ditridecyl Perylene Diimide. *Appl. Phys. Lett.* **2013**, *103*, 203303.
(128) Zhao, Y.; Guo, Y. L.; Liu, Y. Q. 25th Anniversary Article: Recent Advances in n-Type and Ambipolar Organic Field-Effect Transistors. *Adv. Mater.* **2013**, *25*, 5372−5391.
(129) Jeon, H. G.; Oguma, N.; Hirata, N.; Ichikawa, M. Wet-Processed n-Type OTFTs Utilizing Highly-Stable Colloids of a Perylene Diimide Derivative. *Org. Electron.* **2013**, *14*, 19−25.
(130) Mumyatov, A. V.; Leshanskaya, L. I.; Anokhin, D. V.; Dremova, N. N.; Troshin, P. A. Organic Field-Effect Transistors Based on Disubstituted Perylene Diimides: Effect of Alkyl Chains on the Device Performance. *Mendeleev Commun.* **2014**, *24*, 306−307.

DOI: 10.1021/acs.chemrev.5b00312
Chem. Rev. 2015, 115, 11967−11998

(131) Che, Y. K.; Yang, X. M.; Balakrishnan, K.; Zuo, J. M.; Zang, L. Highly Polarized and Self-Waveguided Emission from Single-Crystalline Organic Nanobelts. *Chem. Mater.* **2009**, *21*, 2930−2934.
(132) Li, Y. J.; Liu, T. F.; Liu, H. B.; Tian, M. Z.; Li, Y. L. Self-Assembly of Intramolecular Charge-Transfer Compounds into Functional Molecular Systems. *Acc. Chem. Res.* **2014**, *47*, 1186−1198.
(133) Bao, Q. L.; Goh, B. M.; Yan, B.; Yu, T.; Shen, Z. X.; Loh, K. P. Polarized Emission and Optical Waveguide in Crystalline Perylene Diimide Microwires. *Adv. Mater.* **2010**, *22*, 3661−3666.
(134) Chaudhuri, D.; Li, D. B.; Che, Y. K.; Shafran, E.; Gerton, J. M.; Zang, L.; Lupton, J. M. Enhancing Long-Range Exciton Guiding in Molecular Nanowires by *H*-Aggregation Lifetime Engineering. *Nano Lett.* **2011**, *11*, 488−492.
(135) Shi, M. M.; Tung, V. C.; Nie, J. J.; Chen, H. Z.; Yang, Y. Bulky Rigid Substitutions: A Route to High Electron Mobility and High Solid-State Luminescence Efficiency of Perylene Diimide. *Org. Electron.* **2014**, *15*, 281−285.
(136) Yu, Y. W.; Shi, Q. H.; Li, Y. J.; Liu, T. F.; Zhang, L.; Shuai, Z. G.; Li, Y. L. Solid Supramolecular Architecture of a Perylene Diimide Derivative for Fluorescent Enhancement. *Chem. - Asian J.* **2012**, *7*, 2904−2911.
(137) Liu, H. Y.; Cao, X. Q.; Wu, Y. S.; Liao, Q.; Jiménez, Á. J.; Würthner, F.; Fu, H. B. Self-Assembly of Octachloroperylene Diimide into 1D Rods and 2D Plates by Manipulating the Growth Kinetics for Waveguide Applications. *Chem. Commun.* **2014**, *50*, 4620−4623.
(138) Yu, H.; Bao, Z. N.; Oh, J. H. High-Performance Phototransistors Based on Single Crystalline n-Channel Organic Nanowires and Photogenerated Charge-Carrier Behaviors. *Adv. Funct. Mater.* **2013**, *23*, 629−639.
(139) Liu, Y.; Wang, K. R.; Guo, D. S.; Jiang, B. P. Supramolecular Assembly of Perylene Bisimide with β-Cyclodextrin Grafts as a Solid-State Fluorescence Sensor for Vapor Detection. *Adv. Funct. Mater.* **2009**, *19*, 2230−2235.
(140) Kudo, A.; Miseki, Y. Heterogeneous Photocatalyst Materials for Water Splitting. *Chem. Soc. Rev.* **2009**, *38*, 253−278.
(141) Ismail, A. A.; Bahnemann, D. W. Photochemical Splitting of Water for Hydrogen Production by Photocatalysis: A Review. *Sol. Energy Mater. Sol. Cells* **2014**, *128*, 85−101.
(142) McKone, J. R.; Lewis, N. S.; Gray, H. B. Will Solar-Driven Water-Splitting Devices See the Light of Day? *Chem. Mater.* **2014**, *26*, 407−414.
(143) Hisatomi, T.; Kubota, J.; Domen, K. Recent Advances in Semiconductors for Photocatalytic and Photoelectrochemical Water Splitting. *Chem. Soc. Rev.* **2014**, *43*, 7520−7535.
(144) Wang, X. C.; Maeda, K.; Thomas, A.; Takanabe, K.; Xin, G.; Carlsson, J. M.; Domen, K.; Antonietti, M. A Metal-Free Polymeric Photocatalyst for Hydrogen Production from Water under Visible Light. *Nat. Mater.* **2009**, *8*, 76−80.
(145) Chen, S.; Jacobs, D.; Xu, J. K.; Li, Y. X.; Wang, C. Y.; Zang, L. 1D Nanofiber Composites of Perylene Diimides for Visible-Light-Driven Hydrogen Evolution from Water. *RSC Adv.* **2014**, *4*, 48486−48491.
(146) Chen, S.; Li, Y. X.; Wang, C. Y. Visible-Light-Driven Photocatalytic H_2 Evolution from Aqueous Suspensions of Perylene Diimide Dye-Sensitized Pt/TiO_2 Catalysts. *RSC Adv.* **2015**, *5*, 15880−15885.
(147) Chen, S.; Wang, C.; Bunes, B. R.; Li, Y. X.; Wang, C. Y.; Zang, L. Enhancement of Visible-Light-Driven Photocatalytic H_2 Evolution from Water over g-C_3N_4 through Combination with Perylene Diimide Aggregates. *Appl. Catal., A* **2015**, *498*, 63−68.
(148) Bullock, J. E.; Carmieli, R.; Mickley, S. M.; Vura-Weis, J.; Wasielewski, M. R. Photoinitiated Charge Transport through π-Stacked Electron Conduits in Supramolecular Ordered Assemblies of Donor-Acceptor Triads. *J. Am. Chem. Soc.* **2009**, *131*, 11919−11929.
(149) Chen, Y. L.; Chen, L. N.; Qi, G. J.; Wu, H. X.; Zhang, Y. X.; Xue, L.; Zhu, P. H.; Ma, P.; Li, X. Y. Self-Assembled Organic-Inorganic Hybrid Nanocomposite of a Perylenetetracarboxylic Diimide Derivative and CdS. *Langmuir* **2010**, *26*, 12473−12478.
(150) Kowerko, D.; Krause, S.; Amecke, N.; Abdel-Mottaleb, M.; Schuster, J.; von Borczyskowski, C. Identification of Different Donor-Acceptor Structures via Förster Resonance Energy Transfer (FRET) in Quantum-Dot-Perylene Bisimide Assemblies. *Int. J. Mol. Sci.* **2009**, *10*, 5239−5256.
(151) Zhong, L. N.; Xing, F. F.; Shi, W.; Yan, L. M.; Xie, L. Q.; Zhu, S. R. Synthesis, Spectra, and Electron-Transfer Reaction of Aspartic Acid Functionalized Water-Soluble Perylene Bisimide in Aqueous Solution. *ACS Appl. Mater. Interfaces* **2013**, *5*, 3401−3407.
(152) Llansola-Portoles, M. J.; Bergkamp, J. J.; Tomlin, J.; Moore, T. A.; Kodis, G.; Moore, A. L.; Cosa, G.; Palacios, R. E. Photoinduced Electron Transfer in Perylene-TiO_2 Nanoassemblies. *Photochem. Photobiol.* **2013**, *89*, 1375−1382.
(153) Silva, B. P. G.; de Florio, D. Z.; Brochsztain, S. Characterization of a Perylenediimide Self-Assembled Monolayer on Indium Tin Oxide Electrodes Using Electrochemical Impedance Spectroscopy. *J. Phys. Chem. C* **2014**, *118*, 4103−4112.
(154) Yang, X. L.; Liu, X. Z.; Meng, X. Y.; Wang, X. Y.; Li, G.; Shu, C. Y.; Jiang, L.; Wang, C. R. Self-Assembly of Highly Dispersed Pt and PtRu Nanoparticles on Perylene Diimide Derivatives Functionalized Carbon Nanotubes as Enhanced Catalysts for Methanol Electro-Oxidation. *J. Power Sources* **2013**, *240*, 536−543.
(155) Araújo, R. F.; Silva, C. J. R.; Paiva, M. C.; Franco, M. M.; Proença, M. F. Efficient Dispersion of Multi-Walled Carbon Nanotubes in Aqueous Solution by Non-Covalent Interaction with Perylene Bisimides. *RSC Adv.* **2013**, *3*, 24535−24542.
(156) Liu, Y.; Zhu, E. W.; Bian, L. Y.; Hai, J. F.; Tang, J.; Tang, W. H. Robust Graphene Dispersion with Amphiphlic Perylene-Polyglycidol. *Mater. Lett.* **2014**, *118*, 188−191.
(157) Kirner, J. T.; Stracke, J. J.; Gregg, B. A.; Finke, R. G. Visible-Light-Assisted Photoelectrochemical Water Oxidation by Thin Films of a Phosphonate-Functionalized Perylene Diimide Plus CoO_x Cocatalyst. *ACS Appl. Mater. Interfaces* **2014**, *6*, 13367−13377.
(158) Chen, X. B.; Shen, S. H.; Guo, L. J.; Mao, S. S. Semiconductor-Based Photocatalytic Hydrogen Generation. *Chem. Rev.* **2010**, *110*, 6503−6570.
(159) Cao, S. W.; Yu, J. G. g-C_3N_4-Based Photocatalysts for Hydrogen Generation. *J. Phys. Chem. Lett.* **2014**, *5*, 2101−2107.
(160) Yeh, T. F.; Syu, J. M.; Cheng, C.; Chang, T. H.; Teng, H. Graphite Oxide as a Photocatalyst for Hydrogen Production from Water. *Adv. Funct. Mater.* **2010**, *20*, 2255−2262.
(161) Xiang, Q. J.; Yu, J. G. Graphene-Based Photocatalysts for Hydrogen Generation. *J. Phys. Chem. Lett.* **2013**, *4*, 753−759.
(162) Xiang, Q. J.; Yu, J. G.; Jaroniec, M. Graphene-Based Semiconductor Photocatalysts. *Chem. Soc. Rev.* **2012**, *41*, 782−796.
(163) Zhang, N.; Zhang, Y. H.; Xu, Y. J. Recent Progress on Graphene-Based Photocatalysts: Current Status and Future Perspectives. *Nanoscale* **2012**, *4*, 5792−5813.
(164) Leclerc, M.; Najari, A. Organic Thermoelectrics: Green Energy from a Blue Polymer. *Nat. Mater.* **2011**, *10*, 409−410.
(165) Bubnova, O.; Khan, Z. U.; Malti, A.; Braun, S.; Fahlman, M.; Berggren, M.; Crispin, X. Optimization of the Thermoelectric Figure of Merit in the Conducting Polymer Poly(3,4-Ethylenedioxythiophene). *Nat. Mater.* **2011**, *10*, 429−433.
(166) Yue, R. R.; Xu, J. K. Poly(3,4-Ethylenedioxythiophene) as Promising Organic Thermoelectric Materials: A Mini-Review. *Synth. Met.* **2012**, *162*, 912−917.
(167) Chen, S.; Lu, B. Y.; Duan, X. M.; Xu, J. K. Systematic Study on Chemical Oxidative and Solid-State Polymerization of Poly(3,4-Ethylenedithiathiophene). *J. Polym. Sci., Part A: Polym. Chem.* **2012**, *50*, 1967−1978.
(168) Chen, S.; Lu, B. Y.; Xu, J. K.; Qin, L. Q.; Wang, Z. P.; Duan, X. M. Preparation and Characterization of Aqueous Dispersions of Poly(3,4-Ethylenedithiathiophene-*co*-3,4-Ethylenedioxythiophene)/Poly(Styrene Sulfonate) and Their Conducting Films. *J. Appl. Polym. Sci.* **2013**, *129*, 1717−1725.
(169) Kim, G. H.; Shao, L.; Zhang, K.; Pipe, K. P. Engineered Doping of Organic Semiconductors for Enhanced Thermoelectric Efficiency. *Nat. Mater.* **2013**, *12*, 719−723.

DOI: 10.1021/acs.chemrev.5b00312
Chem. Rev. 2015, 115, 11967−11998

(170) Kumar, M.; George, S. J. Spectroscopic Probing of the Dynamic Self-Assembly of an Amphiphilic Naphthalene Diimide Exhibiting Reversible Vapochromism. *Chem. - Eur. J.* **2011**, *17*, 11102−11106.
(171) Jain, A.; Rao, K. V.; Kulkarni, C.; George, A.; George, S. J. Fluorescent Coronene Monoimide Gels via H-Bonding Induced Frustrated Dipolar Assembly. *Chem. Commun.* **2012**, *48*, 1467−1469.
(172) Kulkarni, C.; Munirathinam, R.; George, S. J. Self-Assembly of Coronene Bisimides: Mechanistic Insight and Chiral Amplification. *Chem. - Eur. J.* **2013**, *19*, 11270−11278.
(173) Molla, M. R.; Gehrig, D.; Roy, L.; Kamm, V.; Paul, A.; Laquai, F.; Ghosh, S. Self-Assembly of Carboxylic Acid Appended Naphthalene Diimide Derivatives with Tunable Luminescent Color and Electrical Conductivity. *Chem. - Eur. J.* **2014**, *20*, 760−771.
(174) Nandre, K. P.; Kobaisi, M. A.; Bhosale, R. S.; Latham, K.; Bhosale, S. V.; Bhosale, S. V. pH Triggered Self-Assembly Induced Enhanced Emission of Phosphonic Acid Appended Naphthalenediimide Amphiphile. *RSC Adv.* **2014**, *4*, 40381−40384.
(175) Rao, K. V.; George, S. J. Synthesis and Controllable Self-Assembly of a Novel Coronene Bisimide Amphiphile. *Org. Lett.* **2010**, *12*, 2656−2659.
(176) Liu, B.; Zhu, W. H.; Wu, W. J.; Ri, K. M.; Tian, H. Hybridized Ruthenium(II) Complexes with High Molar Extinction Coefficient Unit: Effect of Energy Band and Adsorption on Photovoltatic Performances. *J. Photochem. Photobiol., A* **2008**, *194*, 268−274.
(177) Jiang, W.; Li, Y.; Yue, W.; Zhen, Y.; Qu, J.; Wang, Z. One-Pot Facile Synthesis of Pyridyl Annelated Perylene Bisimides. *Org. Lett.* **2010**, *12*, 228−231.
(178) Chen, L.; Li, C.; Müllen, K. Beyond Perylene Diimides: Synthesis, Assembly and Function of Higher Rylene Chromophores. *J. Mater. Chem. C* **2014**, *2*, 1938−1956.
(179) Choi, H.; Paek, S.; Song, J.; Kim, C.; Cho, N.; Ko, J. Synthesis of Annulated Thiophene Perylene Bisimide Analogues: Their Applications to Bulk Heterojunction Organic Solar Cells. *Chem. Commun.* **2011**, *47*, 5509−5511.
(180) Qian, H. L.; Liu, C. M.; Wang, Z. H.; Zhu, D. B. S-Heterocyclic Annelated Perylene Bisimide: Synthesis and Co-Crystal with Pyrene. *Chem. Commun.* **2006**, 4587−4589.
(181) Li, Y. J.; Li, Y. L.; Li, J. B.; Li, C. H.; Liu, X. F.; Yuan, M. J.; Liu, H. B.; Wang, S. Synthesis, Characterization, and Self-Assembly of Nitrogen-Containing Heterocoronenetetracarboxylic Acid Diimide Analogues: Photocyclization of N-Heterocycle-Substituted Perylene Bisimides. *Chem. - Eur. J.* **2006**, *12*, 8378−8385.
(182) Liu, X. L.; Zhang, Y. B.; Pang, X. B.; E, Y.; Zhang, Y. F.; Yang, D. J.; Tang, J. G.; Li, J.; Che, Y. K.; Zhao, J. C. Nanocoiled Assembly of Asymmetric Perylene Diimides: Formulation of Structural Factors. *J. Phys. Chem. C* **2015**, *119*, 6446−6452.
(183) Son, M. J.; Park, K. H.; Shao, C. Z.; Würthner, F.; Kim, D. Spectroscopic Demonstration of Exciton Dynamics and Excimer Formation in a Sterically Controlled Perylene Bisimide Dimer Aggregate. *J. Phys. Chem. Lett.* **2014**, *5*, 3601−3607.
(184) Görl, D.; Zhang, X.; Stepanenko, V.; Würthner, F. Supramolecular block copolymers by kinetically controlled co-self-assembly of planar and core-twisted perylene bisimides. *Nat. Commun.* **2015**, *6*, 7009.
(185) Ogi, S.; Stepanenko, V.; Sugiyasu, K.; Takeuchi, M.; Würthner, F. Mechanism of Self-Assembly Process and Seeded Supramolecular Polymerization of Perylene Bisimide Organogelator. *J. Am. Chem. Soc.* **2015**, *137*, 3300−3307.
(186) Echue, G.; Lloyd-Jones, G. C.; Faul, C. F. J. Chiral Perylene Diimides: Building Blocks for Ionic Self-Assembly. *Chem. - Eur. J.* **2015**, *21*, 5118−5128.
(187) Wang, G.; Chang, X. M.; Peng, J. X.; Liu, K. Q.; Zhao, K. R.; Yu, C. M.; Fang, Y. Towards a New FRET System via Combination of Pyrene and Perylene Bisimide: Synthesis, Self-Assembly and Fluorescence Behavior. *Phys. Chem. Chem. Phys.* **2015**, *17*, 5441−5449.
(188) Weingarten, A. S.; Kazantsev, R. V.; Palmer, L. C.; McClendon, M.; Koltonow, A. R.; Samuel, A. P. S.; Kiebala, D. J.; Wasielewski, M. R.; Stupp, S. I. Self-Assembling Hydrogel Scaffolds for Photocatalytic Hydrogen Production. *Nat. Chem.* **2014**, *6*, 964−970.
(189) Ma, X. J.; Zhang, Y. B.; Zheng, Y. X.; Zhang, Y. F.; Tao, X.; Che, Y. K.; Zhao, J. C. Highly Fluorescent One-Handed Nanotubes Assembled from a Chiral Asymmetric Perylene Diimide. *Chem. Commun.* **2015**, *51*, 4231−4233.
(190) Bu, L. J.; Dawson, T. J.; Hayward, R. C. Tailoring Ultrasound-Induced Growth of Perylene Diimide Nanowire Crystals from Solution by Modification with Poly(3-Hexyl Thiophene). *ACS Nano* **2015**, *9*, 1878−1885.

DOI: 10.1021/acs.chemrev.5b00312
Chem. Rev. 2015, 115, 11967−11998